The Candida albicans Hsp90 co-chaperone complex regulates aspects of virulence

Lyons, Naomi

Award date:
2018

Awarding institution:
University of Bath

The *Candida albicans* Hsp90 co-chaperone complex regulates aspects of virulence

Naomi Lyons

A thesis submitted for the degree of Doctor of Philosophy

University of Bath
Department of Biology and Biochemistry
April 2018

Contents

Acknowledgements

It has been such a privilege to undertake this project; none of it would be possible without the help and support I have had along the way. First, I thank my supervisor, Stephanie Diezmann, for giving me this opportunity in the first place, for her tireless patience and for her attentive guidance all the way through. The best supervisor anyone could hope for.

I am grateful for my second supervisor, Laurence Hurst for the benefit of his experience and calm attitude with all research disasters. Special thanks are owed to Susanne Gebhard for being an honorary third supervisor, offering advice and reassurance while Steph was on maternity leave.

Thank you to all members of the Diezmann and Henk labs, especially to Ruairidh, Leenah, Carolyn, Steve, and Kangzhen, who were there from the beginning, making the office feel like home and keeping the lab ship-shape. My thanks go to Natalie Vaughan for being something of a stress-buddy in trying times.

For tips with statistics and the ever-inscrutable R I have to thank Ben Sharpe, Heath O'Brien, Emanuele Kendrick, and Sion Bayliss.

The advice of Cassidy Bayley, Steve Weston and Elena Corujo was everything I needed for tackling qPCR.

I am indebted to Chris Apark and Chris Vennard for their dedicated care and wealth of experience with the caterpillars.

Most importantly I thank my family for boosting my spirits with nibling updates, and for not asking too many questions when told. Jane, I thank you for all your support, and Ian for inspiring me to finish what you started. Finally, I owe a world of gratitude to Erik for housing and feeding me, and for meeting my stress with eternal good spirits and chocolate surprises.

Abstract

Candida albicans is one of the top five most common causes of nosocomial bloodstream infections, and systemic infections are fatal in 40% of cases in the UK. Treatment of candidiasis presents a challenge owing to a lack of efficacious drugs and a paucity of suitable drug targets for development. Novel drug targets are urgently needed in order to tackle this growing public health problem. Hsp90 is an important regulator of *C. albicans* virulence, but is highly conserved with the human orthologue, making it a poor drug target.

Hsp90 functions in concert with associated co-chaperones, which are less conserved. The sub-telomeric location of co-chaperone genes is reminiscent of virulence gene families, including the *TLO* genes in *Candida.*

The principle aim of this study was to elucidate the roles of five Hsp90 co-chaperones in *C. albicans* virulence; Ssa1, Ssa2, Sba1, Aha1, and Sti1. All five were found to be instrumental in biofilm formation and in killing of an invertebrate host model, *Manduca sexta* fifth instar larvae. Ssa1, Sba1, and Sti1 were identified as regulators of fluconazole resistance. Ssa2 was broadly found to be a repressor of virulence traits, though apparently with an overall fitness benefit to the cells in the host.

The secondary aim was to investigate the silencing effects of histone deacetylases on Hsp90 co-chaperone gene expression. Hst1 was found to

reduce silencing, while Hst2 was found to increase silencing of Hsp90 co-chaperones by heterochromatin formation.

This study enhances understanding of diverse *C. albicans* virulence traits and how the dynamic Hsp90 co-chaperone complex regulates them, as well as how genomic locale implicates genes in virulence functions. This may inform future development of novel antifungal drugs.

1. Introduction

1.1 Candidiasis is a major public health problem

1.1.1 *Candida albicans* is a leading fungal pathogen of humans

Human fungal infections are a neglected public health problem and rates of candidiasis are on the rise [1]. Lack of efficacious drugs makes infections difficult to treat and a paucity of suitable drug targets mean there is a dearth of novel drugs. Identification of novel drug targets is key to tackling fungal infections. Hsp90 is an important regulator of virulence in *Candida albicans* but is highly conserved with its human orthologue [2]. Hsp90 acts in concert with associated co-chaperones, which are less conserved and less well-characterised. The co-chaperones' sub-telomeric locale is reminiscent of other virulence genes [3-5]. The principle aim of this project was to explore the potential of Hsp90 co-chaperones as candidates for development of novel therapeutic strategies to treat systemic *Candida spp.* infections employing the principles of evolutionary medicine. The secondary aim was to elucidate how their expression is regulated with respect to their genomic location.

The opportunistic pathogen *Candida albicans* causes both superficial infections of mucosal surfaces and life-threatening systemic and deep-seated organ infections. Incidence of invasive candidiasis in the UK is currently estimated at >5000 cases per annum, with an overall mortality rate of approximately 40% [6, 7]. *C. albicans* is one of the top five most common nosocomial bloodstream infections [8]. Diagnosis of systemic *C. albicans* infections relies on time-consuming blood culture, which fails to detect 50% of established infections, often causing delays in administering appropriate treatment and increasing the risk of death [9].

The victims of these infections are typically immunocompromised individuals, such as patients who have undergone surgery, chemotherapy patients, organ transplant recipients, and people infected with HIV. The increase in recent years, particularly in more economically developed countries, in the use of therapies with immunosuppressive side-effects has resulted in a larger proportion of the population being susceptible to life-threatening fungal infections [10]. There has been a dramatic increase in use of solid and fluid organ transplants in the last two decades, and for such transplants to be successful suppression of the host immune system is required. Therefore, treatments are needed more than ever before, while antifungal drug resistance is simultaneously an increasing problem. Perhaps the most emotive aspect of life-threatening fungal infections is their prevalence in neonates. Risk factors such as pre-term birth and maternal pre-eclampsia can predispose infants to candidiasis, for which neonates face a death rate of over 40% [11].

C. albicans has the capacity to cause life-threatening systemic infections and the lack of efficacious treatment options, in combination with scarcity of novel antifungal drugs and increasing immunocompromised population, mean that incidence of systemic candidiasis is increasing [1]. Poor diagnostics and the evolution of drug resistance mean that we are ill-equipped to deal with this growing public health threat and that identification of novel and robust drug targets is needed.

1.1.2 *C. albicans* employs a diverse set of virulence mechanisms

C. albicans employs a range of cellular processes to facilitate its thriving in the host environment and subversion of the host immune system.

The most significant virulence factor of *C. albicans* discovered to date is the cytolytic peptide toxin dubbed candidalysin. The first toxin of its kind identified in fungi, candidalysin damages host epithelial cell membranes and induces epithelial immunity. Strains which do not produce candidalysin are avirluent in mucosal models of infection [12]. This recent discovery is an exciting development in the understanding of *Candida spp.* virulence and opens up new avenues of possiblity for how fungal pathogenesis may be undermined in order to tackle problematic fungal infections.

Oxidative stress is induced by oxidative burst from the host's innate immune system, when immune cells such as phagocytes release reactive oxygen species (ROS) into the phagosome, which exert oxidative stress on the invading pathogen [13]. Pathogenic *C. albicans* cells are able to resist this level of oxidative stress and escape from the phagosome unscathed; essential for thriving in the host and causing disease. The Cap1 transcription factor is the principle mediator of the *C. albicans* oxidative stress response, inducing transcription of a wide range of antioxidant enzyme genes to reduce ROS molecules [14-17]. These include catalase and superoxide dismutase enzymes, located intracellularly or anchored in the cell wall [18]. Sod5 is anchored in the cell wall to reduce extracellular ROS, and is specifically induced by englfment by phagocytes, and by hyphal formation [19, 20]. *C. albicans* can also induce hyphal formation as a means to physically escape host immune cells, resulting in death of the phagocyte [21, 22].

The heat shock response is important for adaptation to the host environment, particularly when the pathogen induces fever [23]. Thermal regulation is also intrinsically linked to hyphal morphogenesis and antifungal drug resistance, both of which are major pathogenic traits [24, 25]. A temperature of 42°C constitutes heat shock for *C. albicans* and the heat shock proteins were originally identified by their upregulation in heat stress conditions [26].

Biofilm formation is a ubiquitous virulence trait where cells form a matrix of extracellular polysaccharides allowing them to adhere to diverse surfaces [27]. The biofilm also acts as an impenetrable shield, protecting invasive cells from

drug treatments as well as from the host immune system. Furthermore, the biofilm community can act as a cellular reservoir, allowing for dispersal of cells to seed the infection further afield. Biofilm formation in *C. albicans* is a multigenic trait requiring full functionality of six different transcription factor networks; Bcr1, Brg1, Efg1, Ndt80, Rob1, and Tec1, disruption of any of which leads to defects in biofilm development [28].

The term morphogenesis refers to the switch in phenotype between the yeast and hyphal forms of *Candida albicans*. The ability to change the cell morphology is considered essential for virulence in *C. albicans* and morphological defects can make cells avirulent [29, 30]. *C. albicans* uses hyphal formation as a means to invade host tissues and disseminate into the bloodstream, and is thus a valuable weapon of virulence [31]. The process involves changes in cell wall architecture and composition, and can be induced through different pathways by a variety of environmental cues, such as changes in temperature, pH, or ROS [25, 32, 33].

Drug resistance is becoming an increasingly common virulence trait in the modern world, and renders existing antifungal agents impotent [34]. Hsp90 is considered to govern antifungal drug resistance and the function of this may depend on its associated co-chaperones [35]. The concept of targeting Hsp90 co-chaperones for treatment of systemic candidiasis may also have scope for combinatorial therapy using existing antifungals.

1.1.3 Evolution of antifungal drug resistance is a growing challenge

There are limited fungicidal drugs available for treatment of *C. albicans* infections, and widespread resistance to those there are, resulting in a death rate from systemic infections in excess of 50% [36]. The genetic similarities between fungi and humans also results in a paucity of suitable drug targets which can be used to attenuate the infectious organism whilst avoiding toxic effects on the host. The targets commonly employed in treatment of bacterial infections, such as the bacterial cell wall or cell membrane, are not available in the eukaryotic fungi due to their more recent evolutionary divergence from animals [37, 38].

The problem of antifungal resistance has been sorely neglected, especially when complared to that of antibiotic resistance in bacteria. Whilst there are more than 20 classes of antibacterial drugs available, there are only 4 classes of antifungal drugs on the market today: polyenes, azoles, echinocandins, and pyrimidine analogues. Resistance to any of these is not uncommon [34] and most of them act similarly by disrupting the cell membrane or cell wall synthesis [39]. In 1997 the 30-day mortality rate for systemic candidiasis in the European Union was 37.9% [40], but by 2014 this had increased to 47% [41]. Such a dramatic rise in mortality rate in 17 years, in an age when efficacy of medical treatment should be advancing, must surely be attributable to reduced effectiveness of antifungal drugs. If such trends are allowed to continue, systemic candidiasis may approach imperviousness to treatment.

Of the currently available antifungal drugs, azoles are the most often-used (Fig. 1.1). They induce a strong selective pressure for resistance in fungal communities exposed to the compounds [42]. Azoles act by inhibiting activity of lanosterol 14α demethylase, which is necessary for synthesis of the essential cell membrane component ergosterol, so cell membrane fluidity is disrupted. Ergosterol is an essential component of the fungal cell membrane, balancing stability and fluidity; it fulfils the equivalent role of cholesterol in animal cell membranes. Growth of cells is arrested and toxic precursors to ergosterol build up within the cells, inhibiting growth and development [43]. The pathway of ergosterol synthesis is specific to fungi and, with very few exceptions, conserved across the kingdom [44, 45].

However, binding fidelity of azoles is not perfect and some side-effects can be induced in the host when azoles bind human cytochrome 450 enzymes, which are needed for a range of metabolic functions [46]. Point mutations in *ERG3* and *ERG11* have been found to confer resistance to fluconazole [47].

The problem is exacerbated by use of antifungal compounds in agriculture, with herbicides such as 14α-dimethylase inhibitors (DMIs) and prochloraz used extensively [48]. They are similar in structure and action to triazoles, which are the most commonly used class of antifungal for treatment of infections in humans, and exposure through agriculture encourages cross-resistance to medical triazoles [49]. Azoles are currently the most readily-absorbed class of medical antifungal when administered orally and so

resistance to them poses a real threat to treatment of patients with systemic fungal infections [50].

Echinocandins such as caspofungin act by inhibiting synthesis of cell wall polysaccharides and are fungicidal to *Candida albicans* [51]. They are classified by a cyclic hexapeptide structure with lipid side-chains to anchor in the cell (Fig. 1.1).

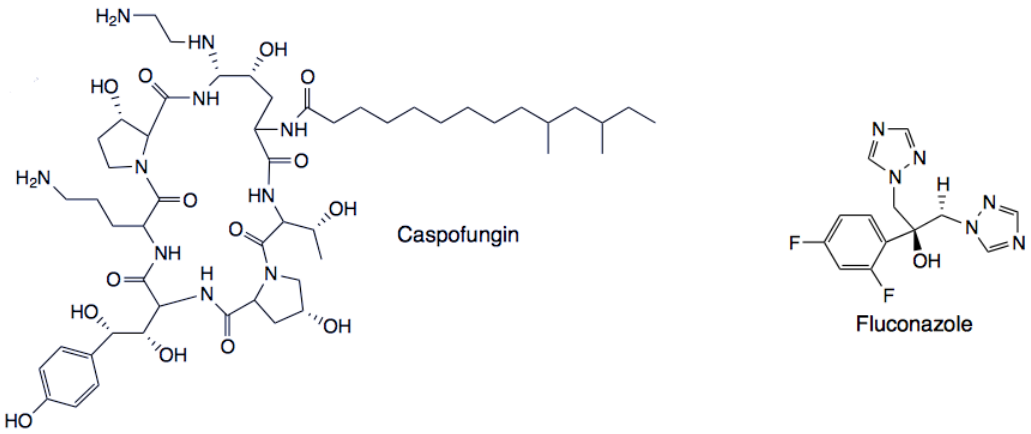

Figure 1.1 Structures representing two of the most commonly used classes of antifungals today [52]; caspofungin, from the echinocandins, and fluconazole, from the azoles.

Employing essential structures of the fungal cell as drug targets, as is the case with the echinocandins, makes the drugs fungicidal. This means that following

exposure to the drug, the surviving fungal population will be resistant. In addition, these are largely broad-spectrum antifungals and so resistance easily becomes widespread in fungal communities, even in the environment outside of the host. Studies of sequential clinical isolates from a single patient have shown that a fluconazole-susceptible strain of *C. albicans* can become completely unresponsive to the drug in under two years [53]. This occurs particularly as antifungal agents such as the azoles are used in agricultural as well as medicinal applications. Targeting cells specifically when they are exhibiting virulent behaviour could help to prevent the spread of resistance as it eliminates the problem of selective pressure on fungi in the environment outside of the host, or on those living commensally in the host.

The study aimed to answer the question of whether Hsp90 co-chaperones regulate fungal virulence and whether they could be exploited as drug targets in the context of evolutionary medicine. Evolutionary medicine is the application of modern evolutionary theory to the understanding of health and disease [54]. The relevance in this case is that the emergence of drug resistance is a result of an organism being challenged by a drug because it targets an essential element of the cell, and therefore exerts a strong selective pressure. As a commensal organism, found on healthy humans and causing disease opportunistically, it is not wholly desirable nor realistic to completely eradicate *C. albicans* from an infected host, and failing to do so with conventional antifungal drugs introduces the risk of leaving behind a drug resistant population.

Drug resistance in pathogens is a growing problem, and leads to deaths of critically ill people. Multiple antimicrobial drugs are often employed sequentially in a single infection, with treatment being changed in response to resistance arising [55]. This raises a multitude of questions for evolutionary medicine; for example, whether the resistance evolves in response to the drug or whether it is acquired from other organisms; or whether drugs could be administered differently to evade resistance pre-emptively. A lack of answers to these questions means that changes to treatment are based on guess-work and are frequently unsuccessful [55].

The principle of evolutionary medicine which this study explored was to identify a target for future drug design which would subvert drug resistance, thereby increasing the value and longevity of the drug, as well as allowing for a simple treatment regimen.

Taking evolutionary mechanisms into account prior to the development of new drugs is prudent; lessons should be learned from the repeated evolution of resistance to antimicrobial compounds. This strategy of drug design to evade resistance is now being employed for health threats as diverse as cancer [56] and malaria [57].

The change from commensal to virulent growth involves significant changes in gene expression in *C. albicans* [58, 59]. Abrogating virulence rather than growth provides a unique opportunity for treatment that would mitigate the problem of drug resistance emerging by reducing the selective pressure for

drug resistance. This would obstruct the ability of *C. albicans* to continue to cause disease, allowing for the host immune system, or a secondary antifungal drug administered combinatorially, to clear the infection efficaciously. This should in turn make the emergence of resistance less likely to occur and more readily lost if acquired; research in *Staphylococcus aureus* has shown that maintaining drug resistance genes is quite costly to the organism and lack exposure to the drug results in loss of resistance [60]. Drug resistance is often a costly trait and in conditions where drug is absent, drug susceptible strains will frequently out-compete the resistant ones [61] so in such conditions it is advantageous for drug resistance to be sacrificed. Indeed, by the same principle, employing non-essential drug targets may additionally extend the usefulness of existing antifungals if they can then be used more sparingly and so reduce the spread of resistance.

In addition, evidence shows that in a hospital setting, bacteria have a tendency to repidly lose acquired resistance to antibiotics, even when the resistance does not confer a fitness cost [62]. This provides further motivation for developing new treatment stategies which employ existing antimicrobial drugs sparingly, in order to avoid problems of widespread resistance.

Evolutionary medicine is a concept yet to be applied to fungal virulence; in the quest for novel drug targets to treat candidiasis Hsp90 is conspicuous as a regulator of virulence [24, 63]. However, due to its essentiality, Hsp90 does not make a suitable drug target for fungal infections, but the Hsp90 co-chaperones may be a new avenue of possibility in treating infections according

to the principles of evolutionary medicine. Whilst most of the co-chaperones being investigated in this study are conserved in humans, they share far less sequence identity than other proteins, such as Hsp90, and so show some potential as more suitable drug targets.

1.2 The molecular chaperone Hsp90 regulates virulence traits in *C. albicans*

1.2.1 Hsp90 is essential and highly conserved

Hsp90 is an essential and well-studied molecular chaperone conserved in all known eukaryotes, with orthologues being universally required for viability [64-66]. In *C. albicans,* Hsp90 interacts with ~4% of the genome, most of which are genes thought to function downstream of Hsp90 as they are not essential in all conditions [67]. In *C. albicans* Hsp90 is a homodimer, which operates in a clamp-like structure; closed when adenosine triphosphate (ATP) is bound, and open when adenosine diphosphate (ADP) is bound (Fig. 1.2) [68, 69].

The name of Hsp90; 90 kDa Heat Shock Protein, was inspired by the size of its orthologue in *Homo sapiens* and its discovery in the 1970s as one of a set of proteins whose expression is increased in response to heat stress in

Drosophila melanogaster [26, 70]. Orthologues are present across the eukaryotic domain, and Hsp90 was identified in yeast later that same decade [71].Although the protein is highly conserved across eukayotes and orthologues share the same name, its size does vary slightly; Hsp90 is only 80.8 kDa in *C. albicans* [72].

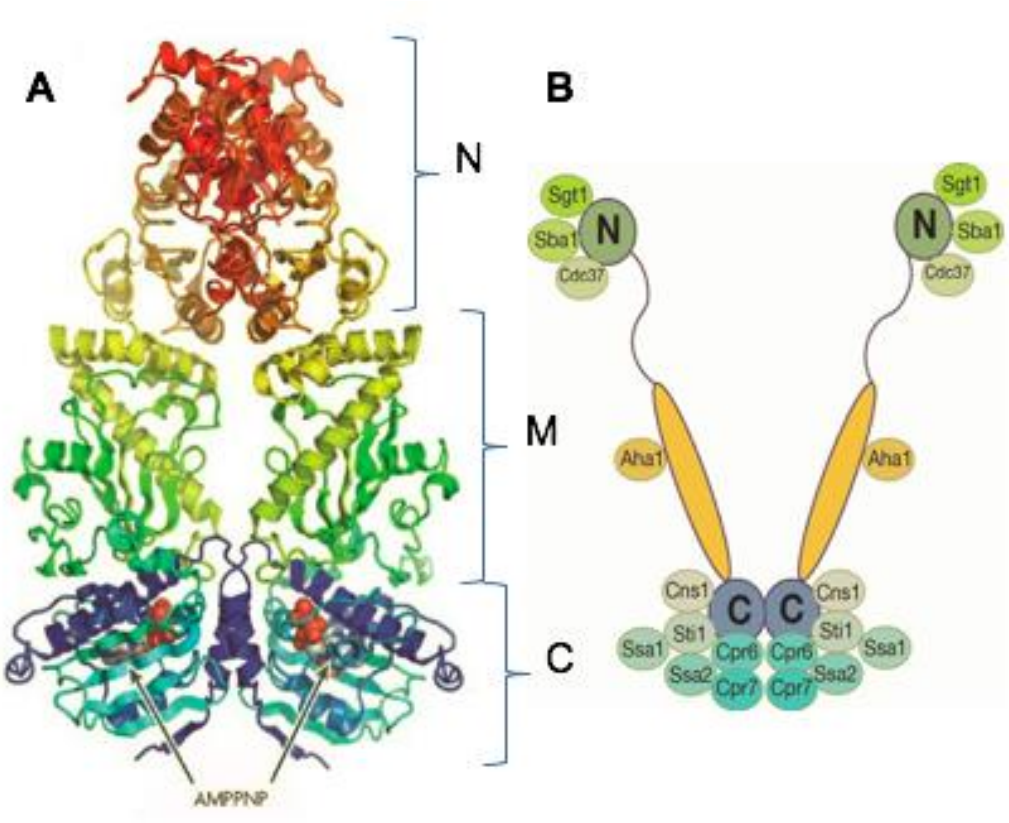

Figure 1.2 [**A**] Crystal structure of *Saccharomyces cerevisiae* Hsp90 [73] with the amino-terminal domain (N), middle domain (M), and carboxy-terminal domain (C) indicated, and [**B**] a simplified diagram of Hsp90 showing which domain the co-chaperones bind to. Aha1 can bind both the middle domain and the N-terminal domain.

Inhibition of Hsp90, which repairs proteins, leads to widespread protein degradation, including proteins responsible for growth. Thus, inhibition of Hsp90 has been shown to limit growth of cancer cells [74] inhibitory compounds based on geldanamycin have even reached clinical trials as anti-cancer drugs [75, 76].

Geldanamycin and radicicol are common Hsp90 inhibitors which operate by binding near the N-terminus of Hsp90, thereby blocking the ATP binding site for the protein [77, 78]. Inhibition is specific to the Hsp90 protein as the particular amino acid motif is atypical of eukaryotic proteins, being more usually found in prokaryotic organisms [79, 80].

More recently, a number of similar compounds have been found to inhibit growth of cells in liver and colon cancers *in vitro*, as well as having antifungal effects on *C. albicans* [81-83]. Preliminary results suggest the mode of action involves suppressing the expression of a number of genes, including *HSP90* and *ERG11*, by inhibiting the necessary transcription factors [47, 48, 84]. Significantly, overexpression of Erg11 is one of the known azole resistance mechanisms [47, 48]; combinatorial therapy with a compound which reduces its expression may act to undermine this resistance and allow for successful treatment of infections.

Hsp90 buffers the effects of deleterious mutations to keep cells phenotypically stable [85, 86]. So as environmental stresses increase in an infection scenario

and the mutation rate of the cells increases in response, Hsp90 helps to lower the associated risks.

1.2.2 In *C. albicans*, Hsp90 regulates important virulence traits

Hsp90 is an essential regulator of virulence and morphogenesis, as well as being required for cell viability [63, 87]. Due to its high level of conservation with the human homologue; 63% sequence identity, Hsp90 is an unsuitable drug target [88]. The shared evolutionary history between mammals and fungi means that this problem of conservation is common in what would otherwise be potential drug targets; inhibiting Hsp90 during systemic candidiasis in a murine model of disease resulted in lethal host toxicity [2]. The essentiality of Hsp90 means that targeting it would also encourage development of resistance, both in the host and in the external environment.

Hsp90 has been shown to be instrumental in the success of drug resistant strains of *C. albicans* and regulates the response and adaptation of the organism to inhibitory compounds [35, 89]. In addition, Hsp90 functions to aid dispersal of *C. albicans* biofilms; a virulence trait which protects cells from drugs and the host immune system as well as seeding the infection [63].

The function of Hsp90 is dependent upon its working in concert with its associated co-chaperones, which provide client specificity and regulate

Hsp90's activity (Fig. 1.2). Hsp90 is essential to *C. albicans* but makes a poor candidate for a drug target due to its high conservation with the human orthologue. The aim of identifying Hsp90 co-chaperones as novel drug targets is to indirectly abrogate Hsp90 function and thus undermine *C. albicans* virulence, including drug resistance.

1.2.3 Hsp90 acts in concert with co-chaperones

The Hsp90 co-chaperone machinery of *C. albicans* involves 14 co-chaperones working in concert with Hsp90; the complex is dynamic with co-chaperones variously regulating localisation, activity, and binding specificity of Hsp90 [90-105]. To date, co-chaperones in *C. albicans* are understudied and poorly understood.

Hsp90 co-chaperones were selected based on their location in the genome (Fig. 1.3). Virulence genes are often found close to the telomeres, with examples including the *TLO* genes in *Candida* [3] and the *VAR* genes in *Plasmodium* [4], and even the effector genes in the causative organism of rice blast, *Magnaporthe* [5], which are all groups of genes implicated in virulence. Orthologous co-chaperone genes in *S. cerevisiae, Candida*'s non-pathogenic relative, are distributed along the whole length of the chromosome. In the pathogenic *C. albicans*, Hsp90 co-chaperone genes are clustered towards the telomeric regions, implying they too may be involved in virulence. This

genomic locale suggests that gene expression can be regulated by heterochromatin formation to silence genes [106, 107].

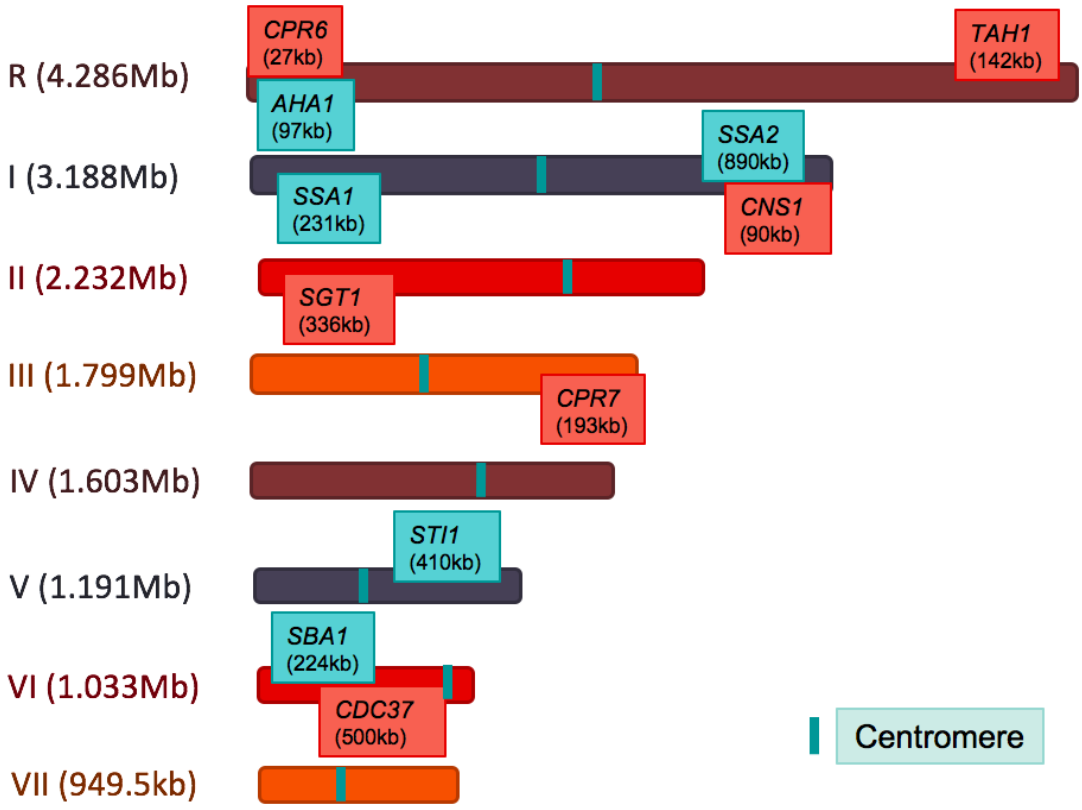

Figure 1.3 Diagram of *C. albicans* chromosomes drawn to scale, labelled with their names and sizes on the left, and positions of co-chaperone genes and centromeres marked on the chromosomes themselves, with distance to the telomere indicated in brackets. Null mutants were generated in this stufy for the co-chaperones shown in blue. The Hsp90 co-chaperone genes are generally located in telomeric regions.

Previous research showed that depleting the co-chaperone Sgt1 in *C. albicans* reduced resistance to azoles and echinocandins [108], implying promise for the rest of the Hsp90 co-chaperones. Yet, Sgt1 is an essential protein and thus not fitting for a project employing the principles of evolutionary medicine.

Conservation of Hsp90 between humans and yeasts is a problem which largely precludes its employment as a drug target. Co-chaperones are less conserved, although conservation for them remains consistent throughout eukaryotes, and evolutionary evidence suggests non-conserved co-chaperones were selectively lost rather than gained [109].

Five co-chaperones were selected for this study to be investigated for their roles in *C. albicans* virulence. All of them were believed to be encoded by non-essential genes, based on generation of mutants in *Saccharomyces cerevisiae.* The aim here was to identify co-chaperones which are essential for virulence, but not required for growth to comply with the principles of evolutionary medicine.

Ssa1 and Ssa2 bind indirectly the C-terminal domain of Hsp90 and are considered to be orthologues of the human Hsp70 family of proteins (Fig. 1.3) [23, 110]. Sti1 is the mediator which binds both the C-terminal domain of Hsp90 and the C-terminal domain of the Hsp70 orthologues; Ssa1 and Ssa2 [111, 112]. Ssa1 and Ssa2 are relevant to this study because of their implication in invasion of host cells [113] and survival of heat shock [114]. Furthermore, their protein levels are increased in biofilm growth, but gene

expression is decreased, so protein translation or protein stability may be disassociated from gene expression levels [115]. The two are very similar to one another, with 85.8% identity in the gene sequences, and 87.2% similarity in their protein sequences [116], which suggests they are alike in structure and function.

The Ssa1 and Ssa2 proteins have been found to be responsible for binding the antimicrobial compound in human saliva, histatin 5 and null mutants of both genes in *Saccharomyces cerevisiae* are resistant to its effects [117]. However, Ssa1 has also been found to mediate invasion of host cells and is therefore instrumental in *C. albicans* virulence [118].

The Sba1 protein has low sequence identity of 23% with the human orthologue, p23 [116] and is induced in the stress response to heavy metals, and protein levels decline in stationary phase growth [119]. Sba1 may have a role in aging as it is implicated in telomere maintenance in *C. albicans* and *S. cerevisiae* null mutants for *SBA1* have been shown to have shorter telomeres [72, 120]. Sba1 binds the N-terminal domain of Hsp90 and of the co-chaperones present in both *C. albicans* and humans, Sba1 has the lowest protein sequence identity [97].

Aha1; “Activator of Hsp90 ATPase”, acts as its name suggests and induces Hsp90 ATPase activity through binding the middle domain and the N-terminal domain of Hsp90. Aha1 has 26.7% protein sequence identity with its human orthologue and is the only known co-chaperone which binds the middle

domain of Hsp90 in *C. albicans* [116]. Depleting Aha1 results in decreased client protein activation, suggesting that Aha1 is responsible for activation, rather than stability [121]. Aha1 is known to be induced by oxidative stress and by heavy metal stress, and to be expressed at higher levels in biofilms relative to planktonic growth in *C. albicans* [15, 115, 122].

The binding sites for Sba1 and Aha1 are overlapping on the N-terminal domain of Hsp90, but Aha1 also binds the middle domain [123], so they are not mutually exclusive components of the Hsp90 complex [121, 124].

Sti1 is also differently expressed in biofilms and is 36.5% conserved in protein sequence with its human orthologue, Hop1, which is the “Hsp70-Hsp90 organising protein” [116]. That Sti1 is not essential for viability shows there may be alternative mechanisms facilitating interaction between Hsp90 and Hsp70 (Ssa1/2). It was recently demonstrated that Hsp90 and Hsp70 do indeed interact directly, with Hsp70 binding a region on the middle domain of Hsp90 in the absence of Sti1 [125]. Disrupting the protein-protein interaction between Hop1 and Hsp90 has shown positive results in reducing growth in breast cancer cells [126].

Tah1 is the only fungal-specific co-chaperone in this group, making it perhaps the most desirable co-chaperone for future development as a drug target. *C. albicans* Tah1 is uncharacterised, and its orthologue in *S. cerevisiae*, Tah18, is known to be essential for viability [127]. In *S. cerevisiae* Tah1 regulates stress responses, including cell death following oxidative stress [128], and

nitric oxide production conferring resistance to high temperature stress [129]. The potential essentiality of Tah1 in *C. albicans* would make it an unsuitable drug target when adhering to the principles of Evolutionary medicine. However, as the only fungal-specific Hsp90 co-chaperone it is desirable to ascertain whether this is the case.

1.3 *C. albicans* virulence genes and their regulation

1.3.1 Heterochromatin and sub-telomeric gene silencing

Regulation of gene expression is required for adaptation to a changeable external environment. In eukaryotes, gene expression can be silenced by formation of heterochromatin, which makes the DNA inaccessible for transcription [130]. DNA in heterochromatin is bound around histones, which are the alkaline proteins key to nucleosome structure. When acetylated, histones are inactive and DNA is in the more open euchromatin structure, allowing for genes to become transcriptionally active [131, 132]. Deacetylation activates histones and triggers heterochromatin formation, thus silencing gene expression. Levels of histone acetylation vary constantly throughout the cell cycle, and so histone deacetylases such as the sirtuins and the Hst group

proteins can regulate gene expression by initiating gene silencing in telomeric regions of the genome [133].

Histone deacetylases are known to be involved in all stages of heterochromatin formation; in initiation, spreading, and maintenance of heterochromatin [134, 135]. Inhibition of histone deacetylase activity has been shown to interfere with heterochromatin in *S. cerevisiae*, thus disrupting regulation of gene expression [136].

1.3.2 Histone deacetylases as regulators of fungal virulence

The sub-telomeric locale of the co-chaperone genes implicates them in virulence because of gene regulation mechanisms in these regions [3, 107]. The sirtuins are a group of histone deacetylases responsible for transcriptional silencing by managing heterochromatin formation, and therefore regulation of gene expression in both humans and fungi [137]. The effects of the sirtuins are most potent in the telomeric regions of the chromosomes, implicating their function in regulation of virulence. The orthologues of the sirtuins in yeast explored in this study are the Hst proteins. This project aimed to develop an understanding of how Hst1 and Hst2 are involved in regulation of co-chaperone gene expression.

In *Candida albicans* the closest orthologue of the human Sirt2 (silent information regulator type 2) is Hst1 [116]. *C. albicans* expresses four sirtuin proteins; Sir2, Hst1, Hst2 and Hst3. Sir2 would seem to be the closest orthologue to the human Sirt2 based in their names, but is less conserved than the Hst proteins. Hst1 and Hst2 were selected for investigation into their role in regulating expression of Hsp90 co-chaperone genes in *C. albicans.* A null mutant for Hst3 could not be generated as it is essential for *C. albicans* viability and was therefore not investigated here [138].

C. albicans has a highly plastic genome, which, as a predominantly clonal fungus, helps in introduction of phenotypic variation [139]. There are mechanisms acting to maintain stability under normal conditions to suppress deleterious mutations [140]. However, mutation rates increase in response to environmental stresses as this increases population diversity and drives faster rates of evolution and thus adaptation to new environmental conditions [141]. Sir2 suppresses recombination activity in plastic sub-telomeric sequences to help maintain genome stability when environmental stress levels are low. When cells are stressed, this suppression is overridden to allow for a higher mutation rate in response [142].

Hst1 and Hst2 are non-essential components of the conserved Set3/Hos2 histone deacetylase complex. Hst1 and Hst2 have been shown to positively regulate white-opaque switching in *Candida albicans* and null mutants have a reduced ability to undergo phenotypic switching [143]. *C. albicans* exhibits a range of different phenotypes in cells with identical genomes, including what

are known as white and opaque cells. The two cell types differ in gene expression, cell morphology, and colony shape, and opaque cells are able to mate, whereas white cells are not. White-opaque switching is a well-studied trait of *C. albicans*, however, the ability to switch is only possessed by cells homozygous for the mating-type locus (*MTL*) and as the majority are heterozygous, they are unable to switch.

Histone deacetylases Hst1 and Hst2 regulate expression of genes in telomeric regions by forming heterochromatin to silence genes. They were selected for study here to investigate their role in regulation of Hsp90 co-chaperone gene expression and hence their potential role in regulation of virulence.

1.4 Investigating the roles of Hsp90 co-chaperones in *C. albicans* virulence traits – experimental approaches

1.4.1 *In vitro* assays to study the role of Hsp90 co-chaperones in fungal virulence

Here, the hypothesis is that Hsp90 co-chaperones govern virulence and that targeting co-chaperones that are not essential for growth but are required for virulence could abrogate Hsp90 function whilst avoiding host toxicity and reducing selective pressure for resistance. Applying the principles of evolutionary medicine; it is desirable to employ a drug target which inhibits the ability of the organism to cause disease, whilst leaving it unaffected in its commensal form [54]. This could discourage the emergence of drug resistance, making the drug more potent and available as an option for disease treatment in the long term, while also carrying the benefit of leaving the host microbiome unscathed by the treatment.

Exploring the potential of Hsp90 co-chaperones as candidates for development of novel therapeutic strategies to treat systemic *Candida spp.* infections and employing the principles of evolutionary medicine was the main aim of this project. Non-essential Hsp90 co-chaperones that regulate *C. albicans* virulence would be suitable candidates for this approach. Yet, *C.*

albicans Hsp90 co-chaperones are largely uncharacterised; little is known about their essentiality and even less about their roles in regulating virulence.

Homozygous null mutant strains for co-chaperone genes were generated from the SN95 background strain [144], referred to here as YSD89. The strain was originally a clinical isolate, SC5314 [145], but has been genetically modified to be auxotrophic for histidine and arginine, which is not the natural case in *C. albicans*. The auxotrophies are conferred by homozygous gene deletion of *HIS1* and *ARG4.*

Once two independent deletion mutants of the *SSA1, SSA2, SBA1, AHA1,* and *STI1* genes were generated, they were assessed for an essential role in four standard growth conditions. These were in rich media and in synthetic defined media at both 30°C and at the physiologically relevant temperature of 37°C. It is important to determine that targeting co-chaperones will not confer a growth defect, making the yeasts less competitive in the environment. The aim was to target cellular aspects that are only required in a virulence setting and will therefore abrogate their capacity to cause disease without impairing commensal populations.

Whilst growth in these two media formulations at the two temperatures would not necessarily be a true and accurate reflection of how the yeasts would grow in their natural environmental conditions, it can be used as an indication of whether a clear growth defect is conferred by the absence of the particular co-chaperone gene.

The impact of co-chaperones on *C. albicans* virulence was then quantified by comparing mutant strains to the wild type in a set of virulence assays. There were five *in vitro* virulence assays; resistance to oxidative stress, heat shock tolerance, drug resistance, morphogenesis, and biofilm formation.

1.4.2 A novel host model of infection

Manduca sexta are established as a model organism for *in vivo* testing of pesticides and bacterial infections [146-148], but the animals have never previously been used as a model for fungal infections. Work in the Diezmann laboratory has optimised their use for fungal infection studies. In accordance with principles of the NC3R [149], this could replace the use of vertebrates such as mice in some studies, thus reducing the number of mice used in laboratory experiments.

The University of Bath has been hosting a resident colony since 1978. This inbreeding colony is maintained by a dedicated technician who follows standard procedure in proliferating animals and preparing them for experiments. Due to their size and weight, *M. sexta* fifth instar larvae can be injected with a defined number of yeast cells. Larvae thrive at 37°C, which is physiologically relevant when carrying out studies of human pathogens. The *M. sexta* genome has recently been published [150], allowing future investigations into host determinants of fungal virulence.

In this study, *M. sexta* fifth instar larvae were infected with *C. albicans* co-chaperone mutants and the wild type strain. Virulence assays were controlled with saline. All animals were screened daily for death, and morbidity was quantified by measuring changes in body weight.

1.4.3 Regulation of co-chaperone genes

Expression of genes in telomeric regions is partly regulated by heterochromatin formation to induce silencing. The roles of histone deacetylases Hst1 and Hst2 on expression of Hsp90 co-chaperones was measured by quantitative real-time polymerase chain reaction (qRT-PCR). Expression of the five co-chaperones of interest was compared between the wild type strain and *hst1ΔΔ* and *hst2ΔΔ* mutants generated in this study.

1.5 Summary

Systemic candidiasis is a public health problem of growing importance due to limited treatment options and the spread of resistance to existing antifungal drugs.

Taking into account the evolutionary mechanisms involved in the emergence of resistance in response to the selective pressure exerted by fungicidal drugs, as well as the simplicity of targeting a pathogen with only one compound. This study aims to identify at least one potential drug target, required for virulence characteristics but not essential for viability in commensal growth, which could be employed for intelligent drug design. Targeting a component of the pathogen exclusive to virulence could subvert the spread of drug resistance.

Such a drug would be intended for use in combinatorial therapy, perhaps with an Hsp90 inhibitor, posing an additional challenge to the pathogen and further discouraging the evolution of resistance. Results presented here demonstrate that Hsp90 co-chaperone mutants exhibit comparable growth to the wild type strain as well as defects in virulence.

2. Materials and Methods

2.1 Strain Construction

Homozygous null mutants were generated for the genes of interest in order to confirm non-essentiality and to investigate their function. Strains were constructed by homologous recombination of a recyclable drug marker encoding resistance to nourseothricin (*NAT*) (a gift from Julia Köhler) using the lithium acetate protocol (Appx. 8.1) [151-153]. The *NAT* cassette is encoded on plasmid pSD3, which additionally encodes a *FLP* recombinase excision gene, expressed by metabolism of maltose. The cassette is then easily excised, resulting in a clean gene deletion. The *NAT* cassette was amplified with Q5 High-Fidelity DNA polymerase and 120-mer primers (Appx. 8.3). Primers correspond to 100 bp upstream and downstream flanking regions of the gene, with 20 bp oligonucleotides homologous to the plasmid encoding the *NAT* cassette. This reaction generated copies of the *NAT* cassette with 100-mer flanking regions homologous to the gene of interest. A total of at least 100 µL PCR product was generated for each transformation reaction. The protocol is optimised for *XmnI*-digested pSD3 plasmid (Table 2.1). Gene sequences were accessed on *candidagenome.org* and primers were designed using *primer3.ut.ee* to identify suitable sequences. Potential primers were searched using the BLAST tool on *candidagenome.org* to ensure that they were unique

sequences in the *C. albicans* genome. The reference genome applied was assembly 22 [154].

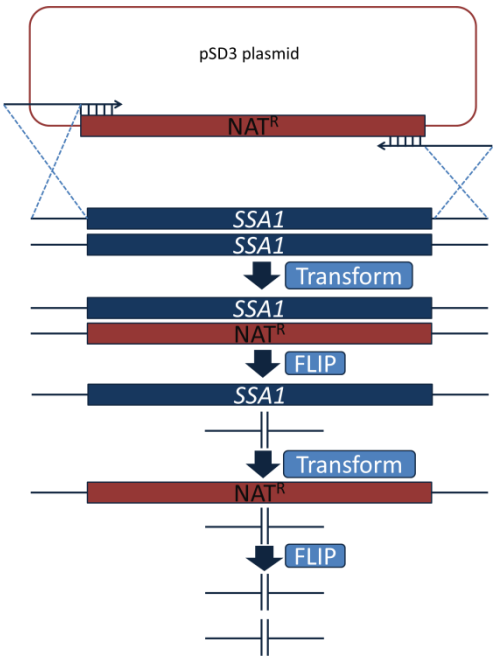

Figure 2.1 Gene deletion strategy using the recyclable *NAT* cassette. The *NAT* cassette was amplified from *XmnI*-digested pSD3 by Q5 PCR using 120-mer primers complementary to the flanking regions of the gene, *SSA1* in this example, with an oligonucleotide region complementary to the *NAT* cassette. As *C. albicans* is an obligate diploid, two rounds of transformation are required to delete both alleles of the wild type gene. The *NAT* cassette is flipped out following each successful transformation reaction, as confirmed by colony PCR, resulting in a complete deletion of both alleles of the wild type gene.

For some genes; *SBA1, AHA1,* and *STI1*, the same 100mer flanking regions were amplified for transformation of both allele deletions. Whereas for others; *SSA1, SSA2, HST1* and *HST2*, a third long primer was used, located outside of the rest, to improve transformation efficiency in removal of the second allele (Fig. 2.2). The result was that one of the long sequences of homology for the second allele deletion was no longer present, precluding the *NAT* cassette from transforming back into the empty locus and thus improving transformation

efficiency. Sequences were checked in design of the third long primer to avoid any disruption of neighbouring alleles.

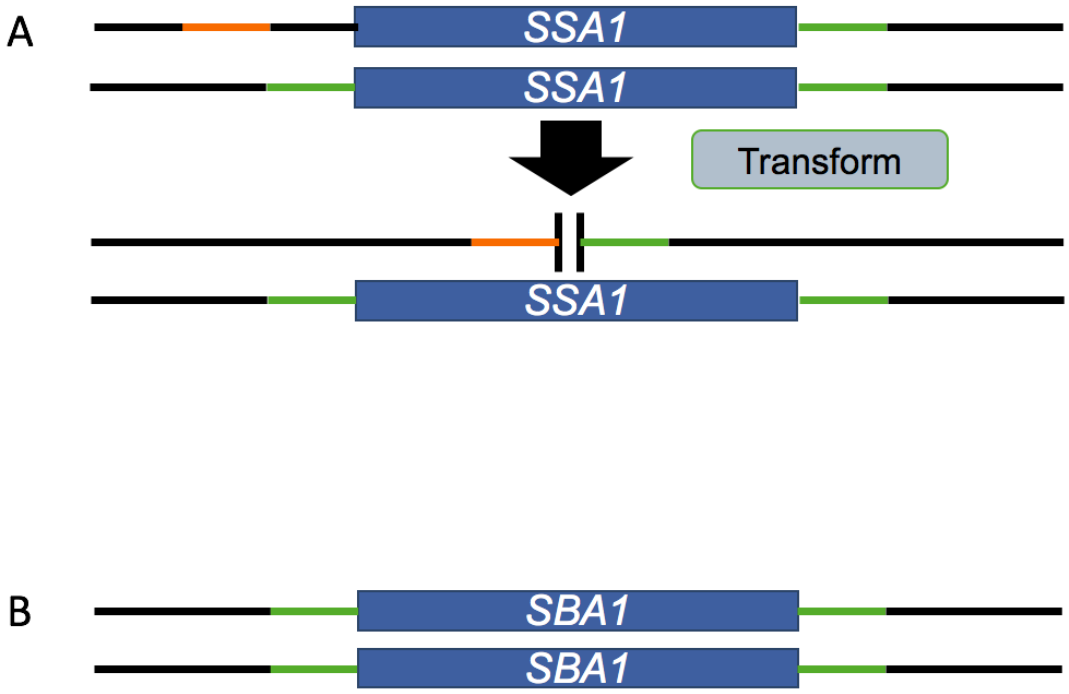

Figure 2.2 A. For some genes, the first allele was transformed using a third long primer further from the native gene, shown in orange. B. For other genes, the same long primers were used for transformation of both alleles.

Successful PCR products, identified by agarose gel electrophoresis, were then purified by ethanol precipitation. To do so, 100 µL PCR product was combined in one 1.5 mL Eppendorf tube. A volume of 10 µL sodium acetate pH 5.2 was added and the tube was inverted twice to mix. Then 220 µL ice cold 100%

ethanol was added and the tube was inverted 5 times to mix and the product was incubated at -20˚C for 30 minutes before being centrifuged at maximum speed for 10 minutes at room temperature. The supernatant was removed and the pellet washed with 70% ethanol. The tube was blotted dry on paper and centrifuged for 30 seconds before the remaining liquid was removed. The pellet was air-dried for 20 minutes to ensure total ethanol evaporation and dissolved in sterile distilled water and stored at 4˚C for up to 2 days prior to transformation.

Table 2.1 PCR reagents and programme for *NAT* cassette amplification; recipe for one 50 µL reaction.

PCR REAGENT	VOLUME (µL)	PCR PROGRAMME	
Water	36.1	98°C 2 min	
5x buffer	10	98°C 30 s	30 cycles
25 mM dNTPs	0.4	55°C 30 s	
100 µM primer (each)	0.25	72°C 3:30 m	
0.1 ng μL^{-1} pSD3	2	72°C 2 min	
Q5 Taq polymerase	1		

To determine purity and concentration of the DNA used for the transformation reaction, the purified PCR product was run on 1% agarose gel dissolved in 1x TAE buffer (40 mM Tris, 20 mM acetic acid, 1 mM EDTA), mixed with SYBR Safe® 10,000x dye. The DNA was separated at 100 V. All PCR products were screened under these conditions prior to use.

In preparation for DNA transformation, *C. albicans* strains were cultured for 16 hours in 10 mL YPD (2% yeast, 1% peptone, 2% dextrose) to a target OD_{600} reading of between 4 and 8. To attain this level of growth, a 1 µL sterile inoculation loop was used to collect a small pellet of cells from a YPD-agar plate to inoculate 10 mL broth. This was then diluted to 1:200 in a fresh tube of broth before incubation at 30°C with 200 rpm orbital shaking. For deleting the first allele of the gene, the wild type strain YSD89 would be transformed. The overnight cultures were diluted 1:10 in water and the OD_{600} was measured. Cultures ranging between OD_{600} 4-8 were then used for transformation. The following formula was employed to standardise the number of yeast cells in each reaction:

$$10/(OD_{600}*1.5) = \text{mL culture per transformation reaction}$$

Cells were washed once with 1mL sterile water and centrifuged for 7 seconds. A volume of 800 µL sterile filtered 50% polyethylene glycol (PEG) 3350 was added to the tube, followed by 260 µL transformation master mix and 50 µL ethanol purified PCR product. The transformation master mix consisted of 100

µL 10x TE, 100 µL 1 M lithium acetate pH 7.4, 40 µL 5 mg mL^{-1} salmon sperm DNA (boiled for 5 minutes and kept on ice), and 20 µL 1 M DTT (dithiothreitol).

Each transformation reaction was incubated in a water bath at 30˚C for 1 hour, before being transferred carefully to 42˚C for 45 minutes; this time was reduced to 30 minutes if the strain was known to be heat-sensitive. The cells were then centrifuged for 8 seconds and the transformation mix was removed. As the *NAT* cassette needs to be expressed prior to exposure to the drug in order to confer resistance, cells were incubated for 4-6 hours in 600 µL YPD at 30˚C 200 rpm, before being plated onto YPD plates containing nourseothricin at a final concentration of 150 µg mL^{-1}, (YPD-NAT). The whole 600 µL volume was plated out and spread as gently as possible. The plates were left to dry before being incubated at 30˚C for three days, when colonies were re-streaked onto fresh YPD-NAT plates.

Table 2.2 PCR reagents and programme for colony genotyping.

PCR REAGENT	VOLUME (µL)	PCR PROGRAMME	
2x master mix	7.5	94°C 5 m	
100 µM Primer (each)	0.1	94°C 30 s	
Water	7.3	53°C 45 s	30 cycles
Colony cells	n/a	72°C 1 m	
		72°C 10 min	

Presence of the *NAT* cassette is detected as well as integration into the proper location by colony PCR (Table 2.2). After deletion of the first allele, potential positive transformants were tested for the presence of the *NAT* cassette. Cells were sampled directly from the transformation plate into the PCR mix. A section of the flanking yeast DNA, overlapping into the *NAT* cassette was amplified, both upstream and downstream of the integrated drug marker. This involved two separate reactions for each colony to detect correct up- and downstream integration (Appx. 8.3). Primers were designed to produce an expected PCR product of ~500 bp in each case.

Once a yeast colony had been identified containing the *NAT* cassette in the appropriate location, the *NAT* marker was excised. Expression of the excision gene on the *NAT* cassette is induced by growth in yeast nitrogen base, with bovine serum albumin and maltose (YNB-BSA-MAL). Cells from the NAT^R colony were inoculated into 5 mL YNB-BSA-MAL and incubated for 2 days at 30˚C while shaking at 200 rpm. This culture was then diluted 1:10,000 in YPD broth and a further 1.6 µL was diluted into 200 µL YPD broth. Of this, 150 µL was plated onto YPD agar and incubated for two days at 30˚C. After incubation, the plate was replicated onto both YPD and YPD + 150 µg mL^{-1} *NAT* agar plates, which were then incubated for two days at 30˚C. Comparison between the two replica plates was then used to identify NAT^S colonies.

Following excision of the *NAT* cassette, it was possible to repeat this method using the same transformation marker for deletion of the second allele. Colonies were then tested for absence of the wild type gene (Table 2.2, Appx.

8.3), involving amplification of ~500 bp of the wild type gene and screening for a negative result. Cells of the wild type strain, YSD89, were used as a positive control for this reaction. Colonies found to be lacking the wild type allele were then tested for upstream and downstream integration of the *NAT* cassette, as above. Once successful deletion of both wild type alleles was ascertained, the *NAT* cassette was once again excised by growth in YNB-BSA-MAL and the gene deletion was complete and the strain prepared for archiving at -80˚C.

In preparation for cryogenic storage, gene deletion mutants were grown overnight in YPD at 30˚C with 200 rpm. The resulting culture was diluted 1:1 in 50% glycerol, giving a final concentration of 25% glycerol, and frozen at -80˚C. Ideally, two independent transformants were generated for each mutation. Two NAT^S colonies were frozen down for each positive transformant, as well as the NAT^R transformant still containing the *NAT* cassette but with the wild type allele removed.

2.2 Co-chaperone Mutant Characterisation

2.2.1 Growth Curve Analysis

Characterising the mutants first involved comparing their growth to that of the wild type strain YSD89 to assess whether mutants had growth defects. Two independent transformants for each gene deletion were tested in a 96-well plate-reader assay in four different conditions; enriched media (YPD) and synthetic defined media (yeast nitrogen base, 2% glucose) at 30˚C and at 37˚C. Strains were grown overnight in the relevant media at 30˚C with 200 rpm orbital shaking for 12-16 hours, cultures were then diluted 1:50 in water and the OD_{600} measured. The OD_{600} was adjusted to 0.05 in fresh media and 96-well plates inoculated; 8 wells were inoculated for each strain as technical replicates and cultures were measured at OD_{595} every 30 minutes throughout the 24-hour assay. Three biological replicates were carried out for each condition. Data were analysed in *R 3.4.1 GUI 1.70 El Capitan build*® using the *Growthcurver* package to obtain and compare growth metrics by ANOVA; maximum carrying capacity, shortest doubling time, and growth rate [155].

2.3 *In vitro* Virulence Assays

2.3.1 Oxidative Stress Resistance

The oxidative stress resistance assay is used to assess whether mutant strains are impaired in their ability to resist the stress induced by the oxidative burst mechanism of the host innate immune system. Cells were grown overnight in YPD at 30˚C with 200 rpm orbital shaking for 12-16 hours and their OD_{600} measured. The culture was adjusted to OD_{600} 0.2 in 10 mL YPD broth and cells were incubated for 3 hours at 30˚C with 200 rpm orbital shaking, until they proliferated to reach OD_{600} between 0.6-0.8, indicative of mid-log phase growth. Using the OD_{600} value and data from a previously plotted standard curve (data not shown), each strain was diluted to 20,000 cfu mL^{-1} in 1x phosphate-buffered saline (PBS) and divided into 2 tubes of 5 mL each. A dilution of 1:10 was made of this inoculum and 100 µL plated onto YPD agar to demonstrate pre-treatment colony growth.

A final concentration of 1 mM hydrogen peroxide was added to one 5 mL culture of each strain, with the second tube serving as no-treatment control. Concentration of hydrogen peroxide was determined by measurements of OD_{240} in quartz cuvette and solving the Beer-Lambert equation with a molar extinction coefficient of 43.6.

Tubes were incubated at 37˚C with 200 rpm orbital shaking for 1 hour. The cultures were diluted 1:10 in 1x PBS before 100 µL was plated onto YPD agar with 5 technical replicates and incubated at 30˚C for 2 days. Colonies were counted to measure the percentage survival of cells exposed to hydrogen peroxide compared to the untreated controls. This experiment was repeated for a total of 3 biological replicates for each mutant strain and data were analysed in *R 3.4.1 GUI 1.70 El Capitan build*® using a mixed linear model and plotted as univariate scatter plots. The univariate scatter plots display every data point measured, as well as the mean and standard deviation values. The mixed linear model compares the rate of survival of the wild type strain; the ratio of cfu with to without exposure to hydrogen peroxide, to the rate of survival of each other strain. Effectively, fold change is compared, with biological repeats treated as random variation nested within date.

2.3.2 Heat Shock Tolerance

The heat shock tolerance assay measures the ability of *C. albicans* strains to adapt to conditions in the host, particularly when the host exhibits fever as a result of the infection. Cells were grown overnight in YPD at 30˚C with 200 rpm orbital shaking for 12-16 hours and their OD_{600} measured. A *tetOff-HSP90/hsp90Δ* mutant was used as the negative control strain in this experiment as it has been shown to be impaired in its response to heat shock; the expression of Hsp90 is repressed by addition of doxycycline to the culture

[24, 156]. However, this strain grows more slowly than the other strains assayed, and so was grown in YPD enriched with nutrient broth to keep the growth rate consistent. The cultures were adjusted to OD_{600} 0.2 in 10 mL YPD broth and cells were incubated for 3 hours, until they proliferated to reach OD_{600} between 0.6-0.8, indicative of mid-log phase growth. For this step, 20 µg mL^{-1} doxycycline was added to the negative control strain *tetO-HSP90/hsp90Δ* to deplete Hsp90 levels. Meanwhile, YPD broth was warmed to 54˚C in a water bath and 100 mL conical flasks were warmed to 42˚C in an incubator.

Prior to heat shock, cultures were diluted to 10^{-4} in 1x PBS and 100 µL was plated onto YPD agar with 5 technical replicates. The 10 mL culture was then mixed with 10 mL of the pre-heated YPD broth in 100 mL conical flasks to induce heat shock and incubated at 42˚C for 2 hours with 200 rpm orbital shaking. For the negative control strain, 20 µg mL^{-1} doxycycline was again added to the pre-heated broth to maintain repression of *HSP90*.

The cultures were then diluted to 10^{-4} in sterile 1x PBS and 200 µL was plated onto YPD agar with 5 technical replicates and incubated at 30˚C for 2 days. Colonies were counted to measure the growth success of cells exposed to heat shock compared to the cultures plated before treatment. This experiment was repeated for a total of 3 biological replicates for each mutant strain and data were analysed in *R 3.4.1 GUI 1.70 El Capitan build*® using a mixed linear model and plotted as univariate scatter plots. The univariate scatter plots display every data point measured, as well as the mean and standard

deviation values. The mixed linear model compares the rate of growth of the wild type strain; the ratio of cfu before to after subjection to heat shock, to the rate of growth of each other strain. Effectively, fold change is compared, with biological repeats treated as random variation nested within date.

2.3.3 Colony Morphology on Solid Growth Media

Colony morphology of the different strains was compared on 6 different solid media formulations; YPD agar, Spider agar, RPMI agar, Sabouraud dextrose (SD) agar with Calcofluor White, SD agar with Congo Red, and Lee's medium (Appx. 8.4). Agar was poured into rectangular omniplates and inoculated using liquid cultures grown in YPD in 96-well plates in a defined layout. A 96-well microplate replicator was used to inoculate the agar plates and replicate the layout from the 96-well plates. The replicator was washed twice with water and ethanol and sterilised by flaming following each inoculation.

Inoculated plates were incubated inverted and static at 37°C for 5 days, while wrapped in aluminium foil to minimise desiccation. Colony morphology was scored according to appearance on the plates (Table 2.3) and compared visually between strains.

Table 2.3 Colony morphology scoring scheme.

MEDIUM	MORPHOLOGY SCORES
YPD	1. Punctiform colonies 2. Less vigorous growth 3. Butyrous, entire colonies
Spider	1. Glabrous colonies, little or no halo 2. Glabrous centre with filiform halo 3. Wrinkled centre with filiform halo 4. Robust wrinkles, little or no halo
RPMI	1. Dry, rough, entire colonies 2. Dry, rough, semi-filiform colonies 3. Dry, rough, filiform colonies
SD + Calcofluor White	1. Glabrous, entire colonies 2. Rough, entire colonies 3. Wrinkly, undulate colonies 4. Robust wrinkles on undulate colonies
SD + Congo Red	1. Glabrous centre with wrinkled halo 2. Wrinkled centre and halo 3. Large, undulate colonies with robust wrinkles
Lee's	1. Dry, entire colonies with robust wrinkles 2. Dry, undulate colonies with elevated wrinkles

2.3.4 Biofilm Formation

Biofilm formation is a potent virulence trait, which affords invasive cell communities protection from drugs and the host immune response, as well as providing a reservoir of cells to seed the infection. Biofilm formation was quantified using the XTT assay, which measures biofilm metabolic activity [157].

For the assay, flat-bottomed 96-well plates were primed with 100 µL bovine serum in each experimental well, with 200 µL 1x PBS pipetted into outermost wells to maintain humidity. The plates were then incubated at 37˚C static overnight. Meanwhile *C. albicans* strains were inoculated into 10 mL YPD and incubated at 30˚C with 200 rpm orbital shaking for 12-16 hours.

On the second day, the yeast cultures were adjusted to OD_{600} 0.5 in Roswell Park Memorial Institute medium (RPMI) 1640 broth (2% maltose, 2% glucose) pH7. The 96-well plate experimental wells were washed once with sterile 1x PBS and filled with 100 µL of the adjusted cultures, with 8 technical replicates of each. Following adhesion at 37˚C static for 90 minutes, the cell suspension was removed by vacuum suction and replaced with fresh RMPI broth. The plates were incubated for 24 hours static at 37˚C, after which mature biofilms were washed 3 times with sterile 1x PBS.

Solutions of XTT and menadione for addition after incubation were prepared in advance and stored in frozen aliquots. XTT (2,3-Bis-(2-Methoxy-4-Nitro-5-

Sulfophenyl)-2H-Tetrazolium-5-Carboxanilide) was diluted to a final concentration of 0.5 mg mL^{-1} in 1x PBS and centrifuged at 3000 rpm for 5 minutes. The supernatant was stored -20°C in 10 mL aliquots. One aliquot was thawed without light exposure for each 96-well plate and 5 µL 10 mM menadione was added immediately before use. Menadione was diluted in ethanol and stored at -80°C in 1 mL aliquots in amber tubes to avoid light exposure.

Of the XTT menadione solution, 100 µL was added to each experimental well and plates incubated for 5 minutes at 37˚C static. Finally, each well was measured at OD_{492} and compared to the wild type YSD89 and the negative control strain *bcr1Δ/Δ* [158]. This experiment was repeated for a total of 3 biological replicates for each mutant strain. The values were plotted as univariate dotplots and compared in *R 3.4.1 GUI 1.70 El Capitan build*® using a mixed linear model and ANOVA. The mixed linear model in this case compared the spread of the values for the wild type with the spread for each other strain. Pairwise comparisons were also conducted to measure differences within mutant pairs.

2.3.5 Antifungal Drug Resistance

Antifungal drug resistance is a growing problem for treatment of systemic fungal infections, and Hsp90 function is considered to be instrumental in conferring this trait [24, 35]. Growth in the presence of fluconazole (FL) at a range of concentrations was measured by optical density in a 96-well plate assay to determine the minimum inhibitory concentration. Cultures were grown overnight in 10 mL YPD broth at 30˚C with 200 rpm orbital shaking for 12-16 hours. Cultures were then adjusted to OD_{600} 0.2 in 5 mL YPD broth for the plate inoculum. Each well was filled with 100 µL YPD broth, except for the right-hand column of wells, in which 180 µL was dispensed. To the 8 wells in the right-hand column, 20 µL fluconazole at a final concentration of 5.12 mg mL^{-1} was added and mixed. From these wells 100 µL of YPD broth with fluconazole was added to the wells in column 11, and so on to serially dilute the drug 1:2 in columns 2-12. The remaining 100 µL of media was then discarded and the wells in column 1 kept drug-free as a positive growth control. This left the wells with a range of concentrations of fluconazole in YPD from 0 µg mL^{-1} to 256 µg mL^{-1}. Inocula were dispensed as follows: 100 µL in each well, with each well in duplicate and the plate was incubated 30˚C static for 48 hours, after which the plate was mixed horizontally and the OD_{600} was measured.

The aim of this experiment was to assess the effect of Hsp90 inhibition on resistance to fluconazole, and so it was repeated with the addition of Hsp90

inhibitors. The assay was carried out with fluconazole alone, with 5 µM geldanamycin in each well in addition to the fluconazole gradient, and again with 5 µM radicicol as well as fluconazole.

Data were normalised for each strain so that the well with no drug was given a growth value of 1. The data were visualised as heat maps using *Java TreeView*® and analysed to compare mutant and wild type strains resistance levels.

2.3.6 Hyphal Morphogenesis

The change in phenotype from yeast to hyphal growth is intrinsic to systemic *C. albicans* infections. Hyphal formation was induced and quantified using Frank Odds' morphology index [159]. Cells were grown overnight in 10 mL YPD broth at 30˚C with 200 rpm orbital shaking for 12-16 hours. Cultures were then adjusted to OD_{600} 0.2 and incubated with shaking for a further 3 hours, until they reached OD_{600} 0.6-0.8. Bovine serum was then added to the cultures to a final concentration of 10% v/v and tubes were incubated once more at, this time at 37˚C with 200 rpm orbital shaking for 90 minutes. Cells were then pipetted onto slides and imaged using a *Nikon i90* microscope. Images were captured using *NIS Elements*® imaging software from multiple fields of view at 40x magnification. For each strain, 100 daughter cells were selected at random and measured using *ImageJ* software. For each cell, measurements

were taken of the width of the septum, the width of the hypha at the widest point, and the full length of the hypha. Morphology index values were determined using the formula [159]:

$$\text{Length} * \text{Septum} / \text{Maximum diameter}^2 = \text{Morphology index value}$$

These values were plotted as boxplots and compared in *R 3.4.1 GUI 1.70 El Capitan build*® using a mixed linear model and ANOVA. The mixed linear model in this case compared the spread of the values for the wild type with the spread for each other strain.

2.4 *In vivo* Virulence Assays using *Manduca sexta* larvae

Manduca sexta fifth instar larvae were employed as a fungal infection model for measurement of the capacity of strains to cause disease and kill an invertebrate host [160]. The animals are grown as part of the University of Bath research colony, which has been established and inbreeding since the 1980s, meaning that the individuals are almost genetically identical. This work is covered under *Defra* licence number 53020/198973.

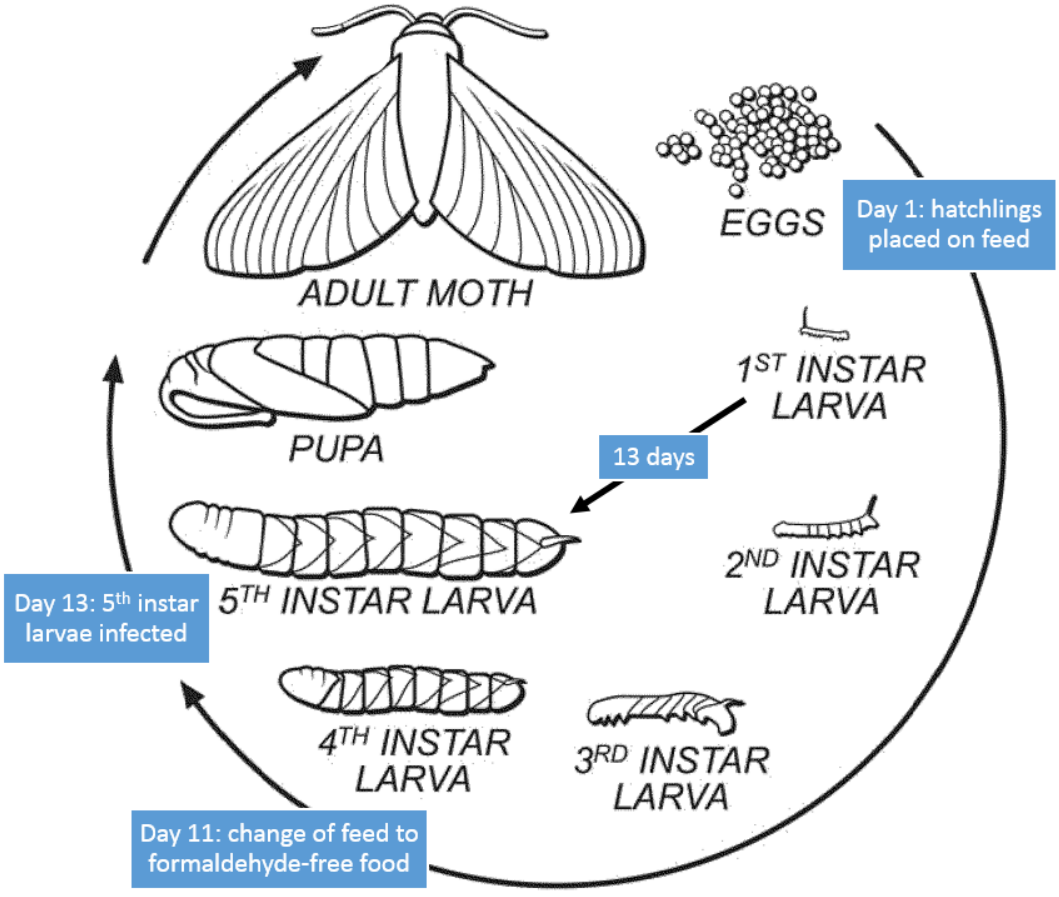

Figure 2.3 The life cycle of *Manduca sexta* [161] annotated with key points in the timeline when used as a model of infection.

Animals were infected 13 days after hatching (Fig. 2.3) and fed on solid cakes containing a mix of nutrients, agar, and antimicrobial additives (Appx. 8.5). For 3 days prior to infection the animals were placed on formaldehyde-free food, to ensure absence of antifungals in their system.

Yeast cells were washed 3 times in sterile 1x PBS and quantified by haemocytometer counting. Cell number was adjusted to 10^7 cells mL^{-1} in 1x PBS and the cell suspension injected into the rear right proleg of the caterpillars. *BD Microlance*™ 0.3 mm * 13 mm needles, and *Terumo*™ 1 mL syringes were used for injection. The dose was 100 µL of cell suspension, equating to 10^6 yeast cells per animal. Injections of 1x PBS only were administered to the control animals.

The caterpillars were then incubated at the physiologically relevant temperature of 37˚C for 4 days and screened every 24h for dead individuals and weight of surviving animals. Death was plotted in Kaplan-Meier and weights were plotted in *R 3.4.1 GUI 1.70 El Capitan build*® as univariate scatter plots. Data were analysed using the Kaplan-Meier estimator and hazard ratio test [162, 163].

2.5 Quantitative real time PCR

Expression of co-chaperone genes of cells in log-phase growth was measured in homozygous null mutants for histone deacetylase genes *HST1* and *HST2* as well as in wild type strain YSD89 using quantitative real-time polymerase chain reactions (qRT-PCR).

Cells were prepared for RNA extraction by overnight growth in YPD at 30°C with 200 rpm orbital shaking, before being adjusted to OD_{600} 0.2 and incubated again until they reached mid-log growth; OD_{600} 0.6-0.8. The concentration of cells in the culture was then calculated and $5*10^7$ cells were harvested, washed in sterile distilled water, and pellets were frozen at -80°C overnight.

RNA was extracted using the Qiagen RNeasy mini kit including DNase digestion. Following extraction, RNA quantity and purity was determined by A260/A280 readings and then used to synthesise cDNA using the Agilent AffinityScript cDNA synthesis kit. A quantity of 250 ng-300 ng RNA was used per cDNA synthesis reaction, depending on yield from extraction. All samples were diluted to the same RNA concentration prior to cDNA synthesis.

The resulting cDNA was used for qRT-PCR (Table 2.5, Appx. 8.6). Double-stranded DNA was detected in the reactions with the aid of 10 µL SYBR Fast

Green dye per reaction. The housekeeping gene *GPD1* was employed as the calibrator.

Table 2.5 Reagents and programme for qRT-PCR.

PCR REAGENT	VOLUME (µL)	PCR PROGRAMME	
2x SYBR Green Fast	10	95°C 20 sec	
Fwd primer 10 µM	0.4	95°C 3 sec	40 cycles
Rev primer 10 µM	0.4	60°C 30 sec	
Water	5.2	Melt curve	
cDNA 2.5 ng μL^{-1}	4		

Data were analysed in *R 3.4.1 GUI 1.70 El Capitan build*® by ΔC_T to compare co-chaperone gene expression in mutant strains and the wild type strain [164].

3. Generation of homozygous null mutants for Hsp90 co-chaperones and assessment of growth

3.1 Strain construction

Homozygous gene deletion mutants for Hsp90 co-chaperones were generated from the wild type strain, YSD89 [144], in order to ascertain that they were not essential for viability and to elucidate the roles of those genes in virulence. Using the lithium acetate method [151] coupled with the recyclable nourseothricin (*NAT*) cassette [153] allowed for the drug resistance marker to be excised by *FLP* expression [152]; resulting in complete allele deletion and allowing for the marker to be used again. Having a recyclable marker was particularly useful in this case as *C. albicans* is an obligate diploid and so each gene deletion involved two rounds of transformation.

3.1.1 Successful deletion of five co-chaperone genes yielding strains for further characterisation

Following PCR amplification of the *NAT* cassette from plasmid pSD3 (a kind gift from Julia Köhler), agarose gel electrophoresis was used to confirm amplification and purity of the cassette, which reliably produced a single bright band. For all transformations, the *NAT* cassette was amplified with 100 bp flanking regions complementary to the native DNA (Appx. 8.3). The sample of amplified cassette was always run alongside a negative control, with no DNA added, to additionally ensure there was no contamination of other genetic material in the reagents. The remaining PCR product of approximately 100 µL was used for the transformation reaction.

Upon completion of the transformation reaction, cells suspensions were spread onto selective media, containing 150 µg mL^{-1} nourseothricin. This means that only nourseothricin resistant colonies were able to grow on the plates, but does not screen for integration site of the cassette. Colonies resistant to nourseothricin were tested for correct integration of the *NAT* cassette by colony PCR.

Colony PCR was used to screen the site of integration of the *NAT* cassette, both upstream and downstream following the first round of transformation, when the first wild type allele was deleted (Fig. 3.1, Fig. 3.3, Appx. 8.3). Unfortunately, this meant that there was no positive control reaction, but a reaction mixture with no cells included was used as a negative control.

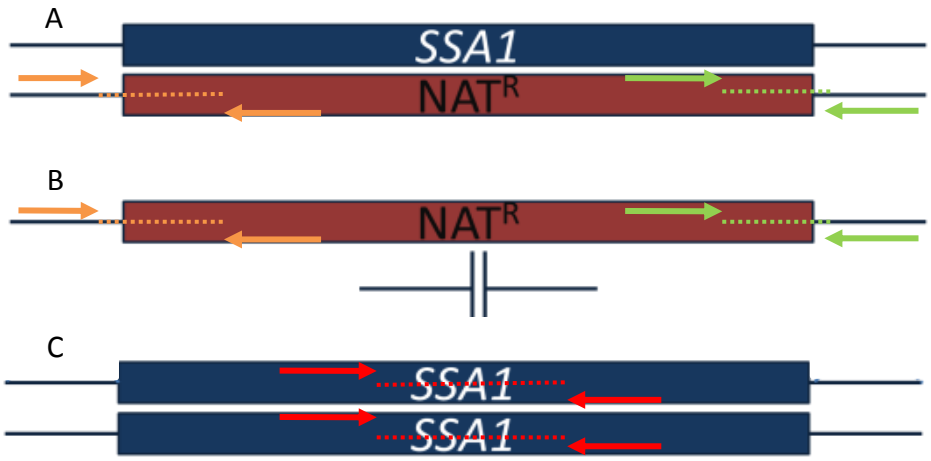

Figure 3.1 Diagram showing sites screened for correct integration of the *NAT* cassette [A and B] and for absence of the wild type allele [C]. Correct integration of the *NAT* cassette was ascertained by amplification of ~500 bp of the junction where the ends of the insert meet the native DNA, shown in orange and green. This was used in both rounds of transformation. Amplification of a ~500 bp fragment in the middle of the gene to ascertain absence of the wild type allele was used only after the second round of transformation; absence of amplification indicated success, shown in red. *SSA1* is used as an example of a native gene here, but the same method was used for screening of all gene deletions.

After the second round of transformation, it was hoped that both alleles of the wild type gene would have been deleted. However, as well as this being quite a low-efficiency reaction, it was possible in some cases for the *NAT* cassette to reintegrate at the site of the first allele. This would leave the remaining wild type allele intact in the genome, so absence of the wild type allele was also screened for by colony PCR (Fig. 3.1, Fig. 3.3, Fig. 3.4, Appx. 8.3). In this case, the wild type strain was used in a positive control reaction, and a reaction mixture without cells was used as a negative control. It was important to have

a positive control for these reactions when screening for negative results. Absence of wild type colony PCR was always repeated to confirm the result was not a false negative due to a failed reaction.

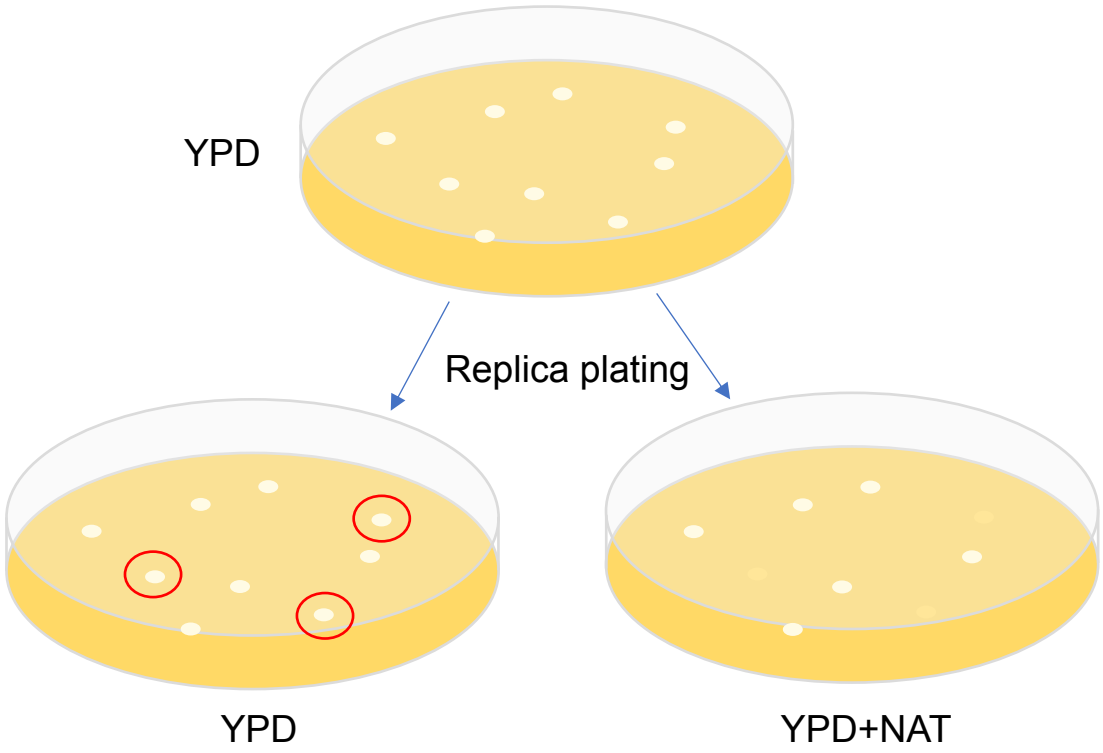

Figure 3.2 Diagram showing identification of nourseothricin-sensitive colonies following “flipping”. When colonies are replicated onto YPD and YPD+NAT in parallel, colonies which grow only in the absence of nourseothricin are sensitive to the drug and have therefore successfully excised the drug selectable marker. Nourseothricin-sensitive colonies are circled in red.

The use of a third long primer in first allelic deletions of *SSA1* and *SSA2* precluded reintegration of the *NAT* cassette at the site of the empty locus in the subsequent round of transformation (Fig. 3.3). Each round of gene deletion was followed by “flipping” out of the *NAT* cassette to complete the homozygous clean gene deletion.

SSA1

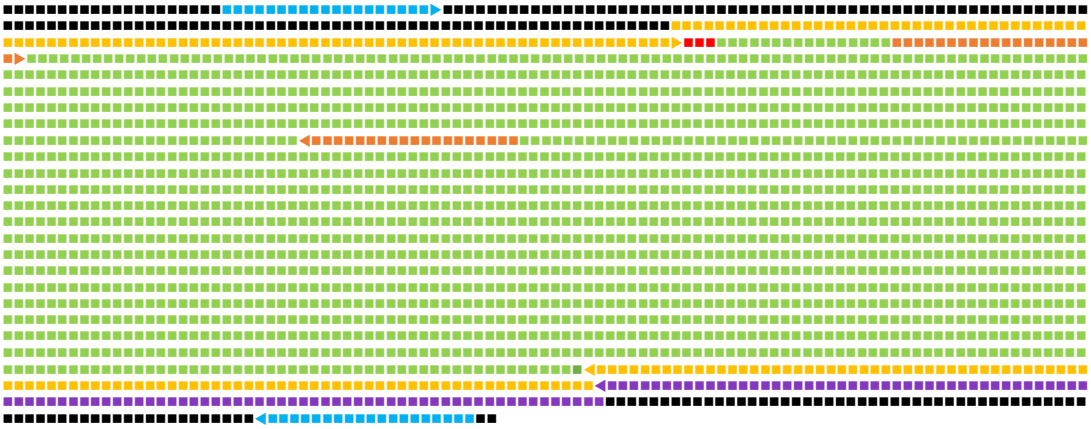

SSA2

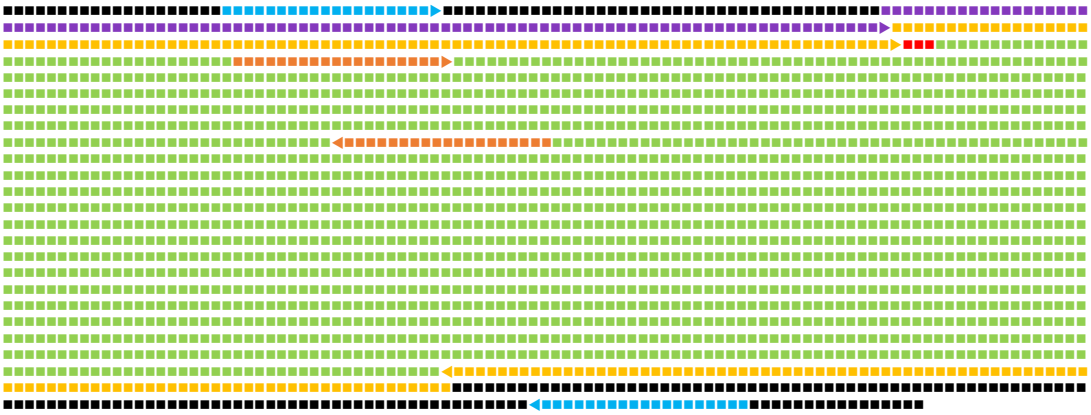

SBA1

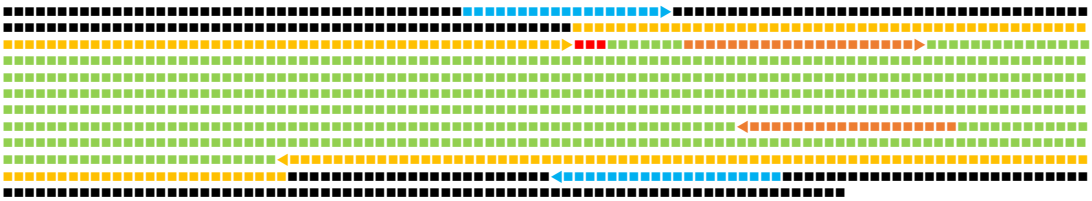

Figure 3.3 Locations of primers used for transformation and genotyping shown within native gene sequences. Figure continues with legend on following page.

AHA1

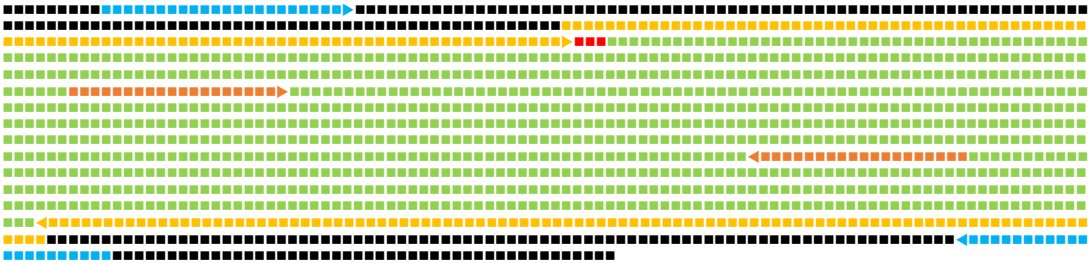

STI1

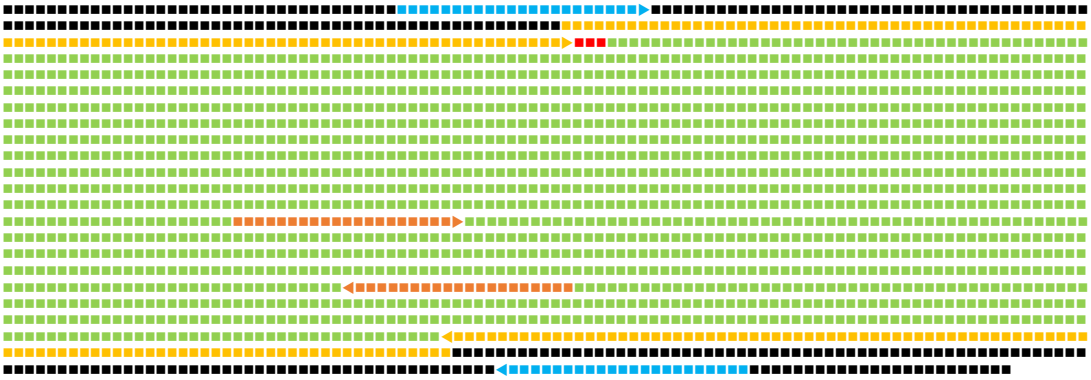

Figure 3.3 Locations of primers used for transformation shown within native gene sequences. Each character denotes a base pair, with colour coding: genes (■), start codons (■), primers of 100-mer flanking regions used for transformation (■), with the third long primer used in first allele deletion for *SSA1* and *SSA2* (■). Short primers were used in genotyping to confirm correct integration of the *NAT* cassette (■), and to verify absence of the wild type allele (■). Small arrows indicate direction of primers (▶).

Once successful integration of the *NAT* cassette at the appropriate site in the genome had been established, the cassette was excised by expression of the flippase (FLP) enzyme encoded on it. Expression of this was induced by growing the cells in YNB-BSA-MAL. The cultures were then diluted 10^{-7} and plated onto non-selective YPD agar to grow individual colonies, which in turn were replica plated onto selective and non-media for growth comparison (Fig. 3.2). Colonies were identified as having successfully "flipped" by sensitivity to nourseothricin.

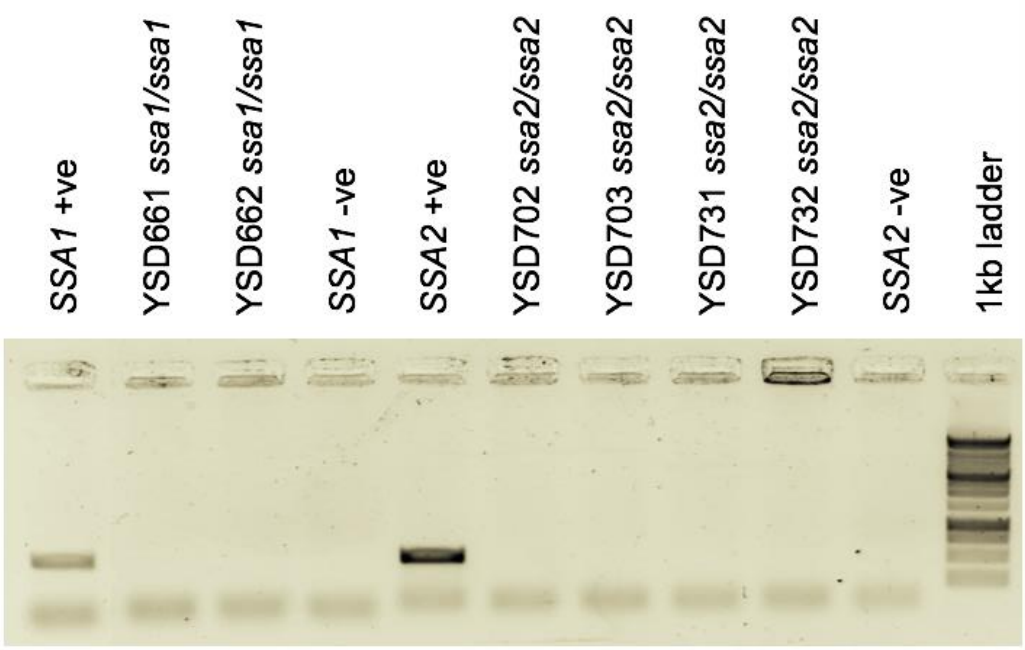

Figure 3.4 Agarose gel showing absence of wild type alleles in homozygous null mutants for *SSA1* and *SSA2* genes, including positive and negative controls and 1 kb labber. Figure continues on following page.

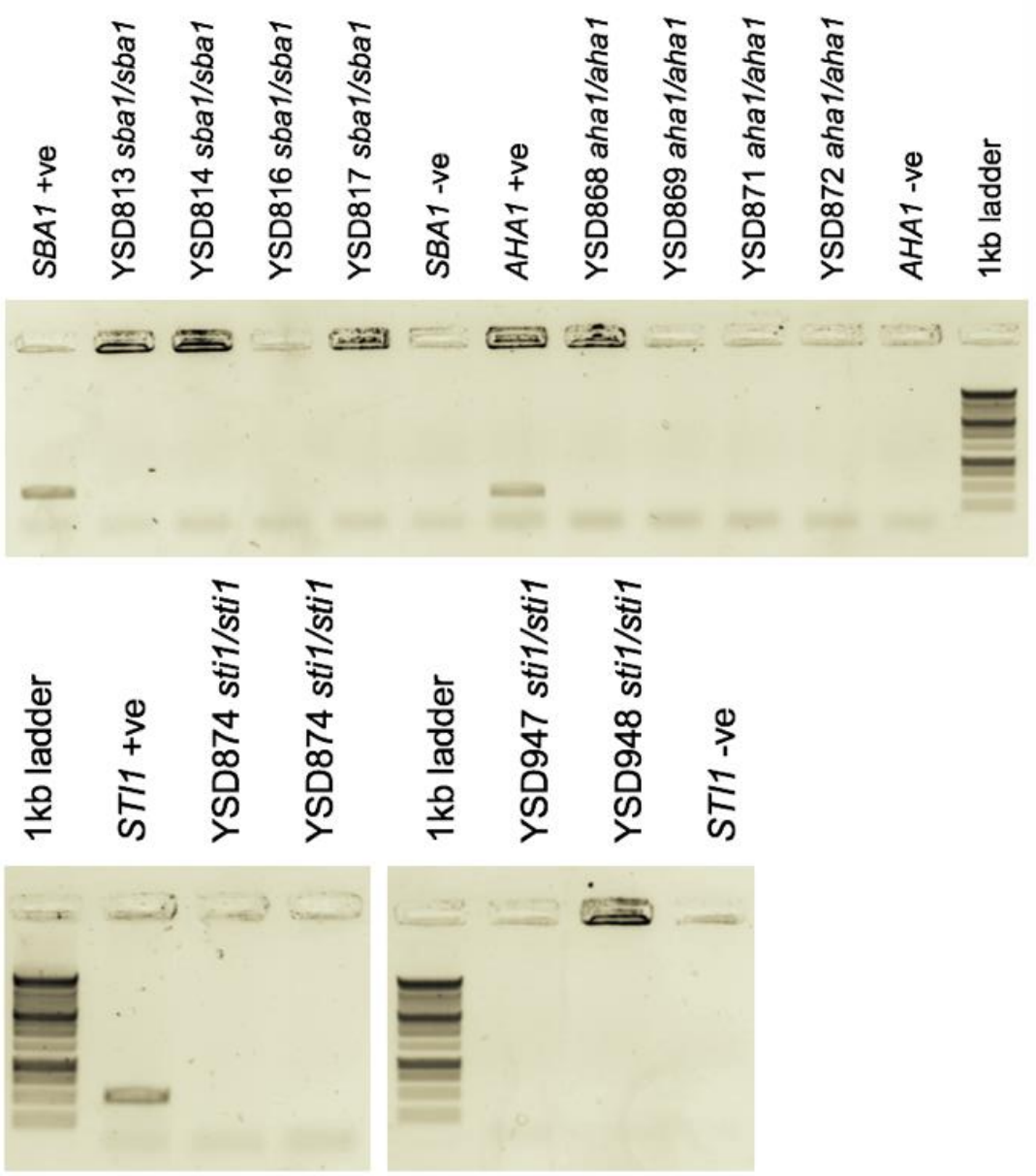

Figure 3.4 Agarose gels showing absence of wild type alleles in homozygous null mutants for *SBA1, AHA1,* and *STI1* genes, including positive and negative controls and 1 kb ladder. Bands show a fragment of the native gene's DNA in the positive controle lanes, which is absent from the mutant strains and from the negatice control lanes.

Once successfully transformed and “flipped”, mutant strains were grown overnight in YPD broth and added to the YSD strain collection at -80°C in a final concentration of 25% glycerol.

The only fungal-specific Hsp90 co-chaperone gene, *TAH1*, could not be deleted in this study as screening of >600 colonies showed the wild type allele still present after attempted deletion of both alleles. It is not yet known whether Tah1 is essential in *C. albicans*, though its orthologue, Tah18, is known to be required for viability in *S. cerevisiae* [127]. A third long primer was used for the first allelic deletion of *TAH1*, so reintegration of the *NAT* cassette at the site of the empty locus can be ruled out (Appx. 8.3).

Additionally, due to the 87.2% protein sequence identity between the Hsp70 orthologues Ssa1 and Ssa2, generation of a double homozygous null mutant was attempted [116]. This was unsuccessful, which may indicate that at least one Hsp70 orthologue is required for viability.

3.2 Selected co-chaperone genes are not essential for viability

Growth assays provide additional detail about the viability of mutants following gene deletion. Generation of homozygous null mutants demonstrates that the gene is not essential for viability, as this would preclude null mutant generation; but growth assays show whether mutants grow with the same success as the wild type strain. In this case, maximum culture density, growth

rate, and minimum generation time was compared between mutants and the wild type strain (Fig. 3.6).

All mutants display comparable growth to the wild type strain, YSD89 (Fig. 3.5). To account for variation between assays, the wild type strain was included in every replicate. The error bars show standard deviation from eight technical replicates and are usually larger at the beginning of the assay before readings stabilise into a consistent pattern. As growth is exponential, log optical density values are plotted on the *y*-axes.

The *ssa1*Δ/Δ mutants, YSD661 and YSD662, generated curves which follow the wild type very closely. The only exception to this is YSD662 in YNB at 37°C, which had a slightly shorter lag phase than the wild type and thus enters the exponential growth phase slightly earlier, but thereafter their respective growth rates and carrying capacities look almost identical.

The *ssa2*Δ/Δ mutants, YSD702 and YSD731, both have a slightly shorter lag phase in YNB at 37°C than the wild type, whilst exhibiting very little variation in the other three conditions. Following the lag phase both strains grow at around the same rate and to the same carrying capacity as the wild type. The same is also the case for the *sba1*Δ/Δ mutants, YSD813 and YSD816 and the *aha1*Δ/Δ mutants, YSD868 and YSD871.

The *sti1*Δ/Δ mutants, YSD874 and YSD947, again show an almost identical growth profile to the wild type strain, but YSD874 does lag very slightly behind

the wild type in all but one condition. The exception is in YNB at 37°C, when the curve for YDS874 is slightly ahead of that of the wild type. YSD947 also lags very slightly behind the wild type in both YPD conditions, and exhibits very large error bars in YNB at 37°C.

Comparing the growth metrics obtained as a proportion of the metric values for the wild type strain in each replicate revealed negligible variation between strains (Fig 3.4, appx. 8.7). All metrics are presented as unit-less proportions rather than absolute values to allow for easier comparisons to the wild type strain and to account for assay variation. The K metric denotes the carrying capacity, or the highest OD_{600} reading the culture reached during the 24-hour growth period as a proportion the K value for the wild type strain. R was measured as number of doubling events of optical density per hour, while T_gen was the fastest single doubling time measured.

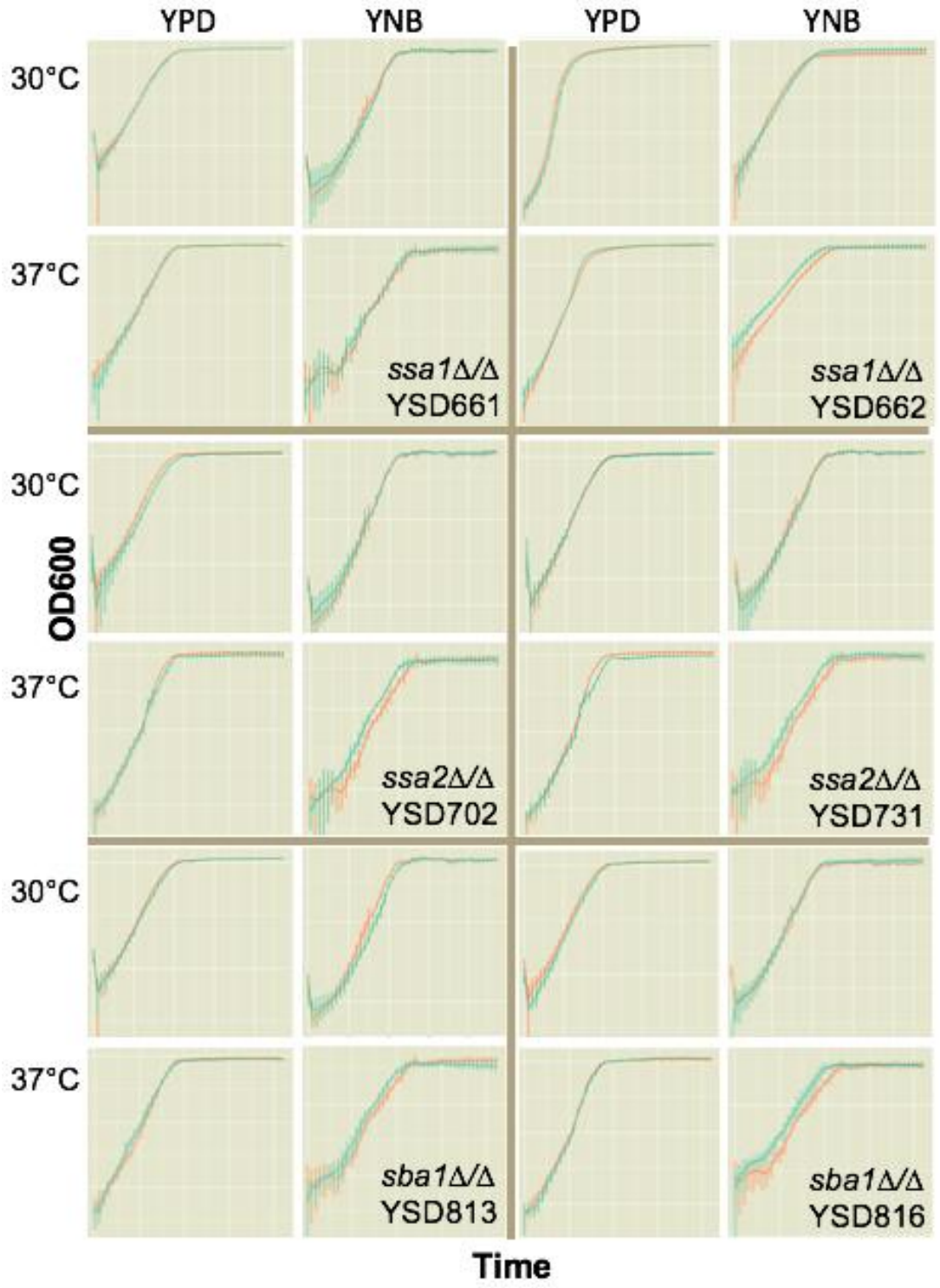

Figure 3.3 Growth curves of mutant strains and wild type strain in four different conditions. Figure continues with legend on the following page.

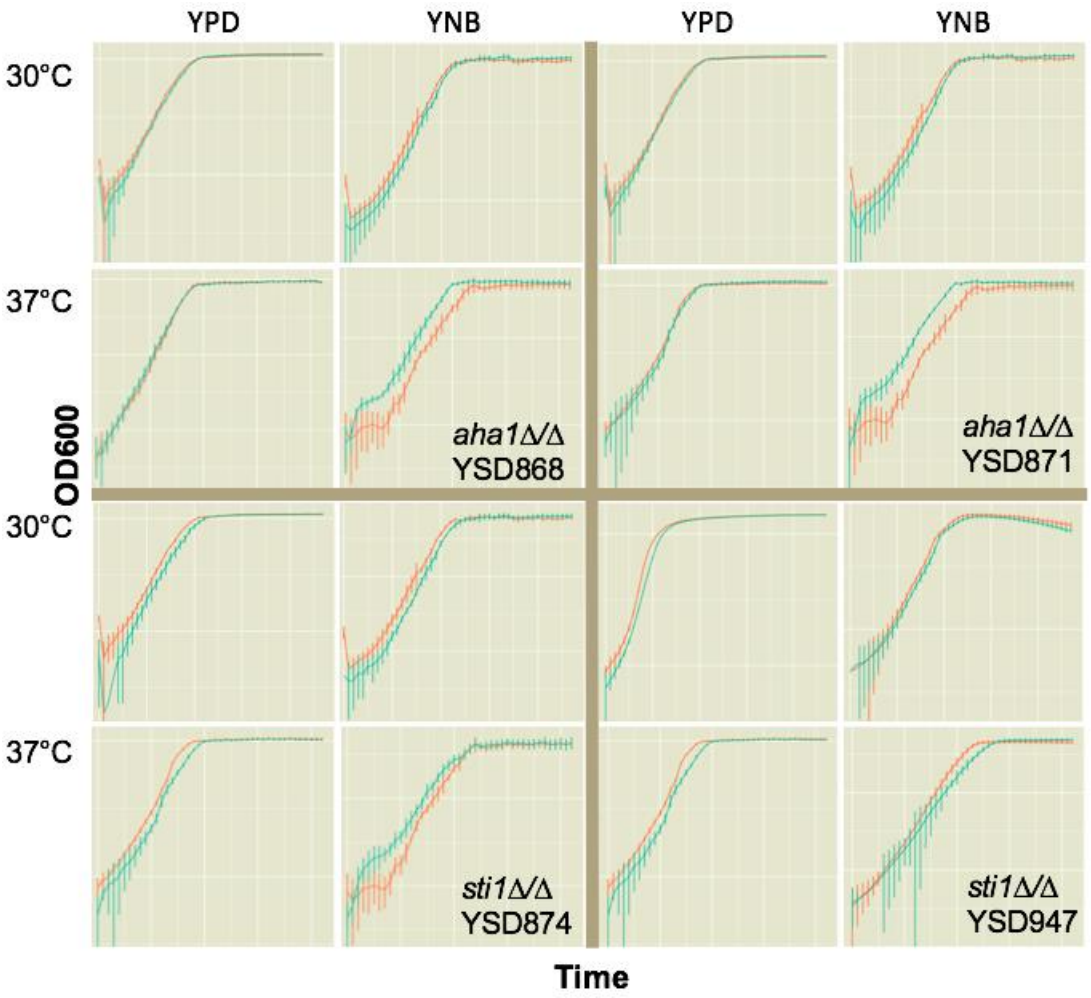

Figure 3.5 continued Growth curves of mutant strains and wild type in four different conditions. Assays were repeated at 30°C and at 37°C, in YPD broth and in YNB broth. Each panel shows the wild type strain in red: — plotted against the mutant strain indicated in blue: —. As growth is exponential, log values of the OD_{600} values were plotted on the *y*-axes. Time is plotted on the *x*-axes; all assays were run for 24 hours. Error bars show standard deviation.

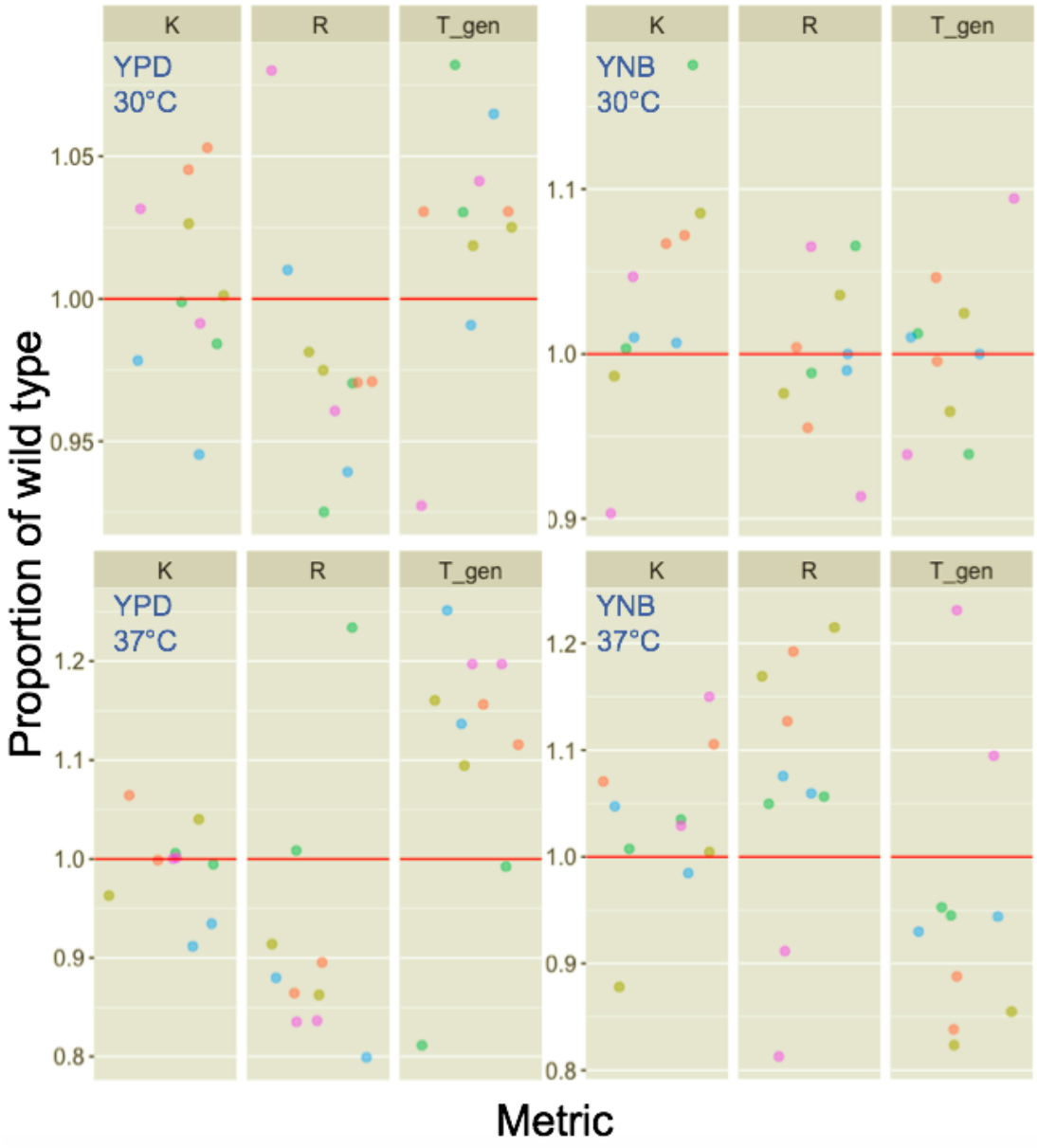

Figure 3.6 Growth metrics of mutants in all conditions relative to the wild type, YSD89 — from their respective repeats presented as univariate scatter plots. "K" indicates carrying capacity of the culture, which was quantified by the maximum optical density reached. "R" denotes the overall rate of growth, while "T_gen" is the fastest doubling time to occur during the assay. Points are coloured according to genotype; *ssa1*Δ/Δ, *ssa2*Δ/Δ, *sba1*Δ/Δ, *aha1*Δ/Δ, *sti1*Δ/Δ.

K or R values >1.00 indicate that the carrying capacity or the growth rate of that strain outperformed that of the wild type strain (Fig. 3.6). Values of <1.00 for K or R indicate that the strain grew to a lower density, or more slowly than the wild type. The inverse is true for the T_gen values; >1.00 is a longer fastest doubling time than the wild type and <1.00 is shorter than wild type. The metrics were compared statistically by ANOVA and Tukey's test.

The carrying capacity (K) for all strains was very similar; almost all were within 10% of the wild type K value and ANOVA analysis of this metric showed no significant deviation from the wild type in any condition ($p>0.1$).

Growth rates and fastest doubling times are intrinsically linked values, Growth rates and fastest doubling times in both YPD and YNB at 30°C were within 10% of the wild type values for all strains. More variation was observed at 37°C, with only YSD661 and YSD813 differing from the wild type by less than 10% in YPD. In YPD at 37°C, the only strain to display a growth rate and generation time higher than the wild type was YSD662, which grew overall 23.3% faster than the wild type strain, and had a shorter minimum doubling time by 18.9%. Nonetheless, these YSD662 did not significantly deviate from the wild type in any condition ($p>0.05$). The remaining strains; YSD816 (*sba1*Δ/Δ), both *ssa2*Δ/Δ mutants, both *aha1*Δ/Δ mutants, and both *sti1*Δ/Δ mutants had growth rates 10%-20% slower than the wild type, and minimum doubling times 11%-25% longer than the wild type. The *ssa2*Δ/Δ mutant strain YSD731 yielded the only statistically significant deviation from the wild type in

YPD at 37°C (p=0.024) in fastest generation time, while carrying capacity and growth rate were similar to the wild type.

Conversely, in YNB at 37°C, several strains outperformed the wild type strain in overall growth rates and minimum doubling times. Only the *sti1*Δ/Δ mutant YSD874 grew more slowly than the wild type, with 18.7% slower growth rate and 23.1% longer minimum doubling time. Both *sba1*Δ/Δ mutants and *aha1*Δ/Δ mutants displayed faster growth rates and shorter minimum doubling times than the wild type strain. Their growth rates were faster by 12%-22%, and their minimum doubling times were shorter by 11%-18%. The remaining five strains all produced values within 10% of the wild type strain in this condition. Nevertheless, none of these differences were statistically significant (p>0.05).

ANOVA analysis showed no statistical significance (p>0.05) in carrying capacity or in overall growth rate in any condition. For fastest generation time, there was a statistically significant difference in time in YPD at 37°C (p=0.018), while in the other three conditions the results were statistically similar. Pairwise comparison showed the outlier strain for fastest generation time in YPD at 37°C was the *ssa2*Δ/Δ strain YSD731, for which the fastest generation time was slower than the wild type (p=0.024). When taking into account that carrying capacity and growth rate did not differ significantly from the wild type, it was concluded that YSD731 did not have a substantial growth defect to preclude it from further testing.

Despite the lack of statistical significance, trends appear to emerge of small differences in growth behaviour between wild type and mutant strains. Both *sti1*Δ/Δ mutants outperformed the wild type in most conditions, and were the only strains to grow more quickly than the wild type strain in YNB broth at 37°C (Fig. 3.6). All of the other strains, with the exception of the *ssa1*Δ/Δ mutants grew at a faster rate than the wild type in YPD at 37°C, but then slower than wild type in YNB at the same temperature. As YNB is the synthetic defined media, this trend implies the mutant strains may thrive while nutrients are abundant, but struggle in nutrient-limiting conditions. This will be something to be mindful of in further investigation of these strains; potential defects in nutrient sequestration or intracellular storage.

Based on the behaviour of these mutants, none of the co-chaperone genes investigated is required for growth under the conditions tested here, and deviations from the metrics of the wild type strain were minor. All of the Hsp90 co-chaperone null mutants were carried forward for further testing of virulence potential.

3.3 Discussion

Transformation using lithium acetate is a reliable method but efficiency of the reaction is low, particularly for deletion of the second allele. Efficiency also differs between genes, depending on factors such as their genomic locale and heterochromatin formation. It is as yet not known whether this is because Tah1 or an Hsp70 orthologue is essential for viability; it may be pertinent in future to try deletion of the genes by another method, such as the recently developed CRISPR [165]. Alternatively, the function of Tah1 and Ssa1/2 could be investigated through insertion of a repressible promoter in place of the native promoter to deplete protein levels in the cell. Established repressible promoters used in *C. albicans* are controlled by various means. These include manipulation of the carbon source, as in the CaMAL2 promoter [166], and addition of amino acids, as with the MET3 promoter [167]. The addition of antibiotics can also control expression, as with the tetracycline-repressible Tet-off promoter, which has been used to suppress other essential genes, such as *HSP90* [168, 169]. Repressible promoters make it possible to deplete levels of essential proteins in cells and to observe the effects thereof.

The growth curves show limited variation between the mutants and the wild type strains. More variation was observed at 37°C than at 30°C with growth in general being less predictable at the higher temperature. There was also more variation in YNB; the synthetically defined medium, than in YPD; the rich broth, suggesting discrepancies in the abilities of strains to grow robustly when nutrients are more limited.

The aim of the growth curve assays was to identify growth defects in mutants, as this was an undesirable trait when trying to identify strains essential for virulence but not for viability or growth. All of the strains were carried forward for further analysis of their virulence potential as none of the gene deletions conferred a growth defect. In fact, the largest differences in growth metrics were in cases when the mutant strain outperformed the wild type strain.

Subtle trends were observed where growth metrics for most strains were clustered either above or below the wild type in the growth assays. This may be worthwhile revisiting in future by assaying strains for growth in conditions more closely imitative of the natural environment; with more nutrient limitation, over longer time periods, and with microbial competition, for example. However, for the purposes of this study, these results were considered adequately informative to dismiss a significant role of these co-chaperones in *C. albicans* avirulent growth.

Homozygous gene deletion strains for Hsp90 co-chaperones were successfully generated for this study, and the initial growth assays show they are not essential for growth. Next, the roles of these co-chaperones in virulence was investigated.

4. Characterisation of Hsp90 co-chaperone null mutants in *in vitro* virulence assays

Virulence factors are the pathogen's armoury which enable it to invade, survive and thrive in the host. Pathogens with attenuated virulence may live as normal in the external environment, but fail to overcome a host's defences. The *C. albicans* Hsp90 co-chaperones are largely uncharacterised and so their role in virulence is unknown. A set of *in vitro* virulence assays was carried out in order to quantify the importance of each co-chaperone in individual virulence traits.

in vitro virulence assays allow for quantification of how different strains are able to manifest virulence factors, known to be important for infection. All of the strains generated and tested in this study are homozygous null for a single gene. This means that when a difference in phenotype is observed it can be deduced that the deleted gene is instrumental in the particular characteristic tested. However, it is important to note that when no difference in phenotype can be observed, it may not mean that the deleted gene plays no role in the phenotype; rather that it does not play a unique or essential role, and that the absence of the gene is compensated for.

For the virulence assays, the strains are split into two groups; group one and group two. There were two mutants generated for each gene deletion, and each group contains one mutant of each pair. The wild type strain, YSD89, was used as a positive control in all assays and included in both groups. There was also a sterile control included in all replicates of all assays, and in some cases an additional negative control.

4.1 *ssa2*Δ/Δ mutants are enhanced in oxidative stress resistance

Resistance to oxidative stress is an important virulence trait for pathogens to survive in the host bloodstream. Oxidative burst is one of the primary defences of the innate immune system employed when phagocytes attack invading organisms with reactive oxygen species [13]. Phagocytes engulf invading pathogens and release reactive oxygen species into the phagosome to exert stress on the pathogen [170].

This assay was optimised using a *hog1Δ/Δ* mutant, YSD883, as Hog1 is known to be important in oxidative stress resistance [171]. The *hog1Δ/Δ* mutant was generated in the same background as the other mutants in this study; YSD89, for consistency in comparing the strains in this assay. A range of hydrogen peroxide concentrations were used in optimisation to find a dose which left the wild type strain unaffected, but the *hog1Δ/Δ* cells inviable (data not shown).

1 mM hydrogen peroxide was fatal for almost all *hog1Δ/Δ* cells but the same concentration left more than 80% of wild type cells unaffected. This shows the clear distinction between a healthy response to oxidative stress and an attenuated response. Higher concentrations were shown to be detrimental to all strains, including the wild type, and so were too concentrated to test for defects in oxidative stress resistance. Due to the high rate of degradation of hydrogen peroxide, the concentration of the stock was checked regularly by spectrophotometer.

Next, group one and group two mutants, each containing one mutant per gene, were compared for their relative colony forming unit (cfu) counts for treated and untreated cells (Fig. 4.2 and 4.3). The wild type strain, YSD89, shows approximately 10% die-off from exposure to hydrogen peroxide, and it was against this metric that the mutant strains were compared. The negative control strain, YSD883 (*hog1*Δ/Δ), clearly exhibits almost complete inability to survive exposure to hydrogen peroxide for one hour; a significant difference between this strain and the wild type strain (Table 4.1).

Interestingly, the homozygous null mutants for *SSA2*; YSD702 and YSD731, both exhibited significantly increased resistance to oxidative stress relative to the wild type strain ($p=0.009$ and $p=0.025$, respectively). This is a consistent and convincing indication that the presence of Ssa2 in some way impedes the oxidative stress response to *C. albicans.*

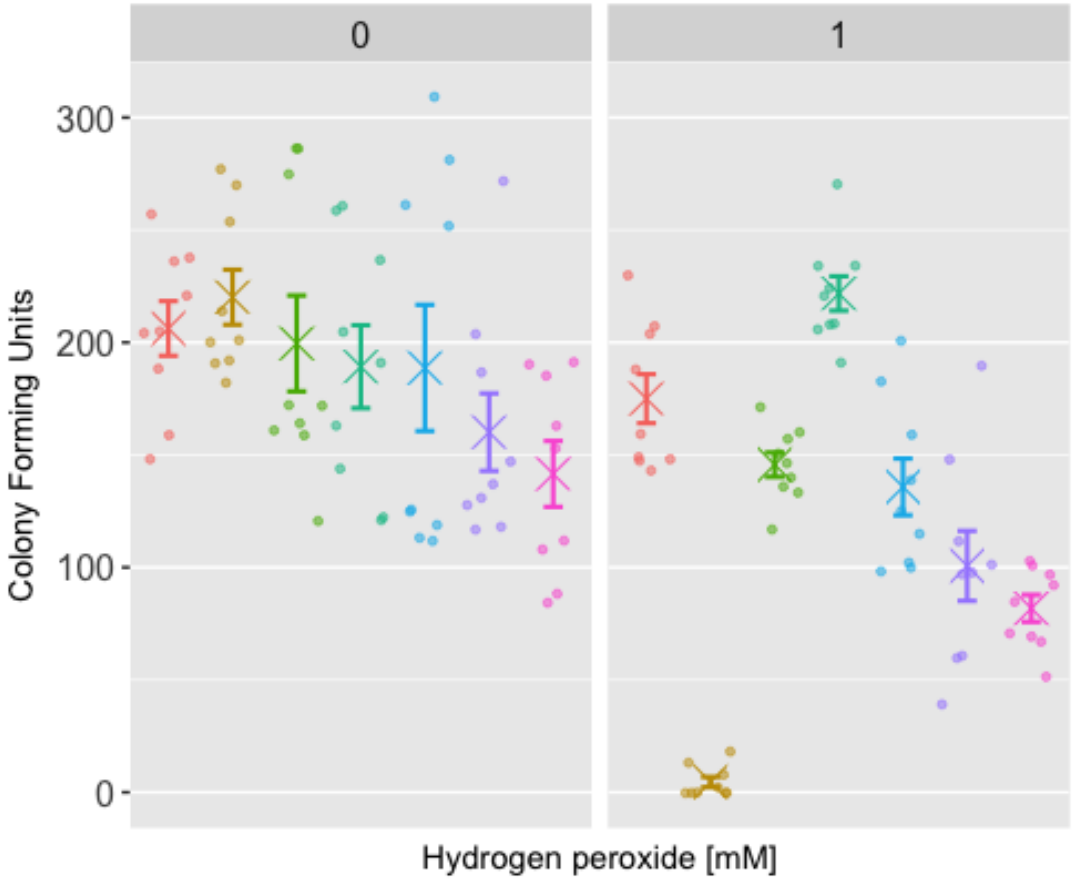

Figure 4.2 Oxidative stress assay results for group one mutants, plotted with positive and negative controls; wild type strain YSD89 and *hog1*Δ/Δ strain YSD883, respectively. The data points denote viable colony forming units (CFU) from the diluted volume plated. The panel on the left shows counts for cells without oxidative stress treatment, and the panel on the right contains counts for cells exposed to 1 mM hydrogen peroxide. Data represent three technical replicates and three biological replicates. Crosses denote mean CFU counts, with standard error bars protruding: YSD89 wild type, YSD883 *hog1*Δ/Δ, YSD661 *ssa1*Δ/Δ, YSD702 *ssa2*Δ/Δ, YSD813 *sba1*Δ/Δ, YSD868 *aha1*Δ/Δ, YSD874 *sti1*Δ/Δ.

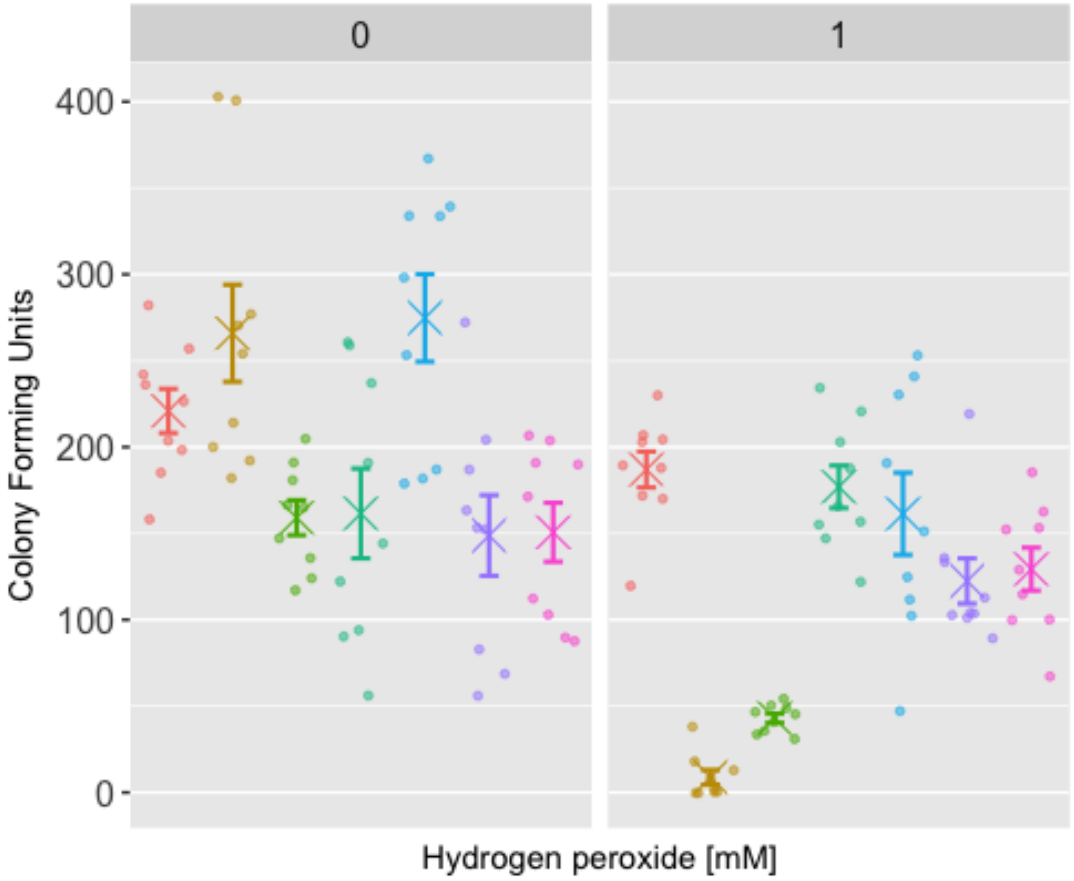

Figure 4.3 Oxidative stress assay results for group two mutants, plotted with positive and negative controls; wild type strain YSD89 and *hog1*Δ/Δ strain YSD883, respectively. The data points denote viable colony forming units (CFU) from the diluted volume plated. The panel on the left shows counts for cells without oxidative stress treatment, and the panel on the right contains counts for cells exposed to 1 mM hydrogen peroxide. Data represent three technical replicates and three biological replicates. Crosses denote mean CFU counts, with standard error bars protruding: YSD89 wild type, YSD883 *hog1*Δ/Δ, YSD662 *ssa1*Δ/Δ, YSD731 *ssa2*Δ/Δ, YSD816 *sba1*Δ/Δ, YSD871 *aha1*Δ/Δ, YSD947 *sti1*Δ/Δ.

Table 4.1 p-values of survival of each strain relative to the wild type strain under oxidative stress calculated by a mixed linear model, with survival rate indicated in comparison to the wild type strain. Significance codes are; "***" p<0.001, "**" 0.001<p<0.01, "*" 0.01<p<0.05.

STRAIN	GENOTYPE	SURVIVAL RATE	LM P-VALUE
YSD883	*hog1*Δ/Δ	Reduced	<0.001***
YSD661	*ssa1*Δ/Δ	Reduced	0.175
YSD662	*ssa1*Δ/Δ	Reduced	0.023*
YSD702	*ssa2*Δ/Δ	Increased	0.009**
YSD731	*ssa2*Δ/Δ	Increased	0.025*
YSD813	*sba1*Δ/Δ	Reduced	0.339
YSD816	*sba1*Δ/Δ	Reduced	0.177
YSD868	*aha1*Δ/Δ	Reduced	0.119
YSD871	*aha1*Δ/Δ	Reduced	0.445
YSD874	*sti1*Δ/Δ	Reduced	0.047*
YSD947	*sti1*Δ/Δ	Reduced	0.444

The homozygous null mutants for *SSA1*; YSD661 and YSD662, show reduced resistance to oxidative stress relative to the wild type. However, this result was not significant for YSD661 (p=0.175), while YSD662 from mutant group two was significantly impaired (p=0.023). These results suggest that Ssa1 may be involved in the oxidative stress response. This is particularly surprising following the increase in survival of oxidative stress seen in the *ssa2*Δ/Δ mutants. Ssa1 and Ssa2, orthologues of Hsp70, share such high similarity in

gene and protein sequences; 85.8% and 87.2%, respectively, that such opposing phenotypes in the mutants was not anticipated [116].

The group one *sti1*Δ/Δ mutant, YSD874, was impaired in its response to oxidative stress relative to the wild type with marginal significance ($p=0.047$), while in group two, YSD947 showed no reduction in oxidative stress resistance ($p>0.1$). This pair of mutants should be genotypically identical so a difference in results was not expected; second-site mutations may have occurred during the transformation reaction.

Neither Sba1 nor Aha1 appear to play an important role in oxidative stress resistance, as the mutants' survival under the conditions tested was statistically similar to the wild type strain (Table 4.1).

4.2 Hsp90 co-chaperones do not appear to be required for heat shock tolerance

Tolerance of heat shock is an important virulence trait in pathogens which induce fever in their hosts. Fever is a facet of the innate immune response which exerts high temperature as a form of stress on the invading pathogen [172, 173]. Tolerance of heat shock and thriving in heat shock conditions is indicative of the ability of the pathogen to adapt to the host environment.

Under normal circumstances, high temperatures increase expression of *HSP90*; as implied by the name, “heat shock protein” [174]. The negative control strain in this assay was the *tetOFF-HSP90/hsp90Δ* strain, YSD106. Addition of 20 µg mL^{-1} doxycycline to the growth media reliably turns off *HSP90* gene expression, thus depleting Hsp90 protein levels [24, 156]. For this assay, doxycycline was added to the cultures when they were adjusted to OD_{600} 0.2 prior to being grown to mid-log growth. The effect of the reduced heat shock tolerance in this assay is stunted growth of the cultures. This means that while the wild type strain, YSD89, almost doubles in colony count over the two-hour period, which is consistent with normal yeast doubling time [175], the negative control strain, YSD106, maintains approximately the same colony count.

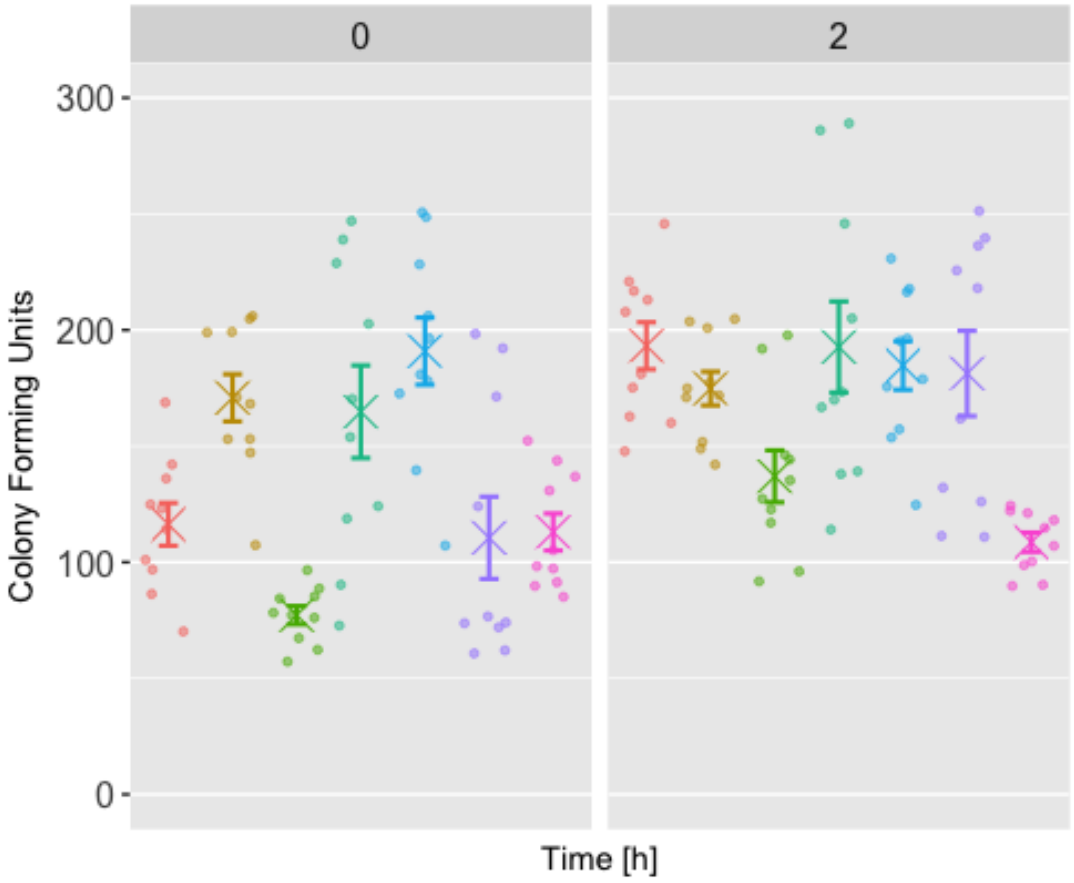

Figure 4.4 Heat shock assay results for group one mutants, plotted with positive and negative controls; wild type strain YSD89 and *tetOFF-HSP90/hsp90Δ* strain YSD106, respectively. The data points denote viable colony forming units (CFU) from the plated culture dilution. The panel on the left shows counts for cells before heat shock treatment, and the panel on the right contains counts for cultures after two hours of incubation at 42°C with orbital shaking at 200 rpm. Data represent five technical replicates and two biological replicates. Crosses denote mean CFU counts, with standard error bars protruding: YSD89 wild type, YSD106 *tetOFF-HSP90/hsp90Δ*, YSD661 *ssa1Δ/Δ*, YSD702 *ssa2Δ/Δ*, YSD813 *sba1Δ/Δ*, YSD868 *aha1Δ/Δ*, YSD874 *sti1Δ/Δ*.

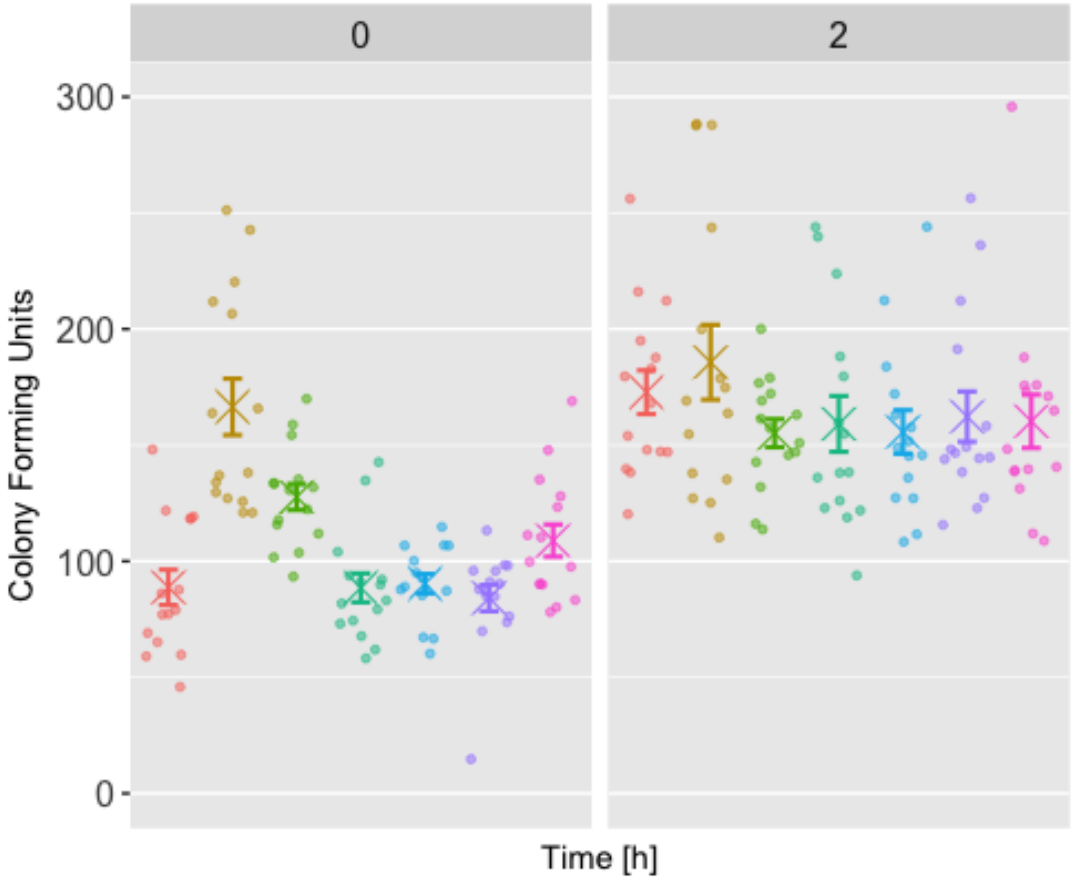

Figure 4.5 Heat shock assay results for group two mutants, plotted with positive and negative controls; wild type strain YSD89 and *tetOFF-HSP90/hsp90Δ* strain YSD106, respectively. The data points denote viable colony forming units (CFU) from the plated culture dilution. The panel on the left shows counts for cells before heat shock treatment, and the panel on the right contains counts for cultures after two hours of incubation at 42°C with orbital shaking at 200 rpm. Data represent five technical replicates and two biological replicates. Crosses denote mean CFU counts, with standard error bars protruding: YSD89 wild type, YSD106 *tetOFF-HSP90/hsp90Δ*, YSD662 *ssa1Δ/Δ*, YSD731 *ssa2Δ/Δ*, YSD816 *sba1Δ/Δ*, YSD871 *aha1Δ/Δ*, YSD947 *sti1Δ/Δ*.

Table 4.2 p-values of growth of mutants at 42°C relative to the wild type strain according to a mixed linear model. Significance codes are; "***" p<0.001, "**" 0.001<p<0.01, "*" 0.01<p<0.05.

STRAIN	GENOTYPE	RELATIVE GROWTH	P-VALUE
YSD106	*HSP90/hsp90*Δ	Reduced	0.005**
YSD661	*ssa1*Δ/Δ	Reduced	0.484
YSD662	*ssa1*Δ/Δ	Reduced	0.040*
YSD702	*ssa2*Δ/Δ	Reduced	0.056
YSD731	*ssa2*Δ/Δ	Reduced	0.742
YSD813	*sba1*Δ/Δ	Reduced	<0.005**
YSD816	*sba1*Δ/Δ	Reduced	0.895
YSD868	*aha1*Δ/Δ	Reduced	0.780
YSD871	*aha1*Δ/Δ	Reduced	0.759
YSD874	*sti1*Δ/Δ	Reduced	<0.002**
YSD947	*sti1*Δ/Δ	Reduced	0.164

While *Candida albicans* is adapted to living at 37°C, a temperature of 42°C constitutes heat shock. Mutants were exposed to heat shock for two hours and growth measured as cfu counts. Colony counts after heat shock were compared to those prior to heat shock and levels of growth were compared with that of the wild type for statistical analyses (Fig. 4.4 and 4.5).

The *ssa1*Δ/Δ mutant in group two, YSD661, was significantly impaired compared to the wild type strain (p=0.040), whereas its counterpart strain was

not (Table 4.2). A similar disparity was seen with the *sba1*Δ/Δ and *sti1*Δ/Δ mutants, with the mutants in group one being impaired in heat shock tolerance, while the group two mutants were not significantly affected. The *sba1*Δ/Δ and *sti*Δ/Δ mutants from group one, YSD813 and YSD874 ($p<0.005$, $p<0.002$), were in fact even outperformed by the negative control strain, YSD106 ($p=0.005$).

The reasons for these stark differences in behaviour between what should be identical pairs of mutants is not clear, but may be due to second-site mutations having arisen during the transformation reaction.

Both pairs of the *ssa2*Δ/Δ mutants, YSD702 and YSD731, as well as both of the *aha1*Δ/Δ mutants, YSD868 and YSD871, grew with comparable success to the wild type in heat shock conditions (Table 4.2). This suggests that neither Ssa2 nor Aha1 plays an important or unique role in tolerance of heat shock.

4.3 *sti1*Δ/Δ mutants are enhanced in morphogenesis on solid growth media

C. albicans is known to grow in three distinct morphological forms; budding yeast, pseudohyphae, and hyphae, and the ability to transition between these is essential for causing disease [30]. Morphology of whole colonies provides information about morphological capabilities and changes in phenotype conferred by gene deletions.

Colonies were grown on six different solid growth media and their morphologies compared to that of the wild type strain, YSD89 (Fig. 4.6). Colonies in the middle of the plate layout were omitted from the analysis as it was evident that their growth was impaired by proximity to other colonies. This meant that two technical replicates and three biological replicates were analysed for each strain, which yielded consistent results across replicates. Each colony was assigned a score according to growth and appearance, and compared to the wild type (Table 2.3).

On YPD agar all strains grew with approximately equal robustness into the familiar butyrous white colony formation typical of *C. albicans*; 3 in the scoring scheme (Fig. 4.6, Table 4.3). This was effectively a control medium for growth at 37°C and major differences in morphology were not expected. Particularly after having assessed the growth rates and capacities of these strains and found them to be similar, morphology on solid rich media was also expected to be consistent.

Spider agar is a rich medium which induces hyphal formation and colony wrinkling in *C. albicans* at 37°C [176]. Almost all of the strains formed wrinkled colonies with a filiform halo of hyphae, a score of 3 in the scheme. This means their phenotype on spider agar did not differ from the wild type strain, YSD89. The notable exception to this was YSD662, which formed glabrous colonies with little filiform halo, a score of 2 according to the scheme. This suggests the strain is defective in formation of wrinkles and of hyphae and, importantly, the same phenotype was not seen in YSD661; the strain with the same gene deletion.

RPMI medium was originally formulated for culturing of mammalian cell lines, and imitates, without serum, nutrient conditions in the host bloodstream [177]. For *Candida spp.* RPMI is used to induce biofilm formation and to test for susceptibility of strains to antifungal drugs [178, 179]. All strains formed dry, rough, filiform colonies on RPMI. The only exception in this case was the *sti1*Δ/Δ mutant YSD947, which formed only semi-filiform colonies. This is an interesting result as this strain exhibited no defects in hyphal formation on any other solid growth media.

SD agar is a selective peptone medium used predominantly to grow fungi [180, 181]. Additional strains were added to the agar in this case for morphological study.

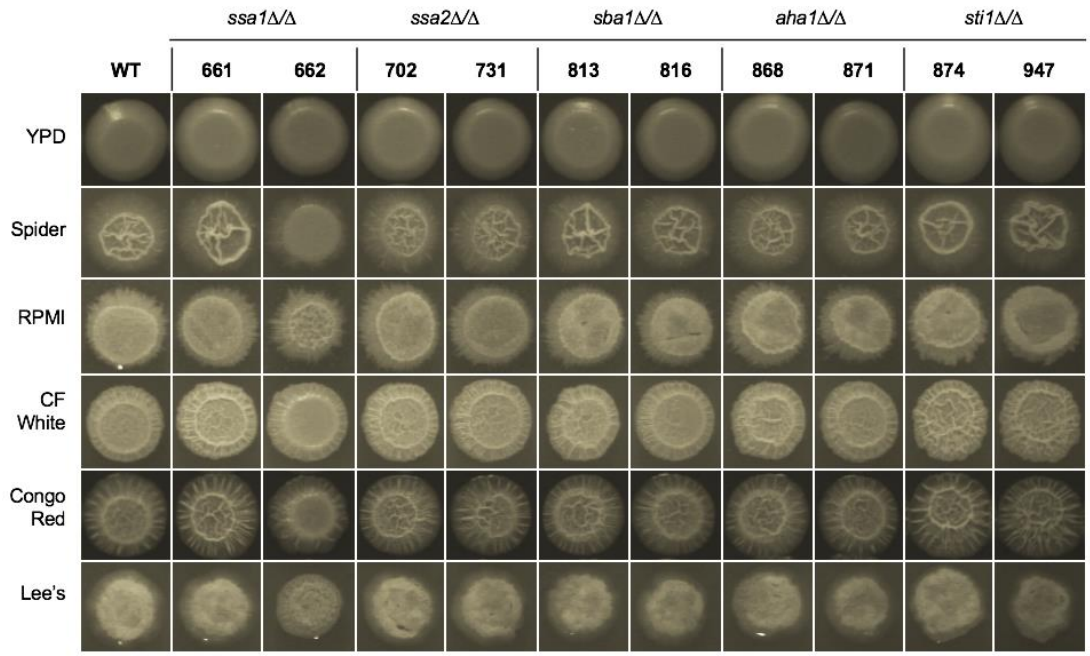

Figure 4.6 Examples of colonies for each strain on each growth medium. "WT" indicates the wild type strain, while the mutant strains are labelled across the top by their genotype and YSD numbers. The column on the left indicates which growth medium the colonies are on.

The Calcofluor White stain has an affinity to chitin and interferes with chitin synthesis and polymerisation, which is essential for proper cell wall formation [182, 183]. This affects cell morphology and Calcofluor White can have the effect of increasing yeast cell wall volume by up to 30% [184]. A range of colony morphologies was seen on this growth medium, with the wild type strain forming colony types 3 and 4 on the scheme; wrinkly, undulate colonies, and robust wrinkles on undulate colonies, respectively. Colony type 3 was predominant for the wild type strain, whereas the *sti1*Δ/Δ mutants; YSD874 and YSD947, formed exclusively colony type 4 with large, robustly wrinkled colonies. The *ssa1*Δ/Δ mutant, YSD662, formed colonies which scored 2; rough colonies, rather than wrinkled.

Congo Red dye similarly affects formation of the fungal cell wall and therefore cell and colony morphology [185]. Most strains formed colony type 2 on this medium; haloed colonies with wrinkles all over. In the case of the *sti1*Δ/Δ mutants; YSD874 and YSD947, the colonies grew larger than the other strains and formed more elevated wrinkles. These are the same strains which grew most robustly on SD agar with Calcofluor White. YSD662 again grew with less success than the other strains and formed colonies with only a wrinkled halo with a glabrous centre; colony type 1.

Table 4.3 Morphology scores for colonies of each strain on each solid growth medium (Table 2.3). Scores are representative of colonies from all replicates as results were consistent. Colours denote equivalence, reduction, or enhancement relative to the wild type.

	WT	ssa1Δ/Δ		ssa2Δ/Δ		sba1Δ/Δ		aha1Δ/Δ		sti1Δ/Δ	
Medium	**89**	**661**	**662**	**702**	**731**	**813**	**816**	**868**	**871**	**874**	**947**
YPD	3	3	3	3	3	3	3	3	3	3	3
Spider	3	3	2	3	3	3	3	3	3	3	3
RPMI	3	3	3	3	3	3	3	3	3	3	2
CF White	3	3	2	3	3	3	3	3	3	4	4
Congo red	2	3	1	2	2	2	2	2	2	3	3
Lee's	2	2	1	2	2	2	2	2	2	2	2

Lee's medium is a synthetic defined growth medium which induces hyphal growth at 37°C [186]. Colony morphology on this medium was consistent, with most strains forming colony type 2; dry, undulate colonies with elevated wrinkles. YSD662 was the only exception to this, forming colony type 1; dry, entire colonies with robust wrinkles. Some strains defective in biofilm formation are known to form colonies on Lee's medium with few wrinkles, or even smooth, so the difference seen in YSD662 is quite minor. However, the different morphology was consistent; this was the only strain to form colony type 1 and it did so in all four technical replicates in all three biological replicates.

Wrinkling of colonies is an indication of biofilm formation; cells in the colony excrete extracellular matrix, causing strain on the colony surface, where the cells act as an elastic skin [187, 188]. The importance of the wrinkles themselves are to increase surface area of the colony to help meet the oxygen demand as the colony expands, and have been found to provide channels for flow of nutrients through the extracellular matrix [189, 190].

The larger, more wrinkled colonies of the *sti1*Δ/Δ strains on media containing Calcofluor White and Congo red dyes imply that Sti may regulate production of extracellular matrix, which is then overproduced in the null mutant. The colonies appear more robust than the other strains, but this may not translate to a fitness advantage.

The *ssa1*Δ/Δ mutant, YSD662, is impaired in wrinkle-formation, but not hyphal growth, as filiform haloes were present on the colonies to the same extent as the wild type strain. Its divergence in morphology from YSD661 suggests that the cause is a second-site mutation, rather than the absence of Ssa1. The smooth colonies suggest that this strain produces less extracellular matrix and should therefore be impaired in biofilm formation.

4.4 Aha1 and Sti1 are required for biofilm formation

Biofilm formation is a potent virulence trait associated with nosocomial systemic infections and drug resistance [27]. Biofilms consist of cells surrounded by a network of extracellular polysaccharides, aiding in their coherence and adherence. This glutinous coating protects microbial communities from both the host immune system and drug treatments. The biofilm also acts as a reservoir of cells to seed the wider infection by gradual dispersal. Biofilm dispersal and drug resistance in *C. albicans* is directed by Hsp90 [63].

Measurements were taken of biofilm metabolic activity using colorimetric dye reduction and OD_{492} readings. As biofilms were washed before measurements were taken, this method means that strains defective in adherence would be classified as “weak”, as any biofilm formed would be washed off the surface. A minimum of 24 biofilms were measured for each strain; 3 biological

replicates containing 8 technical replicates each, with the wild type strain, YSD 89, acting as the positive control for biofilm formation and adherence, and the *bcr1Δ/Δ* strain [158] as a negative control forming poorly adherent biofilms.

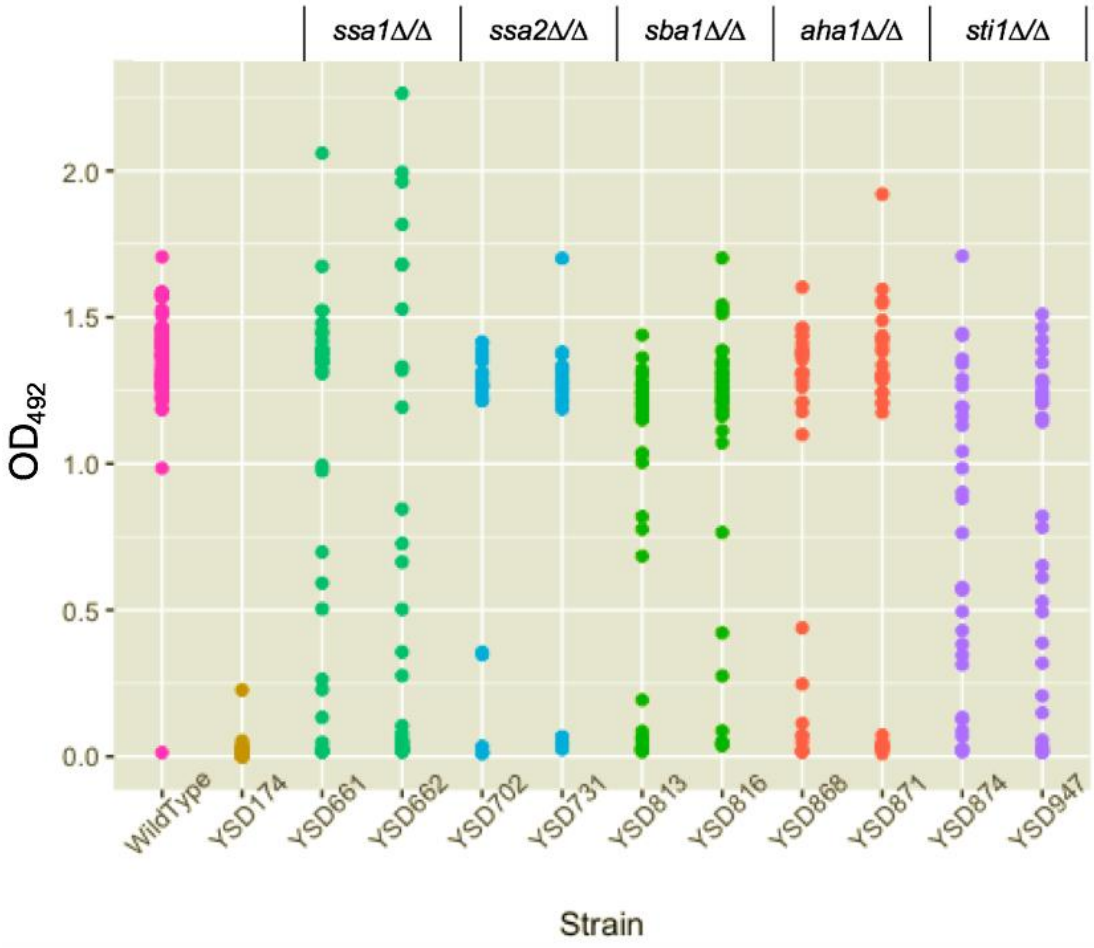

Figure 4.7 Univariate dotplot showing the success of biofilm formation for all strains and all replicates, including the positive and negative controls; the wild type strain YSD89 and the *bcrΔ/Δ* strain YSD174, respectively. Representative of a minimum of 3 biological replicates of 8 technical replicates for each strain.

Results were analysed using ANOVA, which showed significance with $p<0.001$. This was followed by mixed linear analysis comparing each strain to the wild type strain and pairwise comparisons between mutant pairs. All of the strains were found to have significantly weaker biofilm formation compared to the wild type strain, with $p<0.001$ in almost every case (Table 4.4). The only exceptions were the *ssa2*Δ/Δ strain YSD731 ($p=0.015$) and the *sba1*Δ/Δ strain YSD816 ($p=0.002$).

Table 4.4 p-values of biofilm formation of mutant strains relative to the wild type strain, YSD89 according to chi squared 2x2 analysis. Significance codes are; "***" $p<0.001$, "**" $0.001<p<0.01$, "*" $0.01<p<0.05$.

STRAIN	GENOTYPE	WT VS MUTANT	MUTANT PAIRS
YSD174	*bcr1*Δ/Δ	<0.001***	n/a
YSD661	*ssa1*Δ/Δ	<0.001***	0.035*
YSD662	*ssa1*Δ/Δ	<0.001***	
YSD702	*ssa2*Δ/Δ	<0.001***	0.237
YSD731	*ssa2*Δ/Δ	0.015*	
YSD813	*sba1*Δ/Δ	<0.001***	0.028*
YSD816	*sba1*Δ/Δ	0.002**	
YSD868	*aha1*Δ/Δ	<0.001***	0.957
YSD871	*aha1*Δ/Δ	<0.001***	
YSD874	*sti1*Δ/Δ	<0.001***	0.580
YSD947	*sti1*Δ/Δ	<0.001***	

However, there were also statistically significant differences in biofilm success between pairs of mutants which should be identical; *ssa1Δ/Δ* and *sba1Δ/Δ* mutants all showed much lower biofilm success relative to the wild type strain, but differential success to one another to a marginally significant degree (Table 4.4).

The readings for most strains form a bimodal pattern; biofilms either adhered to the wells and gave a high OD_{492} reading, or were almost completely lost in the wash steps and gave a reading close to zero. The *ssa1Δ/Δ* and *sti1Δ/Δ* mutant pairs were the only strains to defy this trend, producing a much more even spread of readings up the scale. The reasons why these strains form biofilms in such an apparently inconsistent manner is as yet unclear.

The *ssa2Δ/Δ, aha1Δ/Δ, and sti1Δ/Δ* mutant pairs showed no significant difference in success between the strains (Table 4.4). It can be concluded from this that Ssa2, Aha1 and Sti1 are instrumental in biofilm formation and adherence, contrary to what the colony morphologies on solid agar implied.

4.5 Ssa2 increases antifungal drug susceptibility, while Sti1 plays a role in resistance

Antifungal drug resistance is a growing threat to the already inadequate treatments for systemic fungal infections [191]. Azoles are the most commonly-prescribed antifungal drug class, and similar compounds are used in arable agriculture. For fungal pathogens, this high frequency of exposure to azoles, both in and out of medical settings, increases the selection pressure for the emergence of resistance.

Hsp90 is instrumental in the evolution of drug resistance [35]. To assess whether Hsp90 is also relevant in co-chaperone-mediated drug resistance, growth of mutants in the presence of fungistatic fluconazole was measured and compared with the wild type strain. The same was then repeated with the addition of Hsp90 inhibitor to investigate how the inhibition of Hsp90 coupled with the absence of each co-chaperone would affect the tolerance of the strains to fluconazole.

Growth in the presence of the drug was quantified by OD_{600} readings, which were normalised to the no-drug control. The strains exhibited high resistance to the fluconazole only condition, and so the minimum inhibitory concentration for inhibition of 40% of total growth (MIC_{40}), rather than 50% (MIC_{50}), as was used in the other two drug conditions. The MIC_{40} for the wild type strain was 8 $\mu g\ mL^{-1}$.

Both of the null strains for *SSA2* showed increased resistance to fluconazole compared to the wild type strain, with MIC_{40} at a dose of 64 μg mL^{-1}. It is well established that Ssa2 mediates entry of histatin 5 into the cell, this result suggests this may also be the case for other antifungal compounds [114, 117].

Six strains, with three different genotypes, showed lower resistance to fluconazole than the wild type. This means that drug resistance is lower when *SSA1*, *SBA1*, and *STI1* are not present in the genome, suggesting that Ssa1, Sba1 and Sti1 are positive regulators of the drug response. The MIC_{40} doses for the *ssa1Δ/Δ* strains; YSD661 and YSD662, were 4 μg mL^{-1} and 2 μg mL^{-1}, respectively. The optical density readings in the raw data (not shown) demonstrate that this is a small difference. For the *sba1Δ/Δ* strains the MIC_{40} doses were 2 μg mL^{-1} and 4 μg mL^{-1}, respectively. The strains in this case show a considerable discrepancy in optical density readings, suggesting there may be an underlying difference in the genomes of the two strains, undetected by genotyping screens. The *sti1Δ/Δ* strains had the same MIC_{40} dose of 4 μg mL^{-1}; one dilution lower than the wild type.

The absence of *AHA1* appears to have no effect on resistance to fluconazole, as MIC_{40} in this case remain stable at 8 μg mL^{-1}. The absence of a difference here suggests that Aha1 is not instrumental in either resistance or susceptibility to fluconazole.

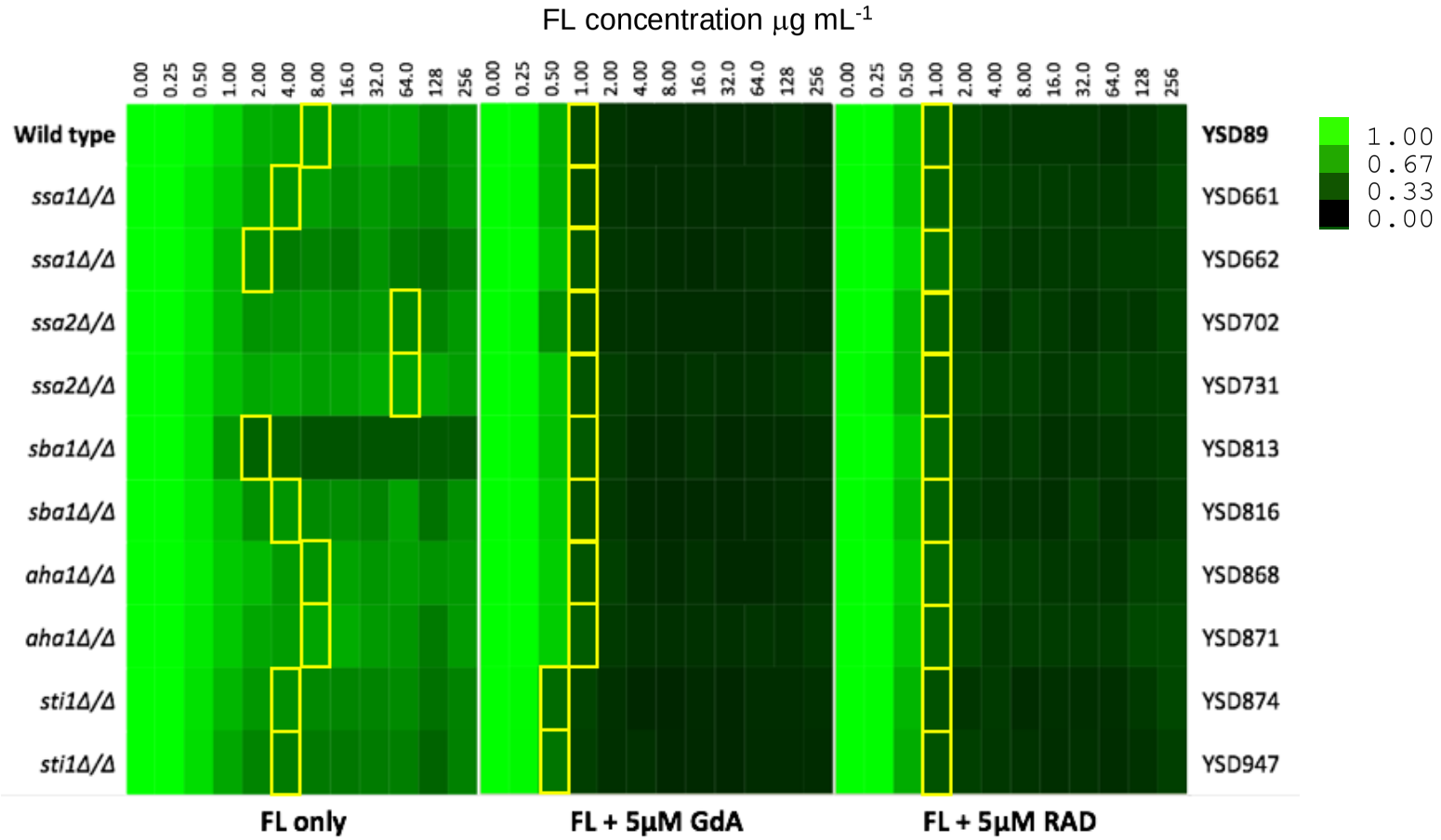

Figure 4.8 Heat maps showing growth of all strains in drug conditions; fluconazole only, fluconazole and geldanamycin, and fluconazole and radicicol. Fluconazole (FL) μg mL^{-1} is shown on the x axis. Geldanamycin (GdA) and radicicol (RAD) concentrations are static (5 μM) where present. Bright green denotes maximum growth, while darker colours show reduced growth. Yellow boxes mark MIC_{40} in fluconazole only, and MIC_{50} in the other two conditions.

It was expected that the addition of geldanamycin and radicicol to the cultures would yield similar effects to one another as they are both Hsp90 inhibitors, although recent research suggests that they target it differently [192]. Hsp90 plays an important role in drug resistance and so a low level of inhibition of its function can abrogate resistance to fluconazole, as well as other antifungal drugs [35, 89].

Geldanamycin and radicicol were added to every well in the 96-well plates, to a final concentration of 5 μM for both. Only fluconazole was added on a gradient ranging from 0 μg mL^{-1} to 256 μg mL^{-1}. Growth in the wells without fluconazole reached the same optical density, regardless of the presence of geldanamycin or radicicol. This shows that 5 μM of Hsp90 inhibitor alone does not affect overall growth success of the cells. The combination of Hsp90 inhibitors with fluconazole, however, had a pronounced effect.

With the addition of geldanamycin, the MIC_{50} dose of fluconazole was 1 μg mL^{-1} for all strains except for the *sti1Δ/Δ* strains; YSD868 and YSD871, which were inhibited by the lower concentration of 0.5 μg mL^{-1}. This emphasises the importance of Hsp90 as its inhibition renders the resistance levels of the mutant strains almost identical to the wild type and masks the effects of gene deletions seen in the fluconazole-only assay.

When radicicol was added, the results were similar to geldanamycin; the MIC_{50} dose was 1 μg mL^{-1} for all strains, this time including the *sti1Δ/Δ* strains. However, both *sti1Δ/Δ* mutants were more inhibited than others at this

concentration as 1 μg mL^{-1} in fact inhibited more than 65% of the growth. This is compared to only 30% inhibition at 0.5 μg mL^{-1} fluconazole with 5 μM radicicol, which is consistent with previous findings [193]. Sti1 plays an important role in drug resistance, meaning that combinatorial therapy using an existing antifungal with a Sti1 inhibitor may prove a useful tactic for treatment of infections.

4.6 Ssa2 suppresses hyphal morphogenesis

Formation of hyphae is known to be instrumental in causing infection, and mutants which are unable to undergo morphogenesis are avirulent. This is in part due to resistance to the host immune system, as yeast cells engulfed by macrophages will filament to escape [194].

To measure the ability of cells to switch from yeast to hyphal morphology, they were grown in 10% bovine serum for 90 minutes at 37ºC during log phase and measured in microscopy images. Odds' morphology index was used to convert measurements from microscopy images of cells into a value for each cell, which could then be compared statistically [195]. A morphology index reading close to 5.0 is considered true hyphae. For each strain, 100 cells were assessed and morphology indices calculated (Fig. 4.9).

The distribution of measurements for all strains is skewed, which is reflected in the average values as each median value is lower than the corresponding mean (Table 4.5). The mean morphology indices for each strain were compared by linear regression analysis and pairs of mutants were compared to one another by analysis of variance.

The *ssa2Δ/Δ* mutants both significantly outperformed the wild type strain in rapid hyphal formation. The boxplots clearly show that the spread of morphological indices for YSD702 and YSD731 extends further towards true hyphae than the wild type strain (Fig. 4.9, Table 4.5). Comparison between the data sets for the two *ssa2Δ/Δ* mutants also shows that they behave almost identically to one another. Ssa2 is known to be a component of the hyphal cell wall so it interesting that its absence should lead to an increase in speed of hyphal formation, while also being impaired in biofilm formation [110].

The mean morphology index for homozygous null mutant for *SSA1,* YSD661 was almost identical to that of the wild type strain, YSD89. However, its counterpart mutant, YSD662 had a smaller average morphology index, with marginal significance ($p=0.014$). This means that YSD662 formed fewer hyphae than the wild type and the cell morphologies were on average closer to the round yeast shape. This result mirrors what was observed in the analyses of colony morphology on solid growth media (Fig. 4.6). When YSD661 and YSD662 were compared to one another by ANOVA they were found to differ significantly ($p=0.004$).

The *sba1Δ/Δ* strains, YSD813 and YSD816, both showed increased hyphal formation relative to the wild type. For YSD813 this was a significant increase ($p=0.002$), whereas for YSD816 the difference was insignificant. However, ANOVA comparison between the two data sets for YSD813 and YSD816 showed that they did not differ significantly from one another.

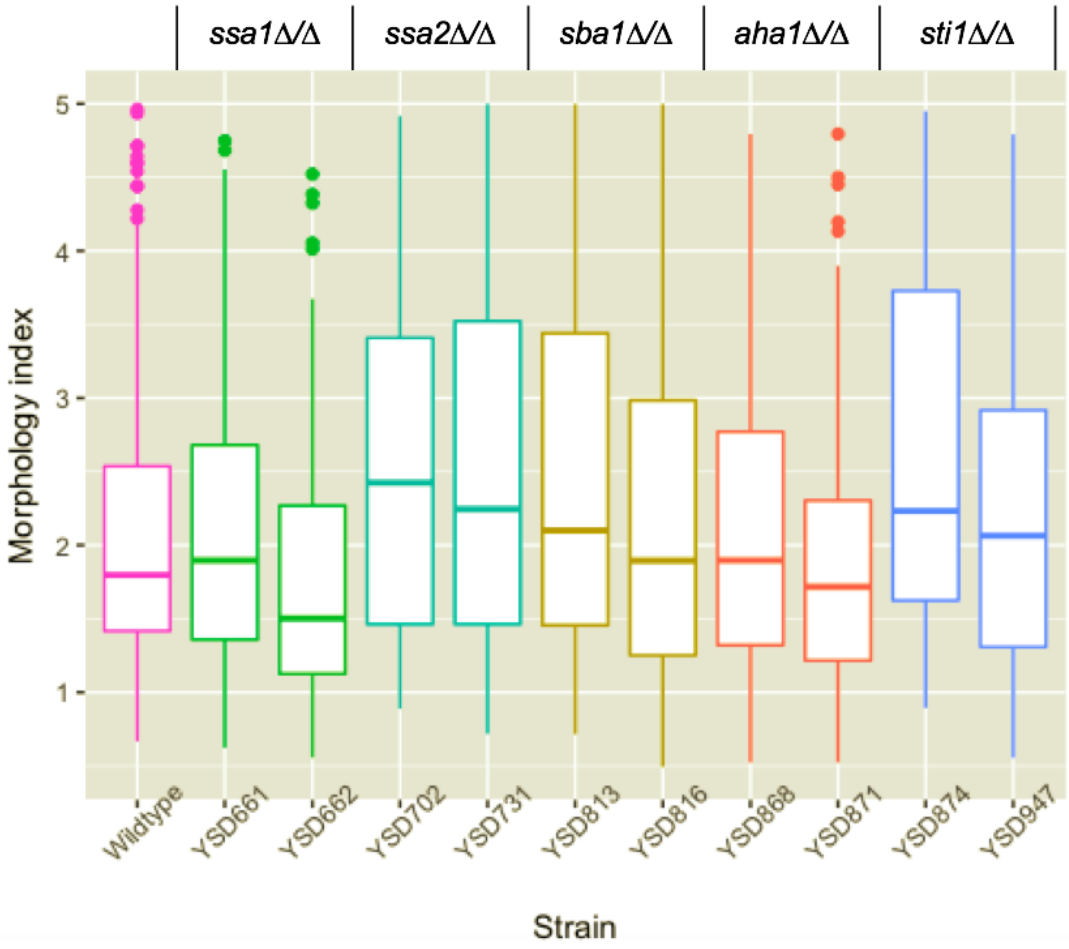

Figure 4.9 Boxplots of morphology indices. Data are based on 100 cells for each strain. Horizontal bars show mean and interquartile range for each strain, while vertical extending bars show the extreme ends of the values. Dots indicate outlier values.

Table 4.5 Summary of hyphal morphogenesis, including mean and median morphology index values for each strain, and statistical p-values. “+/-“ denotes whether the morphology index for each strain is larger (+) or smaller (-) than the wild type strain. “LM p-value” denotes the p-values generated by the mixed linear model used, “A p-value” are the p-values from ANOVA comparison between the mutant pairs. Significance codes are; “***” p<0.001, “**” 0.001<p<0.01, “*” 0.01<p<0.05.

STRAIN	GENOTYPE	MEAN	MEDIAN	+/-	LM P-VALUE	A P-VALUE
YSD89	Wild type	2.107	1.797	n/a	n/a	n/a
YSD661	*ssa1*Δ/Δ	2.158	1.896	+	0.669	0.004**
YSD662	*ssa1*Δ/Δ	1.806	1.502	-	0.014*	
YSD702	*ssa2*Δ/Δ	2.525	2.424	+	0.003**	0.919
YSD731	*ssa2*Δ/Δ	2.546	2.245	+	0.002**	
YSD813	*sba1*Δ/Δ	2.537	2.100	+	0.002**	0.070
YSD816	*sba1*Δ/Δ	2.245	1.894	+	0.214	
YSD868	*aha1*Δ/Δ	2.181	1.897	+	0.671	0.119
YSD871	*aha1*Δ/Δ	1.946	1.717	-	0.181	
YSD874	*sti1*Δ/Δ	2.642	2.233	+	<0.001***	0.011*
YSD947	*sti1*Δ/Δ	2.201	2.065	+	0.534	

Neither of the homozygous null mutants for *AHA1* differed significantly from the wild type in speed of hyphal formation. YSD868 had a very slightly higher morphology index than the wild type, while YSD871 was slightly lower (table 4.4) so the absence of Aha1 was deemed to have no impact on hyphal formation. The two data sets also did not differ from one another (p=0.119).

Homozygous null mutants for *STI1* significantly differed from one another in speed of hyphal formation ($p=0.011$). The disparity is evident in the boxplots (fig. 4.8) with the spread of values for YSD874 extending further towards the higher end of the scale. YSD874 significantly outperformed the wild type strain in speed of hyphal formation ($p<0.001$), while the difference for YSD947 was insignificant ($p=0.534$).

Differences in speed of hyphal formation are, with the exception of *ssa1Δ/Δ* strain YSD662, all due to mutants outperforming the wild type strain. These results defy expectations as morphological switching between yeast and hyphal growth is considered an indispensable virulence trait [29, 30], and deletion of Hsp90 co-chaperone genes was anticipated to confer defects in virulence traits.

4.7 *ssa1*Δ/Δ mutant pair disparities suggest second-site mutations

The phenotypes observed in the mutant pairs, which should be phenotypically identical, are far more variable than expected (Table 4.6). It is possible that second-site mutations occurred in the transformation process which colony PCR genotyping could not detect, as it is only designed to confirm deletion of the intended allele. It is also possible that the variations are due to noisy phenotype data, and so it is important to consider the overall trends observed. In all assays, the *ssa2*Δ/Δ and *aha1*Δ/Δ mutant pairs behaved identically to one another, suggesting that these strains are indeed genotypically identical.

The *sba1*Δ/Δ mutants exhibited differential behaviour in heat shock and drug resistance, but were both identical to wild type in oxidative stress and colony morphology. However, despite differences in the drug resistance assay, the *sba1*Δ/Δ mutants exhibited a similar trend of reduced drug resistance relative to the wild type strain.

The *sti1*Δ/Δ mutants showed disparity in oxidative stress, heat shock, and hyphal formation, while being identical in the other three virulence assays. As well as statistical disparities, the *sti1*Δ/Δ mutants exhibit different trends, with the group one mutant showing defects, while the group two mutant more often shows no phenotypic difference relative to the wild type.

The *ssa1*Δ/Δ mutants were the most dissimilar pair, showing differential behaviour in every virulence assay. The two mutants behave differently not

just statistically in the assaya but also exhibit opposing trends; for example, in the colony morphology assay (Table 4.6). The *ssa1*Δ/Δ mutants showed the same trends as one another only in the biofilm formation and drug resistance assays, but still behaved differentially in both of those. This is a strong suggestion that there are more differences in the genome than the single homozygous gene deletion attempted and there may be multiple second-site mutations, with a range of phenotypic effects. Genome sequencing is advisable here to identify the mutations that have arisen and identify the cause of disparities observed.

The heat shock assay delivered the least consistent results of the *in vitro* virulence assays carried out here. As well as investigating differences of behaviour in the mutants it may be worthwhile to invest in further refinement and optimisation of some of the protocols employed.

Table 4.6 Summary of virulence assays outlining where mutant strains differed from the wild type and whether the virulence trait was reduced, enhanced, or unchanged. The "disparity" column states whether the mutant pairs behaved differently to one another.

ASSAY	GENOTYPE	GROUP 1	GROUP 2	DISPARITY
Oxidative stress	*ssa1*Δ/Δ	None	Reduced	Yes
	*ssa2*Δ/Δ	Enhanced	Enhanced	No
	*sba1*Δ/Δ	None	None	No
	*aha1*Δ/Δ	None	None	No
	*sti1*Δ/Δ	Reduced	None	Yes

ASSAY	GENOTYPE	GROUP 1	GROUP 2	DISPARITY
Heat shock	*ssa1*Δ/Δ	None	Reduced	Yes
	*ssa2*Δ/Δ	None	None	No
	*sba1*Δ/Δ	Reduced	None	Yes
	*aha1*Δ/Δ	None	None	No
	*sti1*Δ/Δ	Reduced	None	Yes
Colony morphology	*ssa1*Δ/Δ	Enhanced	Reduced	Yes
	*ssa2*Δ/Δ	None	None	No
	*sba1*Δ/Δ	None	None	No
	*aha1*Δ/Δ	None	None	No
	*sti1*Δ/Δ	Enhanced	Enhanced	No
Biofilm formation	*ssa1*Δ/Δ	Reduced	Reduced	Yes
	*ssa2*Δ/Δ	Reduced	Reduced	No
	*sba1*Δ/Δ	Reduced	Reduced	Yes
	*aha1*Δ/Δ	Reduced	Reduced	No
	*sti1*Δ/Δ	Reduced	Reduced	No
Drug resistance	*ssa1*Δ/Δ	Reduced	Reduced	Yes
	*ssa2*Δ/Δ	Enhanced	Enhanced	No
	*sba1*Δ/Δ	Reduced	Reduced	Yes
	*aha1*Δ/Δ	None	None	No
	*sti1*Δ/Δ	Reduced	Reduced	No
Hyphal formation	*ssa1*Δ/Δ	None	Reduced	Yes
	*ssa2*Δ/Δ	Enhanced	Enhanced	No
	*sba1*Δ/Δ	Enhanced	None	No
	*aha1*Δ/Δ	None	None	No
	*sti1*Δ/Δ	Enhanced	None	Yes

4.8 Discussion

Homozygous null mutants for *SSA2* appear in most virulence traits to be unimpaired, or even to have an advantage over the wild type strain, YSD89. Thus, Ssa2 appears to be a negative regulator of virulence traits, which are therefore enhanced in its absence.

SSA2 expression is known to be repressed by caspofungin, while human ß-defensins depend on the presence of Ssa2 on the cell surface for their candidacidal activity [196, 197]. Coupled with the effect of increased virulence found here, this suggests that employing Ssa2 as a drug target would be ill-advised.

It was already known that Ssa2 binds antifungal compounds on the surface of the cell, and that its absence therefore confers resistance to some antifungal compounds [114, 117]. It was, however, not previously known that deletion of *SSA2* could confer phenotypic advantages in oxidative stress and hyphal morphogenesis and the reasons for this are thus far unclear. Ssa2 may have a general role in binding extracellular compounds, and therefore increases susceptibility to oxidative stress as well as to antifungal drugs. It is possible that the accelerated growth of hyphae in the mutants may also compromise integrity of the hyphal cell wall structure and thus compromise fitness, but this remains to be seen.

As an Hsp70 orthologue, Ssa2 has been implicated in heat shock tolerance but the homozygous null mutants showed no defects in this study. This result may be explained by the similarity of Ssa1 and Ssa2; with 87.2% protein sequence identity [116], it is possible that Ssa1 is compensating for the absence of Ssa2, and vice versa. Quantification of Ssa1 and Ssa2 protein expression in these strains compared to the wild type may show whether they are each upregulated in response to the other's absence.

It was attempted here to ascertain whether the two Hsp70 orthologues, Ssa1 and Ssa2, compensate for the absence of one another by generating homozygous null mutants for both genes. This was a fruitless venture with the *NAT* recyclable marker, which may be due either to one Hsp70 orthologue being required for viability, or to the inefficiency of the reaction. This gene deletion may be attempted in future using the *CRISPR* method [165], or repressible promoters could be cloned in place of the native promoters to deplete protein levels and investigate essentiality and Ssa1 and Ssa2 in combination [198].

The group two *ssa1*Δ/Δ mutant, YSD662, did exhibit lower tolerance to heat shock, but as the mutants are clearly different to one another, this may not be due to the deletion of *SSA1*. The pair showed similar discrepancies throughout all virulence assays, with YSD662 being the weaker strain in every case. Genome sequencing would help to solve this mystery and identify the additional mutations which are conferring these phenotypes. Although YSD661 performed well in heat shock and hyphal formation, Ssa1 is known to

be required for hyphal formation in heat shock conditions, which highlights the limitations of testing virulence traits individually [199].

The role of Sba1 in these virulence traits is not entirely clear due to the disparity of behaviour between the two strains. A role in oxidative stress resistance can be confidently ruled out as neither strain deviated significantly from the wild type strain in that assay. It can likewise be stated that Sba1 is important for biofilm formation and for fluconazole resistance as both strains were defective in these traits, though to differing degrees. It is as yet uncertain whether these differences are due to experimental variation, or to underlying mutations in the genome having arisen in transformation.

However, the group one *sba1*Δ/Δ mutant (YSD813) exhibited a defective heat shock response and faster speed of hyphal formation, while YSD816 performed the same as the wild type strain in these conditions. It is therefore not known to what degree Sba1 is involved in the heat shock response or in growth of hyphae. However, absence of the wild type allele in both strains was confirmed in duplicate by colony PCR, suggesting that the defects observed in YSD813 are likely to be due to second-site mutations.

The homozygous null mutants for *AHA1* were found to have defects only in biofilm formation, but in no other virulence assay here. Although *AHA1* expression is upregulated in response to oxidative stress and in biofilms [15, 122], these results suggest that it is not actually required for most virulence traits and that its absence is compensated for. In fact, deletion of the *AHA1*

orthologue in *S. cerevisiae* has been shown to increase competitive fitness [200].

Sti1 appears to be required for biofilm formation; although morphology of the null mutants appeared to be enhanced relative to the wild type on solid media they then performed poorly in the biofilm assay. As the biofilm assay includes wash steps, it may be that Sti1 specifically regulates biofilm adherence, which is then compromised in its absence. This is consistent with findings from the *STI1* orthologue in *S. cerevisiae* [201].

For most of the strains tested, the data produced for the biofilm formation assay was bimodal in nature. Strains either successfully formed biofilms with high metabolic activity readings, or biofilms were completely washed off the surface before readings were taken. The negative control strain, ***bcr1*Δ/Δ,** was an extreme example, forming exclusively biofilms which were completely washed off. Otherwise, the ***ssa1*Δ/Δ** and ***sti1*Δ/Δ** mutants were the only strains not to conform to this pattern and produce a spread of OD_{492} readings along the scale.

Very low biofilm readings were considered to be due to poor adherence, as biofilms did form, but were washed off the surface easily. Anecdotally, biofilms which produced very low readings were washed off the surface whole, while intermediate readings were produced when the biofilm came apart slightly wash steps. It appears that as well as biofilm formation and adherence, there is an additional effect of biofilm integrity to be taken into account; the ability of

the cells to adhere to one another as well as to the surface of the plate. This effect may be of relevance in a clinical setting; as an opportunistic pathogen, if *C. albicans* is already present in the host, its ability to form biofilms which adhere strongly to an inorganic surface may be less relevant than the strength with which the cells adhere to one another.

The trend of Hsp90 co-chaperone null mutants outperforming the wild type strain in speed of hyphal formation was not anticipated. The reason may lie in a mechanism of suppression of hyphal formation, which is compromised when these genes are deleted. Hyphal formation is known to be important for biofilm formation, but these mutant strains with faster hyphal formation were all defective in biofilm formation. It appeared that defects in adherence were more relevant to the lack of success for mutant strains in the biofilm assays; all strains formed biofilms, which were then lost in the wash steps. Additionally, strains which form hyphae more quickly may not necessarily form hyphae of equivalent structural integrity than the wild type strain.

It remains, even now, common practice to generate a single null mutant to investigate the role of a gene in *C. albicans* virulence phenotypes [202-204]. The results presented here demonstrate the importance of corroborating phenotype data with multiple mutants, as results between mutant pairs can show significant disparities. Desite the rigorous verification of gene deletion completed in the previous chapter, *in vitro* virulence studies suggest the possibility of underlying mutations, especially in the *ssa1*Δ/Δ mutant strains, YSD661 and YSD662.

Alternatively, the disparities observed, especially the smaller disparities as seen in the *sba1*Δ/Δ and *aha1*Δ/Δ mutant strains may be due to noisy phenotype data produced as an artefact of the protocols used. Protocols were optimised using the extremes of positive and negative controls, with the wild type strain and null mutants such as the *hog1*Δ/Δ and *bcr1*Δ/Δ strains. However, they may not be adequately refined to prevent random variation from confounding the results. The phenotypes observed here should be investigated more thoroughly, using alternative methods and more null mutant strains.

It should also be stated that when a single null mutant is investigated, a complemented strain is typically also generated, to establish that wild type phenotype is restored to the organism when the wild type gene is restored to the genome. This is, however, not always the case, and confirmation of the effects of gene deletion should be carefully considered.

It is impossible to state the importance of particular virulence traits when tested individually, *in vivo* testing gives a more complete picture of the pathogenic capability of the strains. *Manduca sexta* fifth instar larvae were used for this purpose.

5. Characterisation of Hsp90 co-chaperone null mutants in *in vivo* virulence assays with *Manduca sexta* fifth instar larvae

Virulence assays *in vivo* are a holistic approach for comparing the virulence of different strains. Significant defects in individual virulence traits may not always preclude strains from causing morbidity in a host and so the use of a host model compliments the use of *in vitro* virulence assays. Testing of individual virulence traits can never be exhaustive and *in vivo* virulence assays help to give a full and clear picture of the differences in virulence between strains. *Manduca sexta* fifth instar larvae were used in this study as an invertebrate model in keeping with the *NC3R* guidelines to reduce usage of vertebrate hosts [149]. The University of Bath maintains an inbred population that is maintained by a technician following standard operational protocols, ensuring continuity. The colony is regularly used for research, including bacterial and parasitic infection studies [205-207].

It is difficult to ascertain from individual virulence assays how important each trait is in the context of an animal infection. Animal models are a useful tool for quantifying the effect of a pathogen on the whole organism system.

5.1 *C. albicans* infection causes morbidity and mortality in *Manduca sexta* fifth instar larvae

This use of *Manduca sexta* as a model host organism for fungal infections is pioneering [160]. They are however well-established for use in research of flight mechanics [208], toxicology [209-211], and as a model of bacterial infection, including *E. faecalis* and *S. pneumoniae* [146-148]. The crop-pest larvae lend themselves to a study of this type for a number of reasons. Firstly, the caterpillars are cheap to use and carry few ethical implications in comparison to vertebrate infection models, such as mice. Secondly, unlike *Galleria melonella*, which are commonly used as fungal infection models, *M. sexta* larvae are large enough to be injected with a precisely defined dose of fungal cells, and the horn can be clipped to take samples of haemolymph for analysis of the progression of infection during the experiment if desired. Finally, *Manduca sexta* hail from tropical climes [212] and thus the experiment can be run at the physiologically relevant temperature of 37°C, which is often not the case when using invertebrate infection models.

The University of Bath hosts a colony of *Manduca sexta*, also known as the tobacco horn worm. The colony has been inbred since 1978 and so individuals are genetically similar, making them useful for experimental consistency. Research on animals is carried out according to the principles of the *National Centre for Replacement, Refinement & Reduction of Animals in Research* [149, 163].

The experiment starts with caterpillars shedding from fourth instar to fifth instar, and finishes when they are beginning to pupate. During this stage in development the animals will normally increase in body weight up to five-fold; almost doubling each day. A significant infection disrupts their development, so changes in body weight can be used as a measure of morbidity. The animals are also screened each day for death.

What is unknown about the University of Bath *Manduca sexta* colony is how much the animals differ genetically from the published genome [150] having been inbred for almost four decades. In future, the Diezmann lab intends to re-sequence the genome for the University of Bath colony, using the established phenol chloroform method for genomic DNA extraction from insects [213]. The *M. sexta* genome is known to exhibit significant variation between male and female, with female animals having the repetitive W chromosome, not present in male animals [214]. Sexual dimorphism begins in early larval development, with female animals ultimately growing larger than male animals [215]. Dimorphism is known to apply also to the immune system, though evidence for this suggests this divergence begins at a more mature stage than the animals used in this study. There is no statistical indication of sex differences in susceptibility to infection between male and female animals used in *in vivo* infection models [216]. Animals in this study were not screened for sex so it cannot now be determined whether this caused any discrepancies in the data. However, animals were selected and assigned to groups at random so there should be an approximately equal balance of male and female animals in the study.

For these assays, the strains are split into two groups, as before; group one and group two, each containing one mutant of each pair. The wild type strain, YSD89, was used as a positive control in all assays and included in both groups. There was also a saline control included in all replicates.

5.1.1 Deletion of *SSA1* reduces *C. albicans* morbidity in *M. sexta*

Systemic infections, including *C. albicans,* are well-known to cause loss of body weight as a major symptom [217]. Changes in body weight were used as a measure of morbidity in this study and animal weights were measured at 24-hour intervals and compared to the saline control. Animals were weighed daily until either the end of the assay, or until they succumbed to infection.

The starting weight of animals was measured on day 0 and analysed by ANOVA to ensure that animals in different treatment groups were approximately the same weight. No significant differences were found between different treatment groups within any biological replicate, with p-values ranging from p=0.776 to p=0.999. However, variation in initial starting weight is evident from the plots (Fig. 5.1 and 5.2) as the batches of caterpillars can develop at differing speeds. This was accounted for in the analysis as results were nested within date.

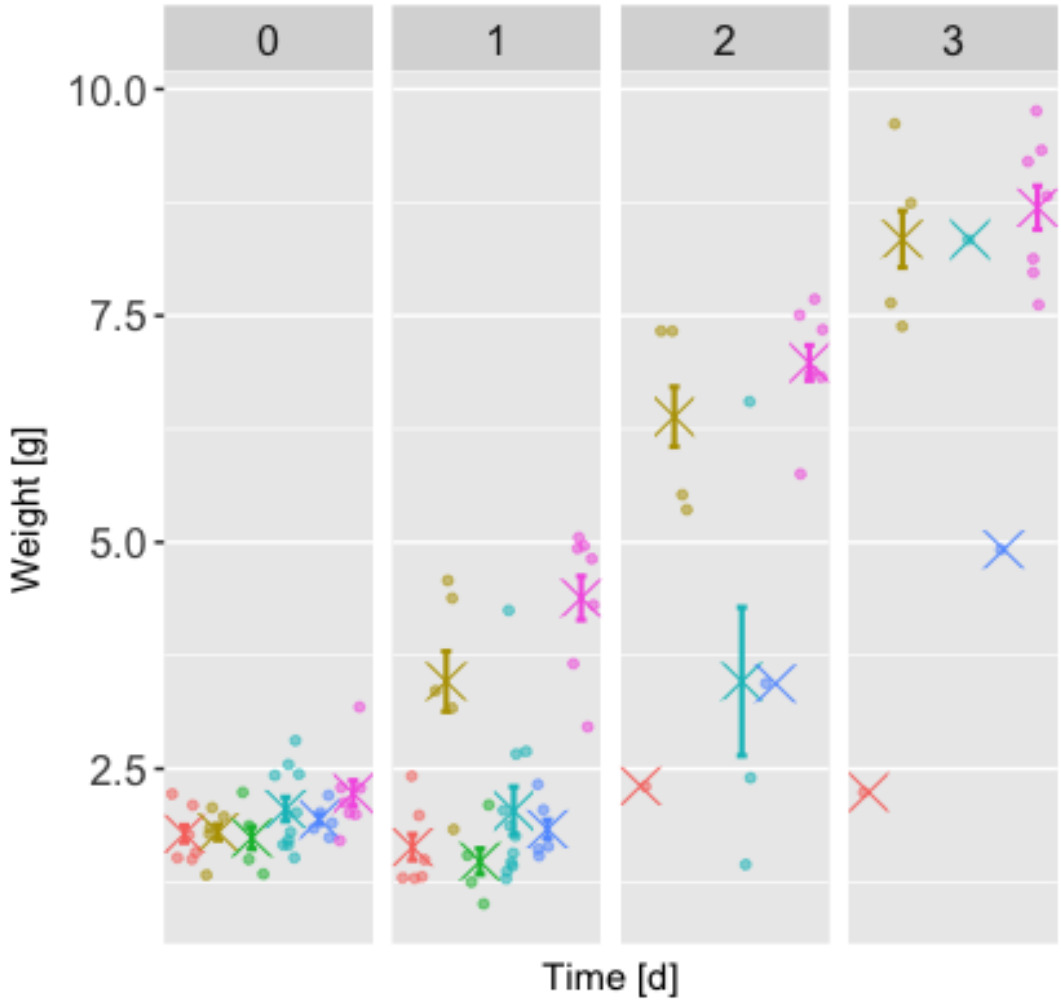

Figure 5.1 The weights of *Manduca sexta* larvae which survived at least one day following infection with group one mutants. The wild type strain does not appear as none of the animals infected with YSD89 survived 24 hours and so no weight changes were observed. The data points denote caterpillar weights in grams plotted against time in days. Data represent three biological replicates. Crosses denote mean weights, with standard error bars protruding: YSD661 *ssa1*Δ/Δ, YSD702 *ssa2*Δ/Δ, YSD813 *sba1*Δ/Δ, YSD868 *aha1*Δ/Δ, YSD874 *sti1*Δ/Δ, saline control.

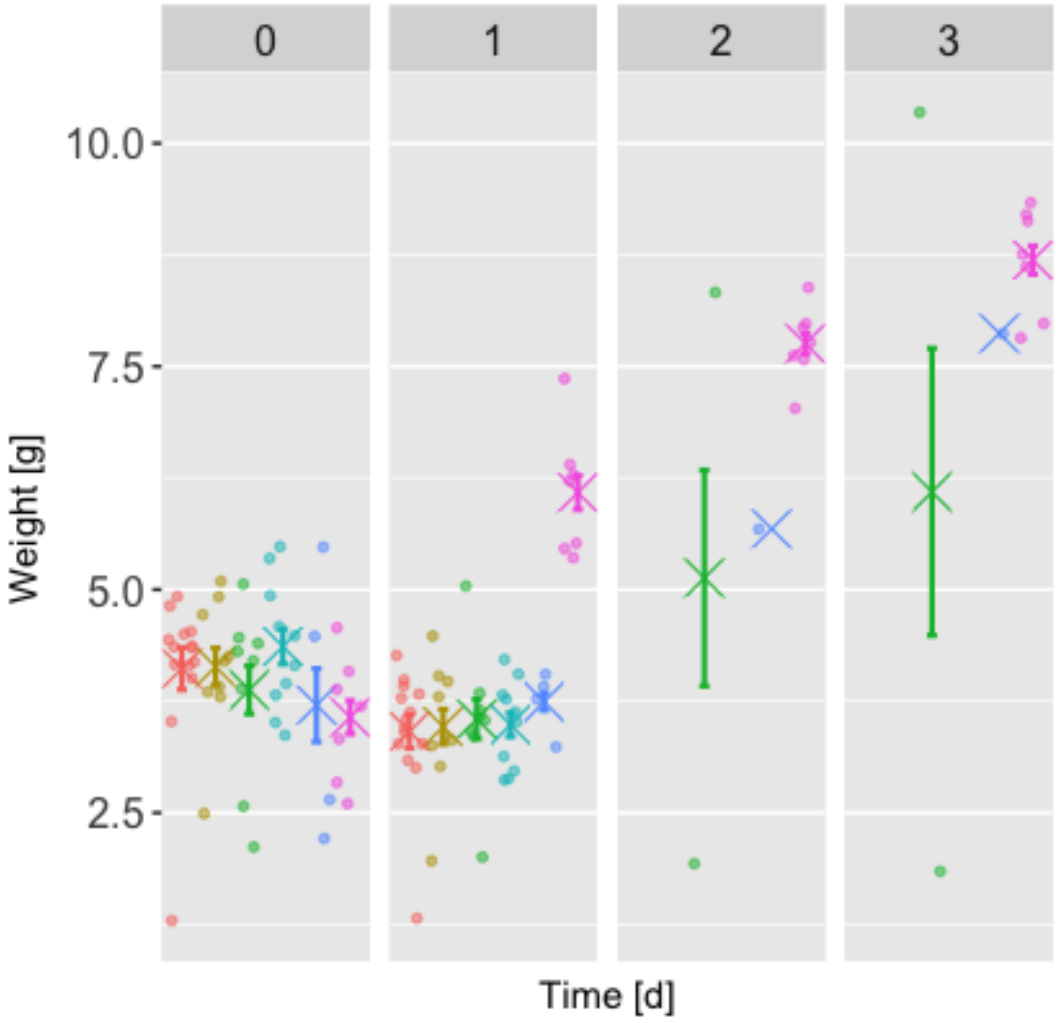

Figure 5.2 The weights of *Manduca sexta* larvae which survived at least one day following infection with group two mutants. The wild type strain does not appear as none of the animals infected with YSD89 survived 24 hours and so no weight changes were observed. The data points denote caterpillar weights in grams plotted against time in days. Data represent three biological replicates. Crosses denote mean weights, with standard error bars protruding: YSD662 *ssa1*Δ/Δ, YSD731 *ssa2*Δ/Δ, YSD816 *sba1*Δ/Δ, YSD871 *aha1*Δ/Δ, YSD947 *sti1*Δ/Δ, saline control.

Morbidity was quantified in surviving animals by changes in body weight. Negative control animals, injected with saline only, gained weight extremely quickly over the course of the experiment; typically starting on day zero under 2.5 g and finishing on day three between 7.5 g and 10 g. This is normal development and demonstrates that the injection of fluid in itself does not exert significant stress on the animals.

Animals injected with phosphate buffered saline (PBS) were used as the control group for statistical analyses of body weight changes in the study. The weights of groups were analysed using ANOVA, which showed significance in weight comparisons between treatments on day one ($p<0.0001$). This was followed by Dunnet's test for multiple comparisons between the weights of animals infected with each strain and the PBS control animals. These again show statistical significance as the control animals developed normally but the infected animals lost weight; the p-values for the Dunnet's test on day one were $p<0.0001$ for all strains except the *ssa2*Δ/Δ mutant strains, which were $p=0.0002$. This means that infection with all strains caused severe morbidity and impaired proper development and growth. Thus, deletion of the co-chaperone genes, though they may be involved in virulence, did not abolish virulence.

On days two and three, the waning numbers of surviving animals mean that the statistical analyses lose power. On day two, the ANOVA test still showed a significant difference in body weights between the treatment groups ($p=0.0367$), but the Dunnet's test comparing the effects of the different strains

to the PBS control animals was only significant for the animals infected with the *ssa1*Δ/Δ mutant strains (p=0.0188). This is because the severely affected animals had succumbed to infection, while the small number of unaffected animals continued to gain weight and increase the mean body weight of the group.

On day three, with only very few animals remaining, the analyses ceased to show any statistical significance in differences of body weights between the treatment groups in any test. In the future, a larger scale of study may help to combat this challenge. Or, alternatively, refining the initial infective dose to an amount which causes morbidity but a lower rate of mortality may serve to make body weight data more informative statistically.

The response of infected animals became bimodal; they would either appear unaffected by the pathogen and gain weight as normal, or lose weight before dying. Based on daily observations and inspections, animals appear to lose weight due to a combination of loss of appetite and dehydration. The usefulness of the mean values in recording weights is dubious; smaller animals die early on in the study and thus the remaining survivors carry undue significance in increasing the average weight.

The bimodal effect in weight-gain is most evident in cases when the infection was most abiding, for example in the two animals which survived until day three when infected with the *sba1*Δ/Δ strain, YSD816. One of the animals was

unaffected and grew to over 10 g, while the other lost a small amount of weight each day but, unusually, did not succumb.

Figure 5.3 Experimental subjects one day post infection. (A) Live caterpillar from the control group, injected with saline only, and (B) dead caterpillar following injection with the wild type strain, YSD89.

Symptoms of morbidity could also be detected visually, with afflicted animals gradually becoming discoloured with spots of melanisation (Fig. 5.3). This was a useful indication at each time point of whether an animal was likely to survive until the next day. They are typically lethargic in isolation even when healthy and so the colour of the animals was indicative of morbidity in the absence of behavioural traits. Anecdotally, it also appeared evident that animals suffering from symptoms were more irritable and sensitive to touch. If this is indeed the case then it may be related to the loss of appetite observed in afflicted animals if sensitivity extends to the chewing mouthparts.

The injection method means that strains in this assay can still cause disease with significant impairment of invasion. To test the capacity of mutant strains to colonise and invade healthy animals it may be possible in future to develop a method for oral infection of *Manduca sexta* larvae with *C. albicans*.

5.1.2 Deletion of Hsp90 co-chaperones slows mortality in an invertebrate model of infection

Manduca sexta fifth instar larvae were injected in the rear right proleg with 10^6 cells in 100 μL phosphate buffered saline (PBS) and kept at 37°C for the duration of the experiment. The wild type strain, YSD89 was used as the positive control, and killed all animals within 24 hours of inoculation.

PBS was used as the negative control; animals were injected with the same volume of saline without cells to verify that they were not stressed by the injection procedure itself. All of the negative control animals survived to the end of the assay. In both groups of mutants, a log rank test showed a significant difference between the treatments ($p<0.0001$). The PBS control had a disproportionate effect on the analysis as all individuals survived, and so was excluded from the remaining analyses. When excluded, there was still significant difference found between the different treatments; $p=0.036$ in group one mutants, and $p=0.023$ in group two mutants.

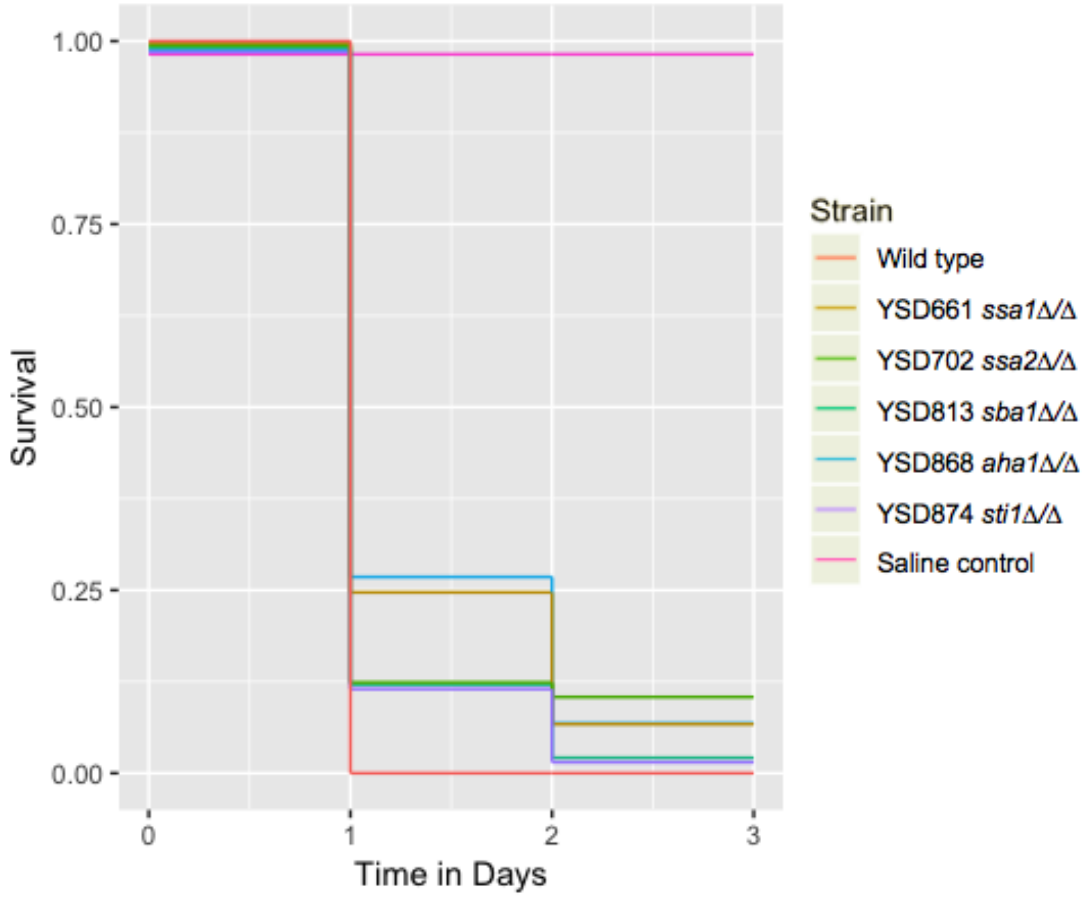

Figure 5.4 Kaplan-Meier plot showing survival of fifth instar *Manduca sexta* larvae infected with group one mutants. The wild type strain, YSD89, was used as a positive control; saline as negative control. Data represent 10 technical replicates and 3 biological replicates. For visibility of data for all strains, *y* values are jittered consecutively by -0.003.

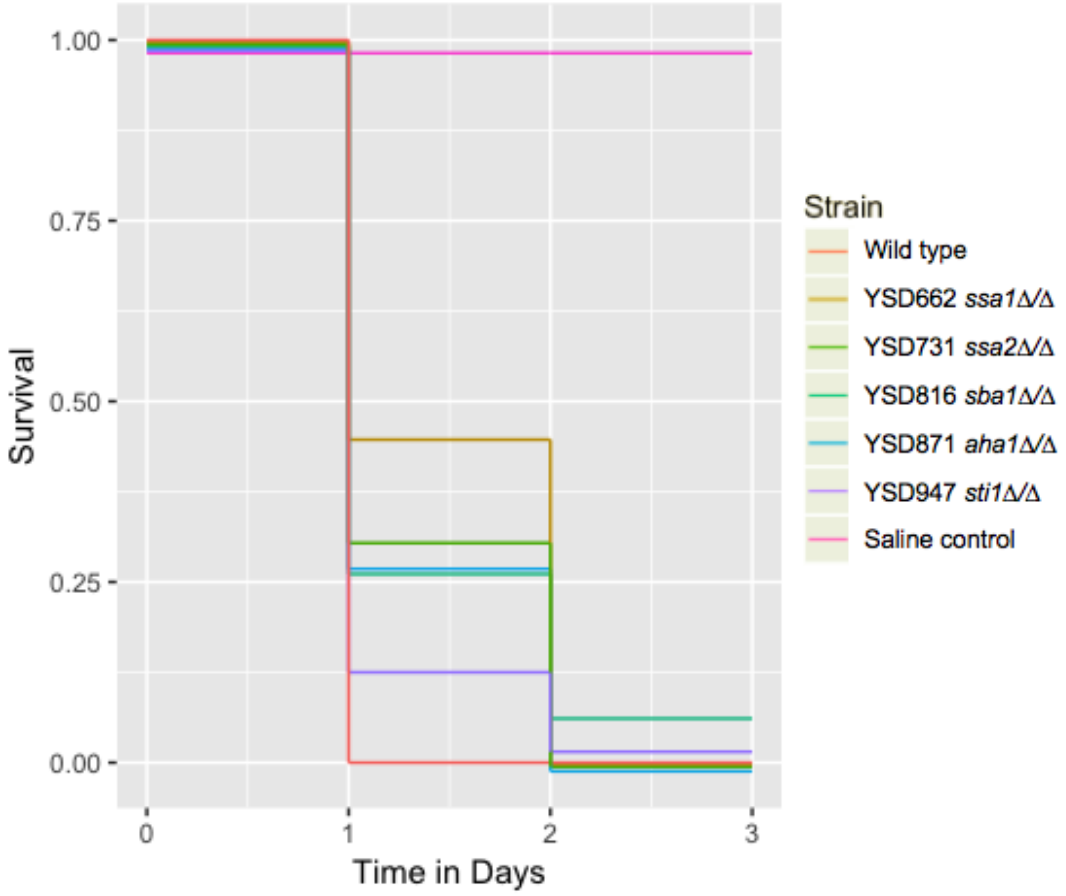

Figure 5.5 Kaplan-Meier plot showing survival of fifth instar *Manduca sexta* larvae infected with group two mutants. The wild type strain, YSD89, was used as a positive control; saline as negative control. Data represent 10 technical replicates and 3 biological replicates. For visibility of data for all strains, *y* values are jittered consecutively by -0.003.

All of the mutant strains exhibited statistically significant differences in the Kaplan-Meier curves relative to the wild type strain; none of them killed all of the animals within one day (Fig. 5.4 and 5.5). The most significant differences, consistent in both groups of mutants, were in the *ssa1*Δ/Δ and *aha1*Δ/Δ mutants, which left the largest proportions of surviving animals one day post-infection.

The curves for the *ssa1*Δ/Δ mutants; YSD661 and YSD662, differed significantly from the wild type YSD89 curves (Table 5.1). This is in keeping with findings from a murine model of infection, where *ssa1*Δ/Δ mutants showed attenuated virulence [110]. The *aha1*Δ/Δ mutant curves; YSD868 and YSD871, also differed significantly from the wild type curves (Table 5.1). The *aha1*Δ/Δ mutants were the only ones for which the group two mutant, YSD871, exhibited slightly less significance in the difference of the killing curve compared with the wild type. In all other strains, the mutant in group two had a lower p-value in the killing curve log-rank test. While the pairs of mutants should be genetically identical, this trend may be due to differences in the groups of animals. The average starting weight for the animals infected with group two mutants was clearly higher than for those infected with group one mutants (Fig. 5.2). This strongly implies that the yeasts were less able to kill the larger animals when the dose was the same. However, as the death rate remained unchanged for the wild type strain, the statistical comparisons remain valid.

The *ssa2*Δ/Δ and *sba1*Δ/Δ mutants also showed significance in Kaplan-Meier analysis (Table 5.1), meaning that they are significantly less able to kill the invertebrate host than the wild type strain.

Table 5.1 p-values for survival of animals infected with mutant strains relative to the wild type, calculated by Mantel-Cox log-rank tests. Significance codes are; "***" p<0.001, "**" 0.001<p<0.01, "*" 0.01<p<0.05.

STRAIN	GENOTYPE	P-VALUE
YSD661	*ssa1*Δ/Δ	0.003**
YSD662	*ssa1*Δ/Δ	<0.001***
YSD702	*ssa2*Δ/Δ	0.011*
YSD731	*ssa2*Δ/Δ	0.001***
YSD813	*sba1*Δ/Δ	0.035*
YSD816	*sba1*Δ/Δ	0.002**
YSD868	*aha1*Δ/Δ	0.001**
YSD871	*aha1*Δ/Δ	0.002**
YSD874	*sti1*Δ/Δ	0.037*
YSD947	*sti1*Δ/Δ	0.031*

The *sti1*Δ/Δ mutants showed the least significance in comparison with the wild type with p=0.037 for YSD874 and p=0.031 for YSD947. This suggests that *STI1* is the least important of the genes tested in these types of infection (Fig. 5.5). The lower level of significance means that the *sti1*Δ/Δ mutants were

closer in virulence capability to the wild type strain. However, that this result is still significant demonstrates that all of the co-chaperones tested here play a role of consequence in the killing of an invertebrate host.

In cases where the ability to kill is impaired, it manifests in this assay as a delay in killing, rather than an inability to kill at all (Fig. 5.4 and 5.5). There was no case in which more than 12% of animals survived until the end of the assay. Thus, the differences in the curves were significant, but ultimately most of the animals died of infection from every strain. It remains to be seen whether this effect has a useful application. However, evidence shows that a delay in treatment of systemic *C. albicans* infections increases the rate of mortality enormously [218, 219].

The Kaplan-Meier analysis, which takes into account time as a variable over the course of the infection, was followed by Cox's hazard ratio analysis, which does not. This means that while the shapes of the Kaplan-Meier curves may be significantly different, removing the time variable means that only the overall chance of death is analysed.

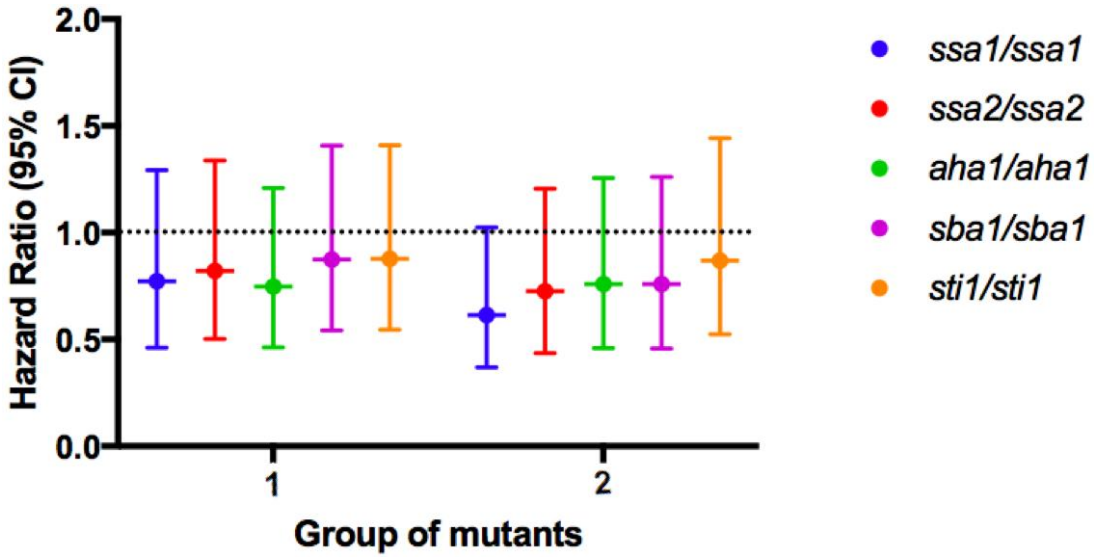

Figure 5.6 Hazard ratios for all strains compared with the wild type strain YSD89. Group one mutants are plotted on the left-hand side, group two mutants are plotted on the right. The points indicate the hazard ratios, while the error bars show the 95% confidence intervals. The dotted line marks a hazard ratio of 1.0, which is equivalent to the wild type strain.

The proportional hazard ratios for all of the mutant strains are lower than that of the wild type (Fig. 5.6), meaning that the risk of animals dying over the whole course of the infection experiment is lower with the mutant strains than with the wild type strain. However, all of the error bars for the 95% confidence interval extend above 1.0, meaning that overall there is no statistically significant lower risk of the animals dying from infection with the mutant strains.

5.2 Discussion

All of the co-chaperone mutant strains demonstrate a slower rate of mortality than the wild type strain, which may be clinically useful where it is essential for treatments to be administered quickly. However, while they were hypothesised to have reduced virulence capability, the mutants ultimately caused severe morbidity and mortality in the animals.

Immunity of the host is an important factor which varies significantly between different species. Data has shown that even with the virulence-attenuated *C. albicans hog1*Δ/Δ mutant, while the *M. sexta* larvae are impervious to the disease, they do not rid the infection from the body and yeast can still be found in the haemolymph and the haemocoel [160]. This is an important factor to consider, however, as *C. albicans* typically causes systemic infections in immunocompromised individuals, an inability to clear the infection, even when virulence is undermined, may be a common feature [9, 217]. Undermining the ability of the organism to cause morbidity may nevertheless be useful in this case as a means of indirectly increasing the tolerance of the patient to the presence of fungal infection in the bloodstream [220]. This may allow for adequate extension of life so that infection can be cleared by application of alternative antifungal treatments in combination with anti-virulence agents.

It would be useful in future to investigate further the persistence of these mutant strains in infected *M. sexta* individuals which survive for multiple time

points. This would be particularly interesting in the cases of those caterpillars which exhibit no symptoms of infection.

Ssa1 is known to mediate host cell invasion and null mutants show reduced virulence in mammalian models of infection [118]. The delay in killing by *ssa1*Δ/Δ observed in *M. sexta* may be a differential manifestation of the same effect, with altered presentation due to the differences in the host immune system and its failure to clear infection.

In future, it would be prudent to refine the optimisation of this assay with a dose-response curve, identifying a specific dose of the wild type strain which results in 50% mortality over the whole course of the assay, This would be useful in allowing for detection of strains which are enhanced in virulence potential, as well as those which are reduced.

This is infection of an invertebrate animal model over a short period of time so conclusions cannot be drawn about how this effect would translate into other species. Factors to be taken into account include invasion, immunity, and time. Any incapacity of the mutants to invade a healthy animal will have been largely masked by the use of the injection method. This was a choice made in order to precisely control and ensure consistency in the infective dose.

6. Measuring the effects of histone deacetylase gene deletion on Hsp90 co-chaperone gene expression

6.1 Histone deacetylases regulate telomeric gene expression

Histone deacetylases are instrumental in chromatin formation in the telomeric regions of the genome, which suppress gene expression by making the genes inaccessible to molecular transcription machinery [130]. The telomere position effect (TPE) is a silencing mechanism which regulates expression of genes in telomeric regions and is understudied in fungi [221]. In human cells telomere length has been found to affect the mechanisms of TPE, and therefore how telomeric genes are differentially expressed as cells age [222]. Due to the trend of virulence genes being located in sub-telomeric regions, it is hypothesised that TPE regulation is relevant in *C. albicans* virulence [3-5].

Sub-telomeric derepression is known to be instrumental in host cell invasion in *Candida glabrata* [223], but its importance in *C. albicans* virulence is not yet known. Heterochromatin-associated proteins, including histone deacetylases, regulate TPE in fungal species [107].

Homozygous null mutants were generated for two histone deacetylase genes; *HST1* and *HST2* using the methods previously described. One mutant strain was generated for *HST1* and a pair of mutants for *HST2. C. albicans* encodes a third Hst protein; Hst3, which was not investigated here as it is essential for viability [138]. These mutants were used to investigate the roles of histone deacetylases on co-chaperone gene expression, which was measured by quantitative real-time PCR (qRT-PCR). Co-chaperone gene expression levels were compared between the wild type strain and the *hst1Δ/Δ* and *hst2Δ/Δ* mutant strains.

The objective was to identify clues as to whether there are evolutionary mechanisms at work selecting for placement of virulence genes in sub-telomeric regions due to the specific way their expression is regulated in the sub-telomeric locale.

6.2 Deletion of histone deacetylases affects co-chaperone gene expression levels

qRT-PCR was completed with three technical replicates and three biological replicates for each gene in each strain, with the housekeeping gene *GPD1* used as a calibrator for ΔC_T calculations. All RNA was purified from cells in log growth. Results for expression of each co-chaperone gene were analysed first by ANOVA and pairwise by Tukey's test. Due to variation in measurements

between biological replicates, the plot shown is of three technical replicates and one biological replicate to simplify the visualisation. Statistical analyses are for all three biological replicates, nested within date.

Figure 6.1 ΔC_T values of co-chaperone genes in wild type strain and histone deacetylase null mutants. Shown are three technical replicates with mean and standard deviation indicated by crosses and error bars, with normalisation against the *GPD1* housekeeping gene.

Results show expression of *SSA1* was significantly higher in all mutant strains relative to the wild type strain, showing that deletion of the histone

deacetylases decreases silencing for *SSA1* (Fig. 6.1, Table 6.1). This is the only gene for which this was the case in all mutants.

Expression for all co-chaperone genes was higher in the *hst1*Δ/Δ strain, YSD1330, relative to the wild type strain, YSD89 (Fig. 6.1). This suggests that Hst1 plays an important role in suppressing gene expression of Hsp90 co-chaperones and that its absence has a significant derepressive effect (Table 6.1). *SBA1* is an exception to this, as its increase in expression relative to the wild type strain is not statistically significant (p=0.061).

For the co-chaperones *SSA2, SBA1, AHA,* and *STI1*, expression was significantly lower in the two *hst2*Δ/Δ strains relative to the wild type strain (Fig 6.1, Table 6.1). The only exception being *SBA1* in YSD1373, for which expression was lower than in the wild type strain, but not to a statistically significant degree (p=0.086). This is a counter-intuitive result as it would be expected that silencing would be reduced as deletion of *HST2* would reduce chromatin silencing and therefore increase telomeric gene expression. However, in *S. cerevisiae*, deletion of both *HST1* and *HST2* are known to have the effect of increasing silencing [224].

Table 6.1 P-values of ANOVA and Tukey tests comparing expression of each co-chaperone gene between strains. ANOVA tested for variation between all strains, while Tukey test shows pairwise comparisons of each mutant strain with the wild type. Significance codes are; "***" p<0.001, "**" 0.001<p<0.01, "*" 0.01<p<0.05.

CO-CHAPERONE	P-VALUE ANOVA	STRAIN	GENOTYPE	P-VALUE TUKEY
SSA1	<0.001***	YSD89	Wild type	-
		YSD1330	*hst1*Δ/Δ	<0.001***
		YSD1373	*hst2*Δ/Δ	0.001**
		YSD1414	*hst2*Δ/Δ	<0.001***
SSA2	<0.001***	YSD89	Wild type	-
		YSD1330	*hst1*Δ/Δ	0.015*
		YSD1373	*hst2*Δ/Δ	0.011*
		YSD1414	*hst2*Δ/Δ	0.028*
SBA1	0.002**	YSD89	Wild type	-
		YSD1330	*hst1*Δ/Δ	0.061
		YSD1373	*hst2*Δ/Δ	0.086
		YSD1414	*hst2*Δ/Δ	<0.001***
AHA1	<0.001***	YSD89	Wild type	-

		YSD1330	*hst1*Δ/Δ	0.008**
		YSD1373	*hst2*Δ/Δ	<0.001***
		YSD1414	*hst2*Δ/Δ	<0.001***
STI1	<0.001***	YSD89	Wild type	-
		YSD1330	*hst1*Δ/Δ	0.028*
		YSD1373	*hst2*Δ/Δ	0.014*
		YSD1414	*hst2*Δ/Δ	0.015*

It is difficult to determine precisely the effects of each histone deacetylase on expression of the co-chaperone genes due to the number and complexity of interactions in the cell. These assays were designed specifically to measure only expression of co-chaperone genes; further work will be needed to fully understand these effects. In *S. cerevisiae* Hst1 is known to suppress expression of the genes responsible for biosynthesis of NAD+, meaning that in *hst1*Δ mutants NAD+ is more abundant and paralogous NAD+-dependent histone deacetylases are more active in silencing [225].

It cannot be ignored that there is some disparity between the two *hst2*Δ/Δ strains, YSD1373 and YSD1414. The difference in expression is statistically significant for the genes *SBA1* (p=0.003), *AHA1* (p<0.001), and *STI1* (p<0.001). Expression of *SSA1* and *SSA2* in the two strains is statistically similar (p=0.414 and p=0.486, respectively). The genotyping method used was

colony PCR, so absence of the wild type allele and of the *NAT* cassette used in transformation is confirmed. However, these results suggest that other genetic changes have arisen in the strains during transformation and so in future genome sequencing may be required to elucidate these differences.

6.3 Histone deacetylase activity is dependent on paralogous histone deacetylase activity

In addition to gene deletion studies, more of the function of the Hst proteins may be elucidated through investigating the effects of overexpression. This approach, though, is also not without its complications as NAD+ biosynthesis has been found to be the limiting factor in activity of NAD+-dependent histone deacetylases in mammalian cells [226]. Overexpression of these enzymes therefore does not guarantee a subsequent increase in their activity, unless additional NAD+ requirements are also catered for. Especially as overexpression of Hst1 is likely to result in reduced production of NAD+ in the cell [225].

There is some overlap in function between Hst1 and Hst2 in *C. albicans*, as both are known to have H3 histone deacetylase activity [72], so there may be a similar effect of NAD+ depletion by deletion of *HST2* in *C. albicans* as there is with deletion of *HST1* in *S. cerevisiae.* In addition, the cells may respond to

the loss of Hst2 by upregulating Hst1 to excess, which would account for the increased silencing effect observed.

Alternatively, if Hst2 activity is responsible for a great deal of chromatin formation, widespread derepression caused by its absence may overwhelm the gene expression machinery, resulting in proportionally lower expression for Hsp90 co-chaperones.

There may be some functional redundancy with Hst1 and Hst3; the essential Hst protein in *C. albicans* as both have H4 histone deacetylase activity. Although both have additional divergent clients, their shared functions may mean that the effects *HST1* gene deletion are buffered. There is thus far no evidence for functional redundancy with Hst2 and Hst3, though Hst1 and Hst2 do share some clients, as described previously [72].

Perhaps, as an essential gene, the function of Hst3 is also instrumental in the expression of the Hsp90 co-chaperones. An approach of chemical depletion or augmentation of Hst3 protein levels may help to elucidate its effects whilst maintaining cell viability. Hst3 is however non-essential in *Saccharomyces cerevisiae*, and studies of null mutants have found that deletion of *HST3* decreases chromatin silencing [224]. Conversely, while deletion of *HST1* increases silencing in *S. cerevisiae* the result here was to reduce silencing of co-chaperone genes in *C. albicans*, so extrapolation of effects observed in *S. cerevisiae* can be problematic.

Opposing effects of deletion of paralogous genes *HST1* and *HST2* were not anticipated, though there are clues to their dissimilarities in function. Orthologues of Hst1 in mammals and in *S. cerevisiae* are exclusively nuclear proteins, whereas Hst2 is also cytosolic; this is also putatively the case in *C. albicans* [72, 227]. The implications of this are not fully understood, but it may indicate a broader range of functions for Hst2 than Hst1, and therefore differing effects of gene deletion.

Candida albicans Hsp90 co-chaperones appear to be subject to TPE silencing, though complex genetic interactions mean that more work is needed to fully understand the mechanisms involved. The pliant nature of this type of regulation of expression lends itself to rapid response to changeable environmental conditions, which is essential in virulence [106]. This is a strong argument for placement of virulence genes, including Hsp90 co-chaperone genes, in sub-telomeric regions being a facet of evolutionary selection.

7. General discussion and future work

7.1 Genome sequencing of co-chaperone gene deletion mutants and avoiding second-site mutations in future

The most important piece of future work to be completed is genome sequencing of the co-chaperone gene deletion mutants to identify second-site mutations which occurred in the transformation process. Comparing the genomes of these strains to the wild type would help to elucidate the reasons behind the discrepancies in phenotypes observed in the assays found here. This would also provide an opportunity to begin understanding how virulence was attenuated in the *ssa1*Δ/Δ mutant YSD662 and whether the phenotypes constitute a novel discovery of gene function in combination with the absence of *SSA1.* The inconsistencies encountered here highlight the necessity of generating at least two independent mutants for each gene deletion to corroborate results [228].

Homologous recombination using the lithium acetate method is a well-established and reliable means of generating homozygous null mutants. However, with its inefficiency and propensity to produce second-site mutations and in the advent of CRISPR, moving onto the more modern method of generating mutants would be advisable for future work [165, 229]. The improved efficiency of this method would allow for homozygous null mutants

to be generated much more rapidly, thus allowing for more time to be devoted to characterising multiple mutants and confirm phenotypic effects.

In addition to identifying additional mutations arising in the transformation process, functions of deleted genes can be further confirmed by replacing the wild type allele into the mutant strains, followed by testing for restoration of the wild type phenotype.

7.2 Biofilm formation and adherence relies on the function of Hsp90 co-chaperones

That all mutant strains were significantly impaired in biofilm formation and adherence suggests that regulation of this virulence trait is multifactorial and highly dependent on functionality of the Hsp90 co-chaperone complex. Although most strains formed wrinkled colonies on solid growth media, indistinguishable in morphology from that of the wild type, biofilm adherence was additionally challenged in the biofilm virulence assay. Further work and alternative quantification methods are necessary to deconstruct the interconnected pathways responsible for biofilm formation and adherence.

Metabolic activity in biofilms could be measured by colorimetric dye reduction, as was done here with XTT [157], with modification made to the wash steps to avoid loss of poorly-attached biofilms. Adherence of biofilms can be quantified

separately by flow cytometry [230], to disentangle biofilm formation and adherence. This is important as it is established that biofilm adherence capability and potency of *C. albicans* infections often do not correlate, while less adherent biofilm formation is still an advantage to the pathogen [231].

7.3 Sti1 and Sba1 are promising candidates for further study as potential novel drug targets

Sti1 makes a promising candidate for a possible future drug target in a combinatorial therapy approach with other antifungal drugs. The protein is known to be required for biofilm formation in *S. cerevisiae*, which has been found here to also be the case in *C. albicans* [201]. It has been found previously that Sti1 regulates resistance to radicicol, which was confirmed here, in addition to Sti1 regulating fluconazole resistance [193]. As deletion of *STI1* partially abrogated *C. albicans* virulence in *M. sexta*, it would be pertinent to assay the effects of fluconazole treatment in an infection model infected with *sti1*Δ/Δ strains to assess whether this increased susceptibility translates to the host environment. As a function of Sti1 is to mediate between Hsp90 and Ssa1/2, the effect of its gene deletion may be to undermine functioning of several forms of the Hsp90 co-chaperone complex, resulting in the observed reduction of several virulence traits [111].

C. albicans Sba1 was previously known to regulate telomere maintenance; implicating it in cell aging, and to be more highly expressed in stress conditions [72, 120]. Here, it has also been shown to be implicated in virulence, as null mutants were more susceptible to fluconazole, less able to form biofilms, and slower to kill *M. sexta* larvae than the wild type. These aspects may, like Sti1, recommend Sba1 as a novel drug target for reduction of *C. albicans* virulence.

7.4 Aha1 has an important but uncharacterised role in *C. albicans* virulence

Findings in this study for the co-chaperone Aha1 are particularly interesting. *C. albicans* Aha1 levels were known to be upregulated in oxidative stress [15], but Aha1 has been shown here to be non-essential for an effective oxidative stress response. Having shown a defect only in biofilm formation, *aha1*Δ/Δ strains then exhibited the most attenuated virulence in the invertebrate host. This demonstrates that Aha1 function is intrinsically linked to virulence, though which specific aspects of virulence it regulates were not fully elucidated here.

This may be investigated in future with assays of other individual virulence traits *in vitro*, such as iron sequestration, or *ex vivo* assays, such as host cell invasion. The effects of loss of Aha1 in the host may also be further dissected by analysing *M. sexta* haemolymph samples during the course of the infection, and even by imaging cross-sections of tissue from the animals.

7.5 Hsp70 orthologues are highly conserved in sequence but differential in function

The Hsp70 orthologues in *C. albicans*; Ssa1 and Ssa2 appear to have surprisingly differential roles considering their 87.2% protein sequence identity [116]. However, Ssa1 is known to mediate host cell invasion and to be required for virulence in a murine infection model [110, 118]. If, therefore, it is proposed as a potential drug target, it is essential to understand the effects of inhibition on Ssa1 and Ssa2 simultaneously, as it is highly unlikely that a compound could be developed with adequate specificity to target one exclusively, given their conservation. With this in mind, Hsp70 orthologues may not be advisable as drug targets as the presence of the Ssa1/2 proteins is instrumental in making *C. albicans* cell vulnerable to the host immune system as well as to some antifungal drugs. Inhibition of Ssa2 may have the unfortunate consequence of undermining the host immune system [196]. However, caspofungin is an antifungal drug in common use and known to suppress expression of Ssa2 [197].

A double null mutant for both Hsp70 orthologues could not be generated in this study, which may indicate that the presence of at least one is required for *C. albicans* viability. Measuring the Ssa1 and Ssa2 protein expression levels in strains which are homozygous null for one of the genes would be a useful step in assessing whether there is compensatory upregulation of one Hsp70 orthologue in response to the absence of the other. This would provide clues as to what extent the two proteins are functionally redundant.

From the results presented here it can be concluded that Ssa2, unlike Ssa1, is a negative regulator of several virulence traits, though the derepression of virulence has an overall fitness cost for the cells in the invertebrate host model. Having outperformed the wild type in oxidative stress resistance, antifungal drug resistance and hyphal formation the *ssa2*Δ/Δ mutants killed *M. sexta* larvae significantly more slowly than the wild type strain.

The results of this study are inconclusive as to the role of Ssa1. The absence of the *SSA1* wild type allele was confirmed in both YSD661 and YSD662, but second-site mutations in the genome are yet to be identified. However, as both strains were the most impaired in killing of *M. sexta* relative to the wild type, it seems likely that Ssa1 promotes virulence. This is in keeping previous findings that *C. albicans ssa1*Δ/Δ strains are less virulent in a murine model of infections and that Ssa1 mediates host cell invasion [110, 118].

7.6 *Manduca sexta* larvae are a useful model of fungal infection

Use of *Manduca sexta* fifth instar larvae has proven a useful tool for measuring virulence in a whole animal infection model. Despite their limitations, they make a relevant and low-cost alternative to vertebrate models of infection for preliminary studies. They are now established as a novel invertebrate model of fungal infection, allows assays to run at the physiologically relevant temperature of 37°C. Refinement of the infective dose of yeast cells would be useful to spread the infection over a longer timescale. This would allow for more morbidity data to be gathered before the animals succumb to infection and hence more complete statistical analyses to be carried out. Having animals infected with the wild type strain survive beyond day one of the study would also allow for detection of enhanced virulence in other strains, as well as reduced virulence.

The model also has potential for more diverse analyses, such as sampling of faeces or haemolymph over the course of the infection to monitor the fungal burnden and whether infection is ever cleared [160]. However, this host is physiologically dissimilar to humans in many ways, which should be kept in mind. Any promising results from *M. sexta* infection studies will need to be verified in a vertebrate infection model.

7.7 Hsp90 co-chaperone inhibition in combination with existing antifungals requires more exploration in the context of evolutionary medicine

Ssa1, Sba1, and Sti1 have all been shown here to positively regulate *C. albicans* resistance to fluconazole, as null mutants were susceptible to lower doses than the wild type strain. This may be useful in considering Hsp90 co-chaperones as drug targets in combinatorial therapy to simply extend the efficacy of existing antifungal drugs. *C. albicans* chaperones have recently been shown to be instrumental in antifungal drug resistance mechanisms [232]. With this in mind, it would be prudent to also complete caspofungin MIC assays on Hsp90 co-chaperone null strains to gather a more complete picture of how and to what extent Hsp90 co-chaperones specifically regulate the drug response.

Combinatorial therapy is gaining favour as a method to subvert drug resistance and extend a drug's usefulness, whereas cycling treatment with individual antimicrobials has been demonstrated to be ineffective, and even in some cases accelerates development of resistance [233, 234]. Choosing the appropriate combinations of drugs to administer is crucial. While targeting the *C. albicans* stress responses has proven useful in this context, it follows that undermining the pathogen's virulence potential, through targeting Hsp90 co-chaperones, would also be of benefit [235]. Despite demonstration of the efficacy of combinatorial therapy using existing antifungals coupled with Hsp90 inhibitors, this is rarely appropriate in a clinical setting. The high

sequence conservation of human and *C. albicans* Hsp90 means that there is a high risk of host toxicity in administering Hsp90 inhibitors to treat systemic fugnal infections. In addition, multidrug-resistant strains of *C. albicans* continue to emerge, and highlight the necessity for new treatment options which will discourage *C. albicans* from developing resistance and thus remain useful [236, 237].

7.8 Employing the principles of evolutionary medicine is the next step in addressing the problem of infectious diseases and drug resistance

Use of antimicrobials drives the, by necessity, the evolution of widespread resistance; persistent and liberal application of antimicrobials eliminates susceptible competitors, thus giving the advantage to resistant cells [238]. Most applications of evolutionary medicine to infectious disease to date have focused on the careful management of existing antimicrobials to minimise the emergence and spread of resistance [239]. What is proposed here as an alternative is the development of antivirulence drugs, to undermine the ability of the infective organism to cause disease, without aiming to kill it or affect normal growth. There is some limited precedence to this concept, possibly owing to the cost and complexity of developing novel drugs through to approved treatment [240, 241].

Under the conditions tested here, none of the Hsp90 co-chaperones investigated appear to be essential for robust growth of *C. albicans,* adhering to the principle of evolutionary medicine that the potential drug targets should be essential only for virulence. Before pursuing these candidates further, however, it would be pertinent to test them in alternative growth conditions, more closely imitating their natural environs. Overall, the robust growth of the mutant strains, coupled with their inhibited virulence, suggests that as a group they do indeed play a significant role in *C. albicans* virulence and may make suitable candidates as antivirulence drug targets.

7.9 Histone deacetylases regulate Hsp90 co-chaperone expression while they are sub-telomerically located

Testing the effects of histone deacetylases on Hsp90 co-chaperone expression on in log phase cells gives preliminary clues as to their involvement. Indeed, the results presented here demonstrate that co-chaperones are subject to regulation by Hst1 and Hst2. However, Hsp90 co-chaperone gene expression in histone deacetylase null mutants should also be measured and compared in virulence conditions to assess their roles specifically in virulence and how they respond to environmental cues. Hst1 and Hst2 clearly have a significant effect on expression of Hsp90 co-chaperones, and TPE (telomeric position effect) regulation allows for the rapid responses to environmental changes demanded by virulence [106, 222].

The influence of TPE regulation on expression of Hsp90 co-chaperones could be further investigated by cloning and relocating co-chaperone genes. Relocating genes whilst maintaining them on their native chromosome arm, away from the telomere and closer to the centromere, along with their upstream regulatory regions, would provide the means to observe the effect of genomic locale on gene expression.

Mutants with centromerically-located Hsp90 co-chaperone genes should then be assessed for their performance in virulence conditions. Likewise, expression of Hsp90 co-chaperones should be measured in these strains to assess whether expression levels are dependent on gene location. This would aid in understanding to what extent sub-telomeric gene location and silencing by heterochromatin formation affect virulence.

This study represents a methodical approach to understanding the roles of *Candida albicans* Hsp90 co-chaperones and their genomic locale in diverse virulence traits. The results presented here have implications for future development of novel antifungal drug targets and elucidation of virulence regulatory pathways in *C. albicans*.

8. Appendices

Appendix 8.1 Strains used in this study. YSD is the accession code preceding numbers for yeast strains in the Diezmann laboratory yeast strain archive.

STRAIN	GENOTYPE	DERIVED FROM
YSD89 (SN95) **[144]**	*arg4/arg4 his1/his1 URA3/ura3::imm434 IRO1/iro1::imm434*	SC5314 [145]
YSD106 **[168]**	*arg4/arg4 his1/his1::TAR-FRT URA3/ura3::imm434 IRO1/iro1::imm434 hsp90::CdHIS1/FRT-tetO-HSP90*	YSD89
YSD174 **[242]**	*arg4/arg4 his1/his1 URA3/ura3::imm434 IRO1/iro1::imm434 bcr1::FRT/bcr1::FRT*	YSD89
YSD883	*arg4/arg4 his1/his1 URA3/ura3::imm434 IRO1/iro1::imm434 hog1::FRT/hog1::FRT*	YSD89
YSD661	*arg4/arg4 his1/his1 URA3/ura3::imm434 IRO1/iro1::imm434 ssa1::FRT/ssa1::FRT*	YSD89
YSD662	*arg4/arg4 his1/his1 URA3/ura3::imm434 IRO1/iro1::imm434 ssa1::FRT/ssa1::FRT*	YSD89
YSD702	*arg4/arg4 his1/his1 URA3/ura3::imm434 IRO1/iro1::imm434 ssa2::FRT/ssa2::FRT*	YSD89

STRAIN	GENOTYPE	DERIVED FROM
YSD731	*arg4/arg4 his1/his1 URA3/ura3::imm434 IRO1/iro1::imm434 ssa2::FRT/ssa2::FRT*	YSD89
YSD813	*arg4/arg4 his1/his1 URA3/ura3::imm434 IRO1/iro1::imm434 sba1::FRT/sba1::FRT*	YSD89
YSD816	*arg4/arg4 his1/his1 URA3/ura3::imm434 IRO1/iro1::imm434 sba1::FRT/sba1::FRT*	YSD89
YSD868	*arg4/arg4 his1/his1 URA3/ura3::imm434 IRO1/iro1::imm434 aha1::FRT/aha1::FRT*	YSD89
YSD871	*arg4/arg4 his1/his1 URA3/ura3::imm434 IRO1/iro1::imm434 aha1::FRT/aha1::FRT*	YSD89
YSD874	*arg4/arg4 his1/his1 URA3/ura3::imm434 IRO1/iro1::imm434 sti1::FRT/sti1::FRT*	YSD89
YSD947	*arg4/arg4 his1/his1 URA3/ura3::imm434 IRO1/iro1::imm434 sti1/sti1::FRT*	YSD89
YSD1327	*arg4/arg4 his1/his1 URA3/ura3::imm434 IRO1/iro1::imm434 hst1::FRT/hst1::FRT*	YSD89

STRAIN	GENOTYPE	DERIVED FROM
YSD1330	*arg4/arg4 his1/his1 URA3/ura3::imm434 IRO1/iro1::imm434 hst1::FRT/hst1::FRT*	YSD89
YSD1373	*arg4/arg4 his1/his1 URA3/ura3::imm434 IRO1/iro1::imm434 hst2::FRT/hst2::FRT*	YSD89
YSD1414	*arg4 /arg4 his1 /his1 URA3/ura3 ::imm434 IRO1/iro1 ::imm434 hst2::FRT/hst2::FRT*	YSD89

Appendix 8.2 List of materials and suppliers used here.

PRODUCT	DESCRIPTION	SUPPLIER
2X PCR MASTERMIX	Mix for PCR	Quantig
96-WELL PLATES FLAT	Growth and biofilm assays	Starstedt
96-WELL REACTION PLATES MICROAMP	qRT-PCR	Fisher
AGAR	For solid growth media	Fluka
AGAROSE	DNA/RNA gels	Sigma
AMMONIUM SULFATE	Media supplement	Sigma
BLUE JUICE LOADING DYE	DNA gel loading dye	Invitrogen
BOVINE SERUM	Hyphal induction	Fisher
BOVINE SERUM ALBUMIN	Media supplement	Sigma
CALCOFLUR WHITE	Media supplement	Sigma
CONGO RED	Media supplement	Sigma
CDNA SYNTHESIS KIT	Synthesise cDNA	Agilent

PRODUCT	DESCRIPTION	SUPPLIER
D-GLUCOSE	Media supplement	Melford
DITHIOTHEITOL	Transformations	Sigma
D-MALTOSE MONOHYDRATE	Media supplement	Sigma
DMSO	Solvent	VWR
DNTP MIX	PCR reagent	Fisher
DOXYCYCLINE	Antibiotic	Melford
ETHANOL	Solvent	Sigma
FLUCONAZOLE	Antibiotic	Sigma
GELDANAMYCIN	Hsp90 inhibitor	Melford
GLYCEROL	Used in -80°C stocks	Sigma
HYDROCHLORIC ACID	pH adjustment	Fluka
HYDROGEN PEROXIDE	Oxidating agent	Sigma
L-ARGININE MONOHYDROCHLORIDE	Amino acid	Sigma
L-HISTIDINE MONOHYDROCHLORIDE MONOHYDRATE	Amino acid	Sigma

PRODUCT	DESCRIPTION	SUPPLIER
LIFEGUARD	Disinfectant	SC Johnson
LITHIUM ACETATE DIHYDRATE	Transformations	Sigma
LURIA BROTH	Growth medium	Invitrogen
MENADIONE	Biofilm assays	Sigma
MICROAMP OPTICAL ADHESIVE FILM	qRT-PCR	Fisher
NOURSEOTHRICIN	Antibiotic	Werner BioAgents
NUTRIENT BROTH	Media supplement	Oxoid
PEPTONE	Media supplement	Fluka
PHOSPHATE BUFFERED SALINE TABLETS	Solvent	Oxoid
POLYETHYLENE GLYCOL 3350	Transformations	Sigma
PRIMERS	PCR reagent	Eurofins
Q5 PCR REACTION BUFFER	PCR reagent	NEB
Q5 TAQ POLYMERASE	PCR reagent	NEB

PRODUCT	DESCRIPTION	SUPPLIER
RADICICOL	Hsp90 inhibitor	Sigma
RNEASY MINI KIT	RNA purification	QIAgen
RNASE-FREE DNASE KIT	RNA purification	QIAgen
RNASE-FREE WATER	PCR reagent	Invitrogen
RPMI MEDIUM 1640	Media supplement	Gibco
SALMON SPERM DNA	Transformations	Applichem
SODIUM ACETATE	DNA purification	Sigma
SODIUM HYDROXIDE	pH adjustment	Sigma
SYBR FAST GREEN MASTER MIX	PCR reagent	Fisher
SYBR SAFE	DNA gel dye	Invitrogen
TE BUFFER (10X)	Buffer	Rockland
TRACK IT 1KB PLUS LADDER	DNA ladder	Invitrogen
URIDINE	Amino acid	Sigma
XTT	Biofilm assays	VWR

PRODUCT	DESCRIPTION	SUPPLIER
YEAST EXTRACT	Media supplement	Oxoid
YEAST NITROGEN BASE	Media supplement	Sigma

Appendix 8.3 Primers used in strain construction and genotype screening. "-100" indicates the primer sequence is complementary to a region beginning 100 bases upstream of the start codon of the gene named. "+100" indicates the primer sequence is complementary to a region beginning 100 bases downstream of the start codon. "F" and "R" indicate whether the primer runs forwards, or reverse respectively; all are presented in 5' to 3' orientation. Long primers were used for amplification of the *NAT* cassette prior to transformation; upper case sections of the sequence are complementary to the flanking regions upstream and downstream of the native genes in *C. albicans*, while lower case sections of sequence are complementary to the *NAT* cassette itself. Short primers were used for genotyping through colony PCR; testing for integration of the *NAT* cassette and absence of the wild type allele.

NAME	SEQUENCE
SSA1_-100F	TATTCTATTTCTTCTTTACTTTTTCTTTAATCAATTCAAT TAGAATTAATAGAATATATTTTTCCAATTAATAAAACAC AATTAAACAAAAAATTAAATTggaaacagctatgaccatg
SSA1_+1971 R	ACAAAAGCAAAGAATCAAAAGAAATAAAAACTAAAATA AAAACCTTTTAAAATTAAACTAAAAAACCAACTCCACAG TAAATTACCTATTTCTTCCTCATgtaaaacgacggccag
SSA1_+2071 R	TACAATTAACAACAATACTAATAAAACAACCCCCCATAA ATAAAAAATTGTTCTAAATATTGTGCTTCTTTCTTTTTTG TTGATCTTTACTTACTTACTTgtaaaacgacggccag
SSA2_-200F	TTTCGACAAAAAGATAAATCAACAACCATCAATAATTTT CAATTTTCAATTTTAAAAAAATTTCATATAAAAAATTTTC AAATCCCAATTGTAATTCTTTggaaacagctatgaccatg
SSA2_-100F	TTTTTTTGGAAATTCTTCTTTCTTTTCCTTTTATAAATTT TTCTTATTGTTTAATTTAATTTAATTCAATTCAATTGATA AATCAACTAATAAATTAATCggaaacagctatgaccatg

NAME	SEQUENCE
SSA2_+1938R	AAAATAAAATTTCTTATCTCAAATTAATATGCGTTTTATTACTGTCTATAAAGTATTACATTATAAATATCTCTAATATATATATACATTATTAATACATgtaaaacgacggccag
SBA1_-100F	CAAATTAATTGATCAATTGTACTTCATTTTAATAATACTCAAATTGAAGGCTTTCAAATTCTGAAATAGAACATTATTTGAAGAAGAAAAATTACTCATTggaaacagctatgaccatg
SBA1_+666R	TTACGAGTAATATTTATTAAATGGTTTGAAATGACTAATAAAATAGACTATTCAACTGTATAATTTTGGTTTTTTTTTTGTATTACTTTGTTATTTGAGAgtaaaacgacggccag
AHA1_-100F	GGAATCTGCAAAAAATTGGAACAATTTAAACAATTGCACCGAATCGAGATTTTTCTTGAAGTAATCAACCTCTCAAAATCAAAACTAAAACAACATAGCAggaaacagctatgaccatg
AHA1_+1041R	ATCCTCAATGCCACAAACTCAACAGAAAAGGTATCATAAGTGATGGTTAATAGAGTAAAATTCTTCTTTATGGATTGCTTGTACGTACATTCTATTTATCgtaaaacgacggccag
STI1_-100F	AAGGGAACCCCTTCCCGAAAAAACTAAAACTAAAACTTCCACCCAAATATCAAATAACCAACTTATCATTCCAACAGATAATATTCCCACTTCAATAACAggaaacagctatgaccatg
STI1_+1770R	ATGACACCAAAAATAGAAAAAAAAGAAACTTTTCAACAACTGTGTAAATAAACCAAATGTGAATTATAAGGGGGTTTTTATTAGTTACTTTTTATCTGGgtaaaacgacggccag
TAH1_-100F	TGGTGTTATCTGGTCGTGCAATTTGCTCAATATCAGAATAGAAAAACATCTGAAAAATTCTATTTATTTTACGGAAGCTACAACCATAACCCCATTAGACggaaacagctatgaccatg
TAH1_-200F	ATTTAATGTTATATACTGACTTAATTATACTCTCATTATACCACTTTACTTACTAATTTGAACTGATATAACATTTACCAATATTGATTTATAGATTCTTggaaacagctatgaccatg

NAME	SEQUENCE
TAH1_+1496R	TGAATATATTCCAGAGTTTTTTCATCCATTGTTTCAACCCTACGATGCTCCTACAAATCTGAAAGGATTAAAGAAAAAATTAGAAATTAAGCATTACTAGgtaaaacgacggccag
HST1_-100F	ATTACTGCAAAATCTCCCAAATTTCTATCAAAACACTCACTTAGTTACATATATATTCTTATTCTTATCAATTGTTACTAATAACAAATAACAATCAATAggaaacagctatgaccatg
HST1_-200F	ACCACCACCACTTCTACCACTTCTACCACCCCCTAATTTTTTACACAATAACTGCAGCAACATTAATTTATTAAAAATTTTCCAACAATAAAAACATTGAggaaacagctatgaccatg
HST1_+1968R	ATATATATAATTAACTAACCACATTAACGTCTATAGTTTATCTATCGGGGCTTTCTCTTCCTCTTTGTCCTCGTTGTCCACTTTATCTTGTTTTGGCTCTgtaaaacgacggccag
HST2_-100F	AAAGATTAGACCTCCCAAAATCAATCAAAGAAAAGCACACTGTGACGACATACAGAAACTCTATACGTACACTTCTTACAACAGACTATAACTTTAAACCggaaacagctatgaccatg
HST2_+996R	TATAAAAGAAAATCTTTGCAACCAAAATATATTTTCTGTTTGTATTTCTCATGTTTTATTCTTTCTTGAAAATGTATATTATATTTTTGTTGAGACATTTgtaaaacgacggccag
HST2_+1096R	TTGAGACTATCTCGGCATTTATTGTAATAAACCCGTATGCACTATCGTCAGTAACTGATAATTGTGATGCTAAAGCCATTTCAACAACTACCCTAGAGGGgtaaaacgacggccag
SSA1_-240F	TTCCAATGAGGGGGGGGGAG
SSA1_+2238R	AAAGAGCAGTAGTTAGAAGT
SSA1_+19F	TTGATTTAGGTACAACCTAT
SSA1_+559R	ATTATGTTCACCTCTGGAAC

NAME	SEQUENCE
SSA2_-260F	AAATTGTTCCATGCAAGGCC
SSA2_+2144R	TTTCCACGGAGAACACTGGT
SSA2_+39F	CTCCTGTGTCGCTCATTTCG
SSA2_+542R	CAGATTTTTTGTCCAAACCG
SBA1_+10F	CAACCACTCAAACTCCAACTGT
SBA1_+510R	GCACTAAGATCGACACCACC
SBA1_-209F	GAACGCTCCTACCTACACCT
SBA1_+790R	CGTACTGATACAACCACCACT
AHA1_+251F	TGGGTCAATCACAATTCCGG
AHA1_+709R	ACGAGTCCATGCACCAATTC
AHA1_-241F	CCTCCTATGTGAAGTAGTAGGCT
AHA1_+1223R	GTCATTCACATAAAGCCTGACG
STI1_+1058F	TGAATTACCCGAAGCAGTGAA
STI1_+1464R	AGTTCTTGCCTCGGTTAAAGT
STI1_-214F	ACATGGTAGCAGCTGATGTATAG
STI1_+1973R	TCGGGCCAATTATTTAACAGTGA
TAH1_-223F	ACACCAACCACAGAGATCAAA
TAH1_+1694R	ACGAAGAAGAAGATTTCAGGCA

NAME	SEQUENCE
TAH1_+258F	CGGAAAGGTATGGCTTTAAAAGG
TAH1_+658R	AGTTGTTTGAGTGTGGTAAGGA
HST1_-383F	AGCTAATTAGATCCCGGCCAA
HST1_+2147R	TTGAATTCCCGCAAAGACCT
HST1_+989F	AACATTTAGGACTTTCGGATCCAC
HST1_+1407R	GTCATCGTCATCATAGGGTTTGTT
HST2_-37F	CACTGTGACGACATACAGAAACT
HST2_+1402R	TGAGAGTGTGACTGAGCCTC
HST2_+85F	TTTCGACAGGTGCAGGGATA
HST2_+468R	TGTTGACAGCTGGGGATCTT

Appendix 8.4 Recipes for solid growth media used in morphology assays. All ingredients were dissolved in a final volume of 1 L distilled water and sterilised either by autoclaving or by filtering through a 0.22 µm filter, as appropriate. Adjustments were made to the pH as necessary.

MEDIA	RECIPE
Spider agar pH 7.2	10 g *Oxoid* enriched nutrient broth 10 g Mannitol 2 g dipotassium phosphate 10 g agar
RPMI agar pH 7.0	10.4 g RPMI 34.35 g 3-(N-morpholino)propanesulfonic acid (MOPS) 20 g glucose 20 g agar
Basic SD agar	1.79 g YNB (without added amino acids of ammonium sulphate) 5 g ammonium sulphate 1.92 g yeast synthetic dropout media (without added uracil) 80 mg uridine 20 g glucose 20 g agar
SD with Calcoflur White	Calcoflur White MR2 powder added to SD agar to a final concentration of 150 µg mL^{-1}
SD with Congo Red	Congo Red powder added to SD agar to a final concentration of 200 µg mL^{-1}
Lee's medium	5 g ammonium sulphate 200 mg magnesium sulphate heptahydrate 2.5 g dipotassium phosphate 5 g sodium chloride

MEDIA	RECIPE
Lee’s medium continued	12.5 g glucose 500 mg L-alanine 1.3 g L-leucine 1 g L-lysine hydrochloride 100 mg L-methionine 71.4 mg L-ornithine 500 mg L-phenylalanine 500 mg L-proline 500 mg L-threonine 50 mg L-arginine hydrochloride 20 mg L-histidine hydrochloride 1 mg Biotin 20 g agar
YPD agar	20 g yeast extract 10 g peptone 20 g glucose 20 g agar

Appendix 8.5 *Manduca sexta* larvae food recipe. The chlorotetracycline and formaldehyde are antimicrobial ingredients used to prevent infections in the colony. Formaldehyde was omitted from the food of animals used in infection assays from 3 days prior to infection.

COMPONENT	INGREDIENTS
Premix	2700 g Wheatgerm
	1260 g Casein
	1080 g Sucrose
	540 g Dried yeast
	360 g Wesson's salt
	36 g Choline chloride
	72 g Cholesterol
	36 g Methyl paraben
	54 g Sorbic acid
Complete food	336 g Premix
	1770 mL Distilled water
	22.5 g Agar
	4 mL Corn oil
	4 mL Linseed oil
	8 mL 4% Formaldehyde
	0.2 g Chlorotetracycline
	0.2 g Vanderssant vitamins
	8 g Ascorbic acid

Appendix 8.6 Primers used in qRT-PCR. “F” indicates the primer is forwards; “R” indicates the primer is reverse. All primers are presented in 5’ to 3’ orientation.

NAME	SEQUENCE
GPD1+570-F	AGTATGTGGAGCTTTACTGGGA
GPD1+766-R	CAGAAACACCAGCAACATCTTC
SSA1_+41F	CTTGTGTTGCTCATTTTGCC
SSA1_+273R	GTTTACCTGCTTTATCAATGAC
SSA2_+49F	CTCATTTCGCTAACGATAGAG
SSA2_+279R	CATTGGTTTACTGGCTTTGTC
SBA1_+362F	TAAATGGGTGGATGAGGATGA
SBA1_535R	CAGCTTGACCCAATTGAGAAG
AHA1_+333F	GCCGAAAATTCAGGTATCACA
AHA1_+491R	GTGGCAGCAATAGTGGATGAT
STI1_+636F	GCATCAGAACCAAAACTGGAA
STI1_+788R	GCTTTAGCATTGTCAGCTTGG

Appendix 8.7 Growth metrics indicated as a proportion of the wild type metrics from their respective repeats. “K” indicates carrying capacity of the culture, which is quantified by the maximum optical density the culture reached. “R” denotes the overall rate of growth, while “T_gen” is the shortest doubling time to occur during the assay.

CONDITION	STRAIN	K	R	T_GEN
YPD 30°C	YSD661	0.999	0.971	1.030
	YSD662	0.984	0.925	1.082
	YSD702	0.945	1.010	0.991
	YSD731	0.978	0.939	1.065
	YSD813	1.001	0.975	1.025
	YSD816	1.026	0.981	1.019
	YSD868	1.053	0.971	1.030
	YSD871	1.045	0.971	1.030
	YSD874	1.031	0.961	1.041
	YSD947	0.991	1.080	0.927
YNB 30°C	YSD661	1.003	1.066	0.939
	YSD662	1.175	0.988	1.012
	YSD702	1.007	1.000	1.000
	YSD731	1.010	0.990	1.010
	YSD813	0.987	1.036	0.965
	YSD816	1.085	0.976	1.025
	YSD868	1.072	0.955	1.046
	YSD871	1.067	1.004	0.996
	YSD874	1.047	0.914	1.094
	YSD947	0.903	1.065	0.939

CONDITION	STRAIN	K	R	T_GEN
YPD 37°C	YSD661	1.006	1.008	0.992
	YSD662	0.995	1.233	0.811
	YSD702	0.935	0.880	1.137
	YSD731	0.911	0.800	1.251
	YSD813	0.963	0.914	1.095
	YSD816	1.040	0.863	1.160
	YSD868	0.999	0.895	1.116
	YSD871	1.064	0.865	1.157
	YSD874	1.004	0.839	1.193
	YSD947	1.001	0.836	1.197
YNB 37°C	YSD661	1.034	1.050	0.953
	YSD662	1.007	1.057	0.945
	YSD702	0.985	1.060	0.944
	YSD731	1.047	1.076	0.929
	YSD813	0.877	1.169	0.855
	YSD816	1.005	1.215	0.824
	YSD868	1.071	1.193	0.839
	YSD871	1.106	1.126	0.888
	YSD874	1.029	0.813	1.231
	YSD947	1.150	0.912	1.095

9. References

1. Harsha, M.V., et al., *Emerging fungal pathogens - a major threat to human life.* International Journal of Pharmaceutical Sciences and Research, 2017. **8**(5): p. 1923-1934.
2. Cowen, L.E., et al., *Harnessing Hsp90 function as a powerful, broadly effective therapeutic strategy for fungal infectious disease.* Proceedings of the National Academy of Sciences of the United States of America, 2009. **106**(8): p. 2818-2823.
3. Anderson, M.Z., et al., *The Three Clades of the Telomere-Associated TLO Gene Family of Candida albicans Have Different Splicing, Localization, and Expression Features.* Eukaryotic Cell, 2012. **11**(10): p. 1268-1275.
4. Duraisingh, M.T., et al., *Heterochromatin silencing and locus repositioning linked to regulation of virulence genes in Plasmodium faiciparum.* Cell, 2005. **121**(1): p. 13-24.
5. Orbach, M.J., et al., *A telomeric avirulence gene determines efficacy for the rice blast resistance gene Pi-ta.* Plant Cell, 2000. **12**(11): p. 2019-2032.
6. Pegorie, M., D.W. Denning, and W. Welfare, *Estimating the burden of invasive and serious fungal disease in the United Kingdom.* Journal of Infection, 2017. **74**(1): p. 60-71.
7. Harrison, D., H. Muskett, and S. Harvey, *Development and validation of a risk model for identification of non-neutropenic, critically ill adult patients at high risk of invasive Candida infection: the Fungal Infection Risk Evaluation (FIRE) Study. Chapter 4, Epidemiology of invasive fungal disease in UK critical care units.* 2013: NIHR Journals Library.
8. Wisplinghoff, H., et al., *Nosocomial bloodstream infections in US hospitals: analysis of 24,179 cases from a prospective nationwide surveillance study. (vol 39, pg 309, 2004).* Clinical Infectious Diseases, 2004. **39**(7): p. 1093-1093.
9. Denning, D.W., et al., *British Society for Medical Mycology proposed standards of care for patients with invasive fungal infections.* Lancet Infectious Diseases, 2003. **3**(4): p. 230-240.
10. Desai, R.J., et al., *Risk of serious infections associated with use of immunosuppressive agents in pregnant women with autoimmune*

inflammatory conditions: cohort study. Bmj-British Medical Journal, 2017. **356**: p. 9.

11. Celebi, S., et al., *Neonatal candidiasis: Results of an 8 year study.* Pediatrics International, 2012. **54**(3): p. 341-349.
12. Moyes, D.L., et al., *Candidalysin is a fungal peptide toxin critical for mucosal infection.* Nature, 2016. **532**(7597): p. 64-+.
13. Nathan, C.F., *SECRETION OF OXYGEN INTERMEDIATES - ROLE IN EFFECTOR FUNCTIONS OF ACTIVATED MACROPHAGES.* Federation Proceedings, 1982. **41**(6): p. 2206-2211.
14. Kusch, H., et al., *Proteomic analysis of the oxidative stress responses in Candida albicans.* Proteomics, 2007. **7**(5): p. 686-697.
15. Wang, Y., et al., *Cap1p is involved in multiple pathways of oxidative stress response in Candida albicans.* Free Radical Biology and Medicine, 2006. **40**(7): p. 1201-1209.
16. Enjalbert, B., A. Nantel, and M. Whiteway, *Stress-induced gene expression in Candida albicans: Absence of a general stress response.* Molecular Biology of the Cell, 2003. **14**(4): p. 1460-1467.
17. Enjalbert, B., et al., *Role of the Hog1 stress-activated protein kinase in the global transcriptional response to stress in the fungal pathogen Candida albicans.* Molecular Biology of the Cell, 2006. **17**(2): p. 1018-1032.
18. Martchenko, M., et al., *Superoxide dismutases in Candida albicans: Transcriptional regulation and functional characterization of the hyphal-induced SOD5 gene.* Molecular Biology of the Cell, 2004. **15**(2): p. 456-467.
19. Fradin, C., et al., *Granulocytes govern the transcriptional response, morphology and proliferation of Candida albicans in human blood.* Molecular Microbiology, 2005. **56**(2): p. 397-415.
20. Heilmann, C.J., et al., *Hyphal induction in the human fungal pathogen Candida albicans reveals a characteristic wall protein profile.* Microbiology-Sgm, 2011. **157**: p. 2297-2307.
21. Lorenz, M.C., J.A. Bender, and G.R. Fink, *Transcriptional response of Candida albicans upon internalization by macrophages.* Eukaryotic Cell, 2004. **3**(5): p. 1076-1087.
22. Lewis, L.E., et al., *Live-cell Video Microscopy of Fungal Pathogen Phagocytosis.* Jove-Journal of Visualized Experiments, 2013(71): p. 5.

23. Sandini, S., et al., *Gene expression of 70 kDa heat shock protein of Candida albicans: transcriptional activation and response to heat shock.* Medical Mycology, 2002. **40**(5): p. 471-478.
24. Singh, S.D., et al., *Hsp90 Governs Echinocandin Resistance in the Pathogenic Yeast Candida albicans via Calcineurin.* Plos Pathogens, 2009. **5**(7): p. 14.
25. Shapiro, R.S. and L.E. Cowen, *Hsp90 orchestrates temperature-dependent Candida albicans morphogenesis via Ras1-PKA signaling.* Virulence, 2010. **1**(1): p. 45-48.
26. Tissieres, A., H.K. Mitchell, and U.M. Tracy, *PROTEIN-SYNTHESIS IN SALIVARY-GLANDS OF DROSOPHILA-MELANOGASTER - RELATION TO CHROMOSOME PUFFS.* Journal of Molecular Biology, 1974. **84**(3): p. 389-+.
27. Uppuluri, P., C.G. Pierce, and J.L. Lopez-Ribot, *Candida albicans biofilm formation and its clinical consequences.* Future Microbiology, 2009. **4**(10): p. 1235-1237.
28. Glazier, V.E., et al., *Genetic analysis of the Candida albicans biofilm transcription factor network using simple and complex haploinsufficiency.* Plos Genetics, 2017. **13**(8): p. 25.
29. Lo, H.J., et al., *Nonfilamentous C-albicans mutants are avirulent.* Cell, 1997. **90**(5): p. 939-949.
30. Saville, S.P., et al., *Engineered control of cell morphology in vivo reveals distinct roles for yeast and filamentous forms of Candida albicans during infection.* Eukaryotic Cell, 2003. **2**(5): p. 1053-1060.
31. Gow, N.A.R., et al., *Candida albicans morphogenesis and host defence: discriminating invasion from colonization.* Nature Reviews Microbiology, 2012. **10**(2): p. 112-122.
32. Baek, Y.U., S.J. Martin, and D.A. Davis, *Evidence for novel pH-dependent regulation of Candida albicans Rim101, a direct transcriptional repressor of the cell wall beta-glycosidase PHR2.* Eukaryotic Cell, 2006. **5**(9): p. 1550-1559.
33. Dantas, A.D., et al., *Thioredoxin Regulates Multiple Hydrogen Peroxide-Induced Signaling Pathways in Candida albicans.* Molecular and Cellular Biology, 2010. **30**(19): p. 4550-4563.
34. Wiederhold, N.P., *The antifungal arsenal: alternative drugs and future targets.* International journal of antimicrobial agents, 2017.

35. Cowen, L.E. and S. Lindquist, *Hsp90 potentiates the rapid evotution of new traits: Drug resistance in diverse fungi.* Science, 2005. **309**(5744): p. 2185-2189.
36. Brown, G.D., et al., *Hidden Killers: Human Fungal Infections.* Science Translational Medicine, 2012. **4**(165): p. 9.
37. Yocum, R.R., J.R. Rasmussen, and J.L. Strominger, *THE MECHANISM OF ACTION OF PENICILLIN - PENICILLIN ACYLATES THE ACTIVE-SITE OF BACILLUS-STEAROTHERMOPHILUS D-ALANINE CARBOXYPEPTIDASE.* Journal of Biological Chemistry, 1980. **255**(9): p. 3977-3986.
38. Velkov, T., et al., *Pharmacology of polymyxins: new insights into an 'old' class of antibiotics.* Future Microbiology, 2013. **8**(6): p. 711-724.
39. Carmona, E.M. and A.H. Limper, *Overview of Treatment Approaches for Fungal Infections.* Clinics in Chest Medicine, 2017. **38**(3): p. 393-+.
40. Tortorano, A.M., et al., *Epidemiology of candidaemia in Europe: Results of 28-month European Confederation of Medical Mycology (ECMM) hospital-based surveillance study.* European Journal of Clinical Microbiology & Infectious Diseases, 2004. **23**(4): p. 317-322.
41. Bassetti, M., et al., *Clinical and Therapeutic Aspects of Candidemia: A Five Year Single Centre Study.* Plos One, 2015. **10**(5): p. 12.
42. Mansfield, B.E., et al., *Azole Drugs Are Imported By Facilitated Diffusion in Candida albicans and Other Pathogenic Fungi.* Plos Pathogens, 2010. **6**(9): p. 11.
43. Lewis, R.E., *Current Concepts in Antifungal Pharmacology.* Mayo Clinic Proceedings, 2011. **86**(8): p. 805-817.
44. Dupont, S., et al., *ERGOSTEROL BIOSYNTHESIS: A FUNGAL PATHWAY FOR LIFE ON LAND?* Evolution, 2012. **66**(9): p. 2961-2968.
45. Weete, J.D., M. Abril, and M. Blackwell, *Phylogenetic Distribution of Fungal Sterols.* Plos One, 2010. **5**(5): p. 6.
46. Townsend, R., et al., *Pharmacokinetic Evaluation of CYP3A4-Mediated Drug-Drug Interactions of Isavuconazole With Rifampin, Ketoconazole, Midazolam, and Ethinyl Estradiol/Norethindrone in Healthy Adults.* Clinical Pharmacology in Drug Development, 2017. **6**(1): p. 44-53.
47. Lockhart, S.R., et al., *Simultaneous Emergence of Multidrug-Resistant Candida auris on 3 Continents Confirmed by Whole-Genome Sequencing and Epidemiological Analyses.* Clinical Infectious Diseases, 2017. **64**(2): p. 134-140.

48. Faria-Ramos, I., et al., *Environmental azole fungicide, prochloraz, can induce cross-resistance to medical triazoles in Candida glabrata.* Fems Yeast Research, 2014. **14**(7): p. 1119-1123.
49. Zhang, J., et al., *Evolution of cross-resistance to medical triazoles in Aspergillus fumigatus through selection pressure of environmental fungicides.* Proceedings. Biological sciences, 2017. **284**(1863).
50. Snelders, E., et al., *Triazole Fungicides Can Induce Cross-Resistance to Medical Triazoles in Aspergillus fumigatus.* Plos One, 2012. **7**(3): p. 11.
51. Deresinski, S.C. and D.A. Stevens, *Caspofungin.* Clinical Infectious Diseases, 2003. **36**(11): p. 1445-1457.
52. Odds, F.C., A.J.P. Brown, and N.A.R. Gow, *Antifungal agents: mechanisms of action.* Trends in Microbiology, 2003. **11**(6): p. 272-279.
53. Redding, S., et al., *Resistance of Candida albicans to fluconazole during treatment of oropharyngeal candidiasis in a patient with AIDS - documentation by in vitro susceptibility testing and DNA subtype analysis.* Clinical Infectious Diseases, 1994. **18**(2): p. 240-242.
54. Williams, G.C. and R.M. Nesse, *THE DAWN OF DARWINIAN MEDICINE.* Quarterly Review of Biology, 1991. **66**(1): p. 1-22.
55. Woods, R.J. and A.F. Read, *Clinical management of resistance evolution in a bacterial infection: A case study*. 2015: Evolution, Medicine and Public Health. p. 281-288.
56. Zahreddine, H. and K.L.B. Borden, *Mechanisms and insights into drug resistance in cancer.* Frontiers in Pharmacology, 2013. **4**: p. 8.
57. Ocampo, D. and M. Booth, *The application of evolutionary medicine principles for sustainable malaria control: a scoping study.* Malaria Journal, 2016. **15**: p. 8.
58. Jarosz, D.F. and S. Lindquist, *Hsp90 and Environmental Stress Transform the Adaptive Value of Natural Genetic Variation.* Science, 2010. **330**(6012): p. 1820-1824.
59. Walker, L.A., et al., *Genome-wide analysis of Candida albicans gene expression patterns during infection of the mammalian kidney.* Fungal Genetics and Biology, 2009. **46**(2): p. 210-219.
60. Gardete, S., et al., *Genetic Pathway in Acquisition and Loss of Vancomycin Resistance in a Methicillin Resistant Staphylococcus aureus (MRSA) Strain of Clonal Type USA300.* Plos Pathogens, 2012. **8**(2): p. 16.

61. Day, T., V. Huijben, and A.F. Read, *Is selection relevant in the evolutionary emergence of drug resistance?* Trends in Microbiology, 2015. **23**(3): p. 126-133.
62. Lipsitch, M., C.T. Bergstrom, and B.R. Levin, *The epidemiology of antibiotic resistance in hospitals: Paradoxes and prescriptions.* Proceedings of the National Academy of Sciences of the United States of America, 2000. **97**(4): p. 1938-1943.
63. Robbins, N., et al., *Hsp90 Governs Dispersion and Drug Resistance of Fungal Biofilms.* Plos Pathogens, 2011. **7**(9): p. 18.
64. Gupta, R.S., *PHYLOGENETIC ANALYSIS OF THE 90 KD HEAT-SHOCK FAMILY OF PROTEIN SEQUENCES AND AN EXAMINATION OF THE RELATIONSHIP AMONG ANIMALS, PLANTS, AND FUNGI SPECIES.* Molecular Biology and Evolution, 1995. **12**(6): p. 1063-1073.
65. Chen, B., D.B. Zhong, and A. Monteiro, *Comparative genomics and evolution of the HSP90 family of genes across all kingdoms of organisms.* Bmc Genomics, 2006. **7**: p. 19.
66. Borkovich, K.A., et al., *HSP82 IS AN ESSENTIAL PROTEIN THAT IS REQUIRED IN HIGHER CONCENTRATIONS FOR GROWTH OF CELLS AT HIGHER TEMPERATURES.* Molecular and Cellular Biology, 1989. **9**(9): p. 3919-3930.
67. Diezmann, S., et al., *Mapping the Hsp90 Genetic Interaction Network in Candida albicans Reveals Environmental Contingency and Rewired Circuitry.* Plos Genetics, 2012. **8**(3): p. 15.
68. Wegele, H., L. Muller, and J. Buchner, *Hsp70 and Hsp90 - a relay team for protein folding.* Reviews of Physiology, Biochemistry and Pharmacology, 2004. **151**: p. 1-44.
69. Grenert, J.P., et al., *The amino-terminal domain of heat shock protein 90 (hsp90) that binds geldanamycin is an ATP/ADP switch domain that regulates hsp90 conformation.* Journal of Biological Chemistry, 1997. **272**(38): p. 23843-23850.
70. Lindquist, S., *THE HEAT-SHOCK RESPONSE.* Annual Review of Biochemistry, 1986. **55**: p. 1151-1191.
71. McAlister, L., et al., *ALTERED PATTERNS OF PROTEIN-SYNTHESIS INDUCED BY HEAT-SHOCK OF YEAST.* Current Genetics, 1979. **1**(1): p. 63-74.

72. Skrzypek, M.S., et al., *The Candida Genome Database (CGD): incorporation of Assembly 22, systematic identifiers and visualization of high throughput sequencing data.* Nucleic Acids Research, 2017. **45**(D1): p. D592-D596.
73. Pearl, L.H., C. Prodromou, and P. Workman, *The Hsp90 molecular chaperone: an open and shut case for treatment.* Biochemical Journal, 2008. **410**: p. 439-453.
74. Sherman, M. and G. Multhoff, *Heat shock proteins in cancer.* Stress Responses in Biology and Medicine: Stress of Life in Molecules, Cells, Organisms, and Psychosocial Communities, 2007. **1113**: p. 192-201.
75. Solit, D.B., et al., *Phase II Trial of 17-Allylamino-17-Demethoxygeldanamycin in Patients with Metastatic Melanoma.* Clinical Cancer Research, 2008. **14**(24): p. 8302-8307.
76. Pacey, S., et al., *A Phase II trial of 17-allylamino, 17-demethoxygeldanamycin (17-AAG, tanespimycin) in patients with metastatic melanoma.* Investigational New Drugs, 2012. **30**(1): p. 341-349.
77. Stebbins, C.E., et al., *Crystal structure of an Hsp90-geldanamycin complex: Targeting of a protein chaperone by an antitumor agent.* Cell, 1997. **89**(2): p. 239-250.
78. Prodromou, C., et al., *Identification and structural characterization of the ATP/ADP-binding site in the Hsp90 molecular chaperone.* Cell, 1997. **90**(1): p. 65-75.
79. Bergerat, A., et al., *An atypical topoisomerase II from archaea with implications for meiotic recombination.* Nature, 1997. **386**(6623): p. 414-417.
80. Dutta, R. and M. Inouye, *GHKL, an emergent ATPase/kinase superfamily.* Trends in Biochemical Sciences, 2000. **25**(1): p. 24-28.
81. Dede, B., F. Karipcin, and M. Cengiz, *Novel homo- and hetero-nuclear copper(II) complexes of tetradentate Schiff bases: Synthesis, characterization, solvent-extraction and catalase-like activity studies.* Journal of Hazardous Materials, 2009. **163**(2-3): p. 1148-1156.
82. Demirci, S., et al., *A Schiff base derivative for effective treatment of diethylnitrosamine-induced liver cancer in vivo.* Anti-Cancer Drugs, 2015. **26**(5): p. 555-564.
83. Dogan, A., et al., *A NOVEL SCHIFF BASE DERIVATIVE FOR EFFECTIVE TREATMENT OF AZOXYMETHANE INDUCED COLON CANCER.* International Journal of Pharmaceutical Sciences and Research, 2014. **5**(8): p. 3544-3550.

84. Yoğurtçu, B.M., et al., *Anticandidal activity of hetero-dinuclear copper(II) Mn(II) Schiff base and its potential action of the mechanism*. 2017, Springer Science+Business Media: World J Microbiol Biotechnol.
85. Queitsch, C., T.A. Sangster, and S. Lindquist, *Hsp90 as a capacitor of phenotypic variation.* Nature, 2002. **417**(6889): p. 618-624.
86. Rutherford, S.L. and S. Lindquist, *Hsp90 as a capacitor for morphological evolution.* Nature, 1998. **396**(6709): p. 336-342.
87. Swoboda, R.K., et al., *Structure and regulation of the HSP90 gene from the pathogenic fungus Candida albicans.* Infection and Immunity, 1995. **63**(11): p. 4506-4514.
88. Swoboda, R.K., et al., *STRUCTURE AND REGULATION OF THE HSP90 GENE FROM THE PATHOGENIC FUNGUS CANDIDA-ALBICANS.* Infection and Immunity, 1995. **63**(11): p. 4506-4514.
89. Hoehamer, C.F., et al., *Changes in the Proteome of Candida albicans in Response to Azole, Polyene, and Echinocandin Antifungal Agents.* Antimicrobial Agents and Chemotherapy, 2010. **54**(5): p. 1655-1664.
90. Prodromou, C., et al., *Regulation of Hsp90 ATPase activity by tetratricopeptide repeat (TPR)-domain co-chaperones.* Embo Journal, 1999. **18**(3): p. 754-762.
91. Chen, S.Y. and D.F. Smith, *Hop as an adaptor in the heat shock protein 70 (Hsp70) and Hsp90 chaperone machinery.* Journal of Biological Chemistry, 1998. **273**(52): p. 35194-35200.
92. Wandinger, S.K., K. Richter, and J. Buchner, *The Hsp90 chaperone machinery.* Journal of Biological Chemistry, 2008. **283**(27): p. 18473-18477.
93. Pal, M., et al., *Structural Basis for Phosphorylation-Dependent Recruitment of Tel2 to Hsp90 by Pih1.* Structure, 2014. **22**(6): p. 805-818.
94. Marsh, J.A., K.M. Kalton, and R.F. Gaber, *Cns1 is an essential protein associated with the Hsp90 chaperone complex in Saccharomyces cerevisiae that can restore cyclophilin 40-dependent functions in cpr7 Delta cells.* Molecular and Cellular Biology, 1998. **18**(12): p. 7353-7359.
95. Hainzl, O., et al., *Cns1 is an activator of the Ssa1 ATPase activity.* Journal of Biological Chemistry, 2004. **279**(22): p. 23267-23273.
96. Johnson, J.L. and D.O. Toft, *BINDING OF P23 AND HSP90 DURING ASSEMBLY WITH THE PROGESTERONE-RECEPTOR.* Molecular Endocrinology, 1995. **9**(6): p. 670-678.

97. Ali, M.M.U., et al., *Crystal structure of an Hsp90-nucleotide-p23/Sba1 closed chaperone complex.* Nature, 2006. **440**(7087): p. 1013-1017.
98. Meyer, P., et al., *Structural basis for recruitment of the ATPase activator Aha1 to the Hsp90 chaperone machinery.* Embo Journal, 2004. **23**(3): p. 511-519.
99. Hernandez, M.P., A. Chadli, and D.O. Toft, *HSP40 binding is the first step in the HSP90 chaperoning pathway for the progesterone receptor.* Journal of Biological Chemistry, 2002. **277**(14): p. 11873-11881.
100. Flom, G.A., et al., *Farnesylation of Ydj1 Is Required for In Vivo Interaction with Hsp90 Client Proteins.* Molecular Biology of the Cell, 2008. **19**(12): p. 5249-5258.
101. Liu, X.D., K.A. Morano, and D.J. Thiele, *The yeast Hsp110 family member, SSE1, is an Hsp90 cochaperone.* Journal of Biological Chemistry, 1999. **274**(38): p. 26654-26660.
102. Shaner, L. and K.A. Morano, *All in the family: atypical Hsp70 chaperones are conserved modulators of Hsp70 activity.* Cell Stress & Chaperones, 2007. **12**(1): p. 1-8.
103. Caplan, A.J., A.K. Mandal, and M.A. Theodoraki, *Molecular chaperones and protein kinase quality control.* Trends in Cell Biology, 2007. **17**(2): p. 87-92.
104. Zhang, M.H., et al., *Structural and functional coupling of Hsp90-and Sgt1-centred multi-protein complexes.* Embo Journal, 2008. **27**(20): p. 2789-2798.
105. Martins, T., et al., *Sgt1, a co-chaperone of Hsp90 stabilizes Polo and is required for centrosome organization.* Embo Journal, 2009. **28**(3): p. 234-247.
106. Doheny, J.G., R. Mottus, and T.A. Grigliatti, *Telomeric Position Effect-A Third Silencing Mechanism in Eukaryotes.* Plos One, 2008. **3**(12): p. 15.
107. Palmer, J.M., et al., *Telomere position effect is regulated by heterochromatin-associated proteins and NkuA in Aspergillus nidulans.* Microbiology-Sgm, 2010. **156**: p. 3522-3531.
108. Shapiro, R.S., et al., *The Hsp90 Co-Chaperone Sgt1 Governs Candida albicans Morphogenesis and Drug Resistance.* Plos One, 2012. **7**(9): p. 12.
109. Johnson, J.L., *Evolution and function of diverse Hsp90 homologs and cochaperone proteins.* Biochimica Et Biophysica Acta-Molecular Cell Research, 2012. **1823**(3): p. 607-613.
110. LopezRibot, J.L., et al., *Evidence for presence in the cell wall of Candida albicans of a protein related to the hsp70 family.* Infection and Immunity, 1996. **64**(8): p. 3333-3340.

111. Pratt, W.B. and D.O. Toft, *Regulation of signaling protein function and trafficking by the hsp90/hsp70-based chaperone machinery.* Experimental Biology and Medicine, 2003. **228**(2): p. 111-133.
112. Kimmins, S. and T.H. MacRae, *Maturation of steroid receptors: an example of functional cooperation among molecular chaperones and their associated proteins.* Cell Stress & Chaperones, 2000. **5**(2): p. 76-86.
113. Wang, Y.Y., et al., *The yeast Hsp70 Ssa1 is a sensor for activation of the heat shock response by thiol-reactive compounds.* Molecular Biology of the Cell, 2012. **23**(17): p. 3290-3298.
114. Li, X.W.S., et al., *Candida albicans Ssa1/2p is the cell envelope binding protein for human salivary histatin 5.* Journal of Biological Chemistry, 2003. **278**(31): p. 28553-28561.
115. Diezmann, S., *Determining the consequences of transcriptional silencing during C. albicans biofilm formation*. 2013: Unpublished raw data.
116. Pearson, W.R., et al., *Comparison of DNA sequences with protein sequences.* Genomics, 1997. **46**(1): p. 24-36.
117. Li, X.W.S., et al., *Candida albicans cell wall Ssa proteins bind and facilitate import of salivary histatin 5 required for toxicity.* Journal of Biological Chemistry, 2006. **281**(32): p. 22453-22463.
118. Sun, J.N., et al., *Host Cell Invasion and Virulence Mediated by Candida albicans Ssa1.* Plos Pathogens, 2010. **6**(11): p. 14.
119. Kusch, H., et al., *A proteomic view of Candida albicans yeast cell metabolism in exponential and stationary growth phases.* International Journal of Medical Microbiology, 2008. **298**(3-4): p. 291-318.
120. Toogun, O.A., W. Zeiger, and B.C. Freeman, *The p23 molecular chaperone promotes functional telomerase complexes through DNA dissociation.* Proceedings of the National Academy of Sciences of the United States of America, 2007. **104**(14): p. 5765-5770.
121. Holmes, J.L., et al., *Silencing of HSP90 cochaperone AHA1 expression decreases client protein activation and increases cellular sensitivity to the HSP90 inhibitor 17-allylamino-17-demethoxygeldanamycin.* Cancer Research, 2008. **68**(4): p. 1187-1196.
122. Nett, J.E., et al., *Time Course Global Gene Expression Analysis of an In Vivo Candida Biofilm.* Journal of Infectious Diseases, 2009. **200**(2): p. 307-313.
123. Pearl, L.H. and C. Prodromou, *Structure, function, and mechanism of the Hsp90 molecular chaperone.* Protein Folding in the Cell, 2002. **59**: p. 157-186.

124. Harst, A., H.Y. Lin, and W.M.J. Obermann, *Aha1 competes with Hop, p50 and p23 for binding to the molecular chaperone Hsp90 and contributes to kinase and hormone receptor activation.* Biochemical Journal, 2005. **387**: p. 789-796.
125. Kravats, A.N., et al., *Functional and physical interaction between yeast Hsp90 and Hsp70.* Proceedings of the National Academy of Sciences of the United States of America, 2018. **115**(10): p. E2210-E2219.
126. Cortajarena, A.L., F. Yi, and L. Regan, *Designed TPR modules as novel anticancer agents.* Acs Chemical Biology, 2008. **3**(3): p. 161-166.
127. Giaever, G., et al., *Functional profiling of the Saccharomyces cerevisiae genome.* Nature, 2002. **418**(6896): p. 387-391.
128. Vernis, L., et al., *A Newly Identified Essential Complex, Dre2-Tah18, Controls Mitochondria Integrity and Cell Death after Oxidative Stress in Yeast.* Plos One, 2009. **4**(2): p. 14.
129. Nishimura, A., N. Kawahara, and H. Takagi, *yy The flavoprotein Tah18-dependent NO synthesis confers high-temperature stress tolerance on yeast cells.* Biochemical and Biophysical Research Communications, 2013. **430**(1): p. 137-143.
130. Heitz, E., *Heterochromatin , Chromocentren , Chromomenen .* 1929: Berichte der. Deutschen Botanischen Gesellschaft. p. 274-284.
131. Narlikar, G.J., R. Sundaramoorthy, and T. Owen-Hughes, *Mechanisms and Functions of ATP-Dependent Chromatin-Remodeling Enzymes.* Cell, 2013. **154**(3): p. 490-503.
132. Blossey, R. and H. Schiessel, *Kinetic proofreading of gene activation by chromatin remodeling.* Hfsp Journal, 2008. **2**(3): p. 167-170.
133. Ayer, D.E., *Histone deacetylases: transcriptional repression with SINers and NuRDs.* Trends in Cell Biology, 1999. **9**(5): p. 193-198.
134. Kang, J.K., et al., *Coordinated change of a ratio of methylated H3-lysine 4 or acetylated H3 to acetylated H4 and DNA methylation is associated with tissue-specific gene expression in cloned pig.* Experimental and Molecular Medicine, 2007. **39**(1): p. 84-96.
135. Tasselli, L., W. Zheng, and K.F. Chua, *SIRT6: Novel Mechanisms and Links to Aging and Disease.* Trends in Endocrinology and Metabolism, 2017. **28**(3): p. 168-185.
136. Ekwall, K., et al., *Transient inhibition of histone deacetylation alters the structural and functional imprint at fission yeast centromeres.* Cell, 1997. **91**(7): p. 1021-1032.

137. Buck, S.W., C.M. Gallo, and J.S. Smith, *Diversity in the Sir2 family of protein deacetylases.* Journal of Leukocyte Biology, 2004. **75**(6): p. 939-950.
138. Oh, J., et al., *Gene Annotation and Drug Target Discovery in Candida albicans with a Tagged Transposon Mutant Collection.* Plos Pathogens, 2010. **6**(10): p. 18.
139. Selmecki, A., A. Forche, and J. Berman, *Genomic Plasticity of the Human Fungal Pathogen Candida albicans.* Eukaryotic Cell, 2010. **9**(7): p. 991-1008.
140. Lazzerini-Denchi, E. and A. Sfeir, *Stop pulling my strings - what telomeres taught us about the DNA damage response.* Nature Reviews Molecular Cell Biology, 2016. **17**(6): p. 364-378.
141. Larsen, D.H. and M. Stucki, *Nucleolar responses to DNA double-strand breaks.* Nucleic Acids Research, 2016. **44**(2): p. 538-544.
142. Freire-Beneitez, V., et al., *Sir2 regulates stability of repetitive domains differentially in the human fungal pathogen Candida albicans.* Nucleic Acids Research, 2016. **44**(19): p. 9166-9179.
143. Hnisz, D., T. Schwarzmuller, and K. Kuchler, *Transcriptional loops meet chromatin: a dual-layer network controls white-opaque switching in Candida albicans.* Molecular Microbiology, 2009. **74**(1): p. 1-15.
144. Noble, S.M. and A.D. Johnson, *Strains and strategies for large-scale gene deletion studies of the diploid human fungal pathogen Candida albicans.* Eukaryotic Cell, 2005. **4**(2): p. 298-309.
145. Maestrone G, S.R. *Establishment and treatment of cutaneous Candida albicans infection in the rabbit*. in *Naturwissenschaften*. 1968.
146. Holt, J.F., et al., *Enterococcus faecalis 6-Phosphogluconolactonase Is Required for Both Commensal and Pathogenic Interactions with Manduca sexta.* Infection and Immunity, 2015. **83**(1): p. 396-404.
147. Hussa, E. and H. Goodrich-Blair, *Rearing and Injection of Manduca sexta Larvae to Assess Bacterial Virulence.* Jove-Journal of Visualized Experiments, 2012(70): p. 5.
148. Roth, A., P. Reichmann, and R. Hakenbeck, *The Capsule of Streptococcus pneumoniae Contributes to Virulence in the Insect Model Manduca sexta.* Journal of Molecular Microbiology and Biotechnology, 2012. **22**(5): p. 326-334.
149. Trust, N.R.B.D.M.N.W., *Responsibility in the use of animals in bioscience research: expectations of the major research councils and charitable funding bodies. London: NC3Rs*. 2017.

150. Kanost, M.R., et al., *Multifaceted biological insights from a draft genome sequence of the tobacco hornworm moth, Manduca sexta.* Insect Biochem Mol Biol, 2016. **76**: p. 118-47.
151. Schiestl, R.H. and R.D. Gietz, *High-efficiency transformation of intact yeast-cells using single stranded nucleic-acids as a carrier.* Current Genetics, 1989. **16**(5-6): p. 339-346.
152. Morschhauser, J., S. Michel, and P. Staib, *Sequential gene disruption in Candida albicans by FLP-mediated site-specific recombination.* Molecular Microbiology, 1999. **32**(3): p. 547-556.
153. Shen, J.Q., W.H. Guo, and J.R. Kohler, *CaNAT1, a heterologous dominant selectable marker for transformation of Candida albicans and other pathogenic Candida species.* Infection and Immunity, 2005. **73**(2): p. 1239-1242.
154. Muzzey, D., et al., *Assembly of a phased diploid Candida albicans genome facilitates allele-specific measurements and provides a simple model for repeat and indel structure.* Genome Biology, 2013. **14**(9).
155. Sprouffske, K. and A. Wagner, *Growthcurver: an R package for obtaining interpretable metrics from microbial growth curves.* Bmc Bioinformatics, 2016. **17**: p. 4.
156. Leach, M.D., et al., *Hsf1 and Hsp90 orchestrate temperature-dependent global transcriptional remodelling and chromatin architecture in Candida albicans.* Nature Communications, 2016. **7**: p. 13.
157. Pierce, C.G., et al., *A simple and reproducible 96-well plate-based method for the formation of fungal biofilms and its application to antifungal susceptibility testing.* Nature Protocols, 2008. **3**(9): p. 1494-1500.
158. Dwivedi, P., et al., *Role of Bcr1-Activated Genes Hwp1 and Hyr1 in Candida Albicans Oral Mucosal Biofilms and Neutrophil Evasion.* Plos One, 2011. **6**(1): p. 9.
159. Mersondavies, L.A. and F.C. Odds, *A MORPHOLOGY INDEX FOR CHARACTERIZATION OF CELL-SHAPE IN CANDIDA-ALBICANS.* Journal of General Microbiology, 1989. **135**: p. 3143-3152.
160. Diezmann, S., *Of caterpillars and yeasts: Introducing a new model system for the study of fungal virulence*. 2015, Figshare.
161. Lal, A., et al., *Surgically implanted micro-platforms and microsystems in arthropods and methods based thereon*. 2010, Google Patents.

162. Goel, M.K., P. Khanna, and K. Jugal, *Understanding Survival Analysis: Kaplan-Meier Estimate.* 2010, PMC: *International Journal of Ayurveda Research*. p. 274-278.
163. Festing, M.F.W. and D.G. Altman, *Guidelines for the design and statistical analysis of experiments using laboratory animals.* ILAR journal, 2002. **43**(4): p. 244-58.
164. Najafi, M., *How to Analyse Real Time qPCR Data?* 2013: Biochemistry & Physiology: Open Access.
165. Vyas, V.K., M.I. Barrasa, and G.R. Fink, *A Candida albicans CRISPR system permits genetic engineering of essential genes and gene families.* Science Advances, 2015. **1**(3): p. 6.
166. Backen, A.C., et al., *Evaluation of the CaMAL2 promoter for regulated expression of genes in Candida albicans.* Yeast, 2000. **16**(12): p. 1121-1129.
167. Care, R.S., et al., *The MET3 promoter: a new tool for Candida albicans molecular genetics.* Molecular Microbiology, 1999. **34**(4): p. 792-798.
168. Pearl, L.H. and C. Prodromou, *Structure and mechanism of the Hsp90 molecular chaperone machinery*, in *Annual Review of Biochemistry*. 2006, Annual Reviews: Palo Alto. p. 271-294.
169. Nakayama, H., et al., *Tetracycline-regulatable system to tightly control gene expression in the pathogenic fungus Candida albicans.* Infection and Immunity, 2000. **68**(12): p. 6712-6719.
170. Baldridge, C.W. and R.W. Gerard, *The extra respiration of phagocytosis*. 1932: American Journal of Physiology-Legacy Content. p. 235-236.
171. Yin, Z.K., et al., *A proteomic analysis of the salt, cadmium and peroxide stress responses in Candida albicans and the role of the Hog1 stress-activated MAPK in regulating the stress-induced proteome.* Proteomics, 2009. **9**(20): p. 4686-4703.
172. Lindquist, S. and E.A. Craig, *The heat-shock proteins.* Annual Review of Genetics, 1988. **22**: p. 631-677.
173. Morimoto, R.I., *Cells in stress - transcriptional activation of heat-shock genes.* Science, 1993. **259**(5100): p. 1409-1410.
174. Parsell, D.A., J. Taulien, and S. Lindquist, *The role of heat-shock proteins in thermotolerance.* Philosophical Transactions of the Royal Society of London Series B-Biological Sciences, 1993. **339**(1289): p. 279-286.

175. Dabrowa, N., J.W. Landau, and V.D. Newcomer, *Generation time of Candida albicans in synchronized and nonsynchronized cultures*. 1968: Sabouraudia. p. 51-56.
176. Liu, H.P., J. Kohler, and G.R. Fink, *Suppression of hyphen formation in Candida albicans by mutation of a Ste12 homolog.* Science, 1994. **266**(5191): p. 1723-1726.
177. Moore, G.E., R.E. Gerner, and H.A. Franklin, *Culture of normal human leukocytes.* Journal of the American Medical Association, 1967. **199**(8): p. 519-&.
178. Espinelingroff, A., et al., *Collaborative comparison of broth macrodilution and microdilution antifungal susceptibility tests.* Journal of Clinical Microbiology, 1992. **30**(12): p. 3138-3145.
179. Daniels, K.J., et al., *Impact of Environmental Conditions on the Form and Function of Candida albicans Biofilms.* Eukaryotic Cell, 2013. **12**(10): p. 1389-1402.
180. Odds, F.C., *Sabouraud(s) Agar.* Journal of Medical and Veterinary Mycology, 1991. **29**(6): p. 355-359.
181. Sabouraud, R., *Contribution a l'étude de la trichophytie humaine*. 1892-3: *Annales de Dermatologie 3rd series III* p. 1061 – 1087.
182. Duran, A. and E. Cabib, *Solubilization and partial-purification of yeast chitin synthetase - confirmation of zymogenic nature of enzyme.* Journal of Biological Chemistry, 1978. **253**(12): p. 4419-4425.
183. Merzendorfer, H., *Chitin synthesis inhibitors: old molecules and new developments.* Insect Science, 2013. **20**(2): p. 121-138.
184. Liesche, J., M. Marek, and T. Gunther-Pomorski, *Cell wall staining with Trypan blue enables quantitative analysis of morphological changes in yeast cells.* Frontiers in Microbiology, 2015. **6**: p. 8.
185. Roncero, C. and A. Duran, *Effect of Calcofluor white and Congo red on fungal cell-wall morphogenesis - in vivo activation of chitin polymerization.* Journal of Bacteriology, 1985. **163**(3): p. 1180-1185.
186. Lee, K.L., C.C. Campbell, and H.R. Buckley, *Amino-acid liquid synthetic medium for development of mycelial and yeast forms of Candida albicans.* Sabouraudia-Journal of Medical and Veterinary Mycology, 1975. **13**(JUL): p. 148-153.
187. Chen, L., et al., *Two-Dimensionality of Yeast Colony Expansion Accompanied by Pattern Formation.* Plos Computational Biology, 2014. **10**(12): p. 14.

188. Vandeparre, H. and P. Damman, *Wrinkling of stimuloresponsive surfaces: Mechanical instability coupled to diffusion.* Physical Review Letters, 2008. **101**(12): p. 4.
189. Morales, D.K., et al., *Control of Candida albicans Metabolism and Biofilm Formation by Pseudomonas aeruginosa Phenazines.* Mbio, 2013. **4**(1): p. 9.
190. Trejo, M., et al., *Elasticity and wrinkled morphology of Bacillus subtilis pellicles.* Proceedings of the National Academy of Sciences of the United States of America, 2013. **110**(6): p. 2011-2016.
191. Perlroth, J., B. Choi, and B. Spellberg, *Nosocomial fungal infections: epidemiology, diagnosis, and treatment.* Medical Mycology, 2007. **45**(4): p. 321-346.
192. Schmid, S., M. Gotz, and T. Hugel, *Effects of inhibitors on Hsp90's conformational dynamics, cochaperone and client interactions*. 2018: bioRxiv.
193. Ondeyka, J., et al., *Isolation, Structure Elucidation, and Biological Activity of Virgineone from Lachnum virgineum Using the Genome-Wide Candida albicans Fitness Test.* Journal of Natural Products, 2009. **72**(1): p. 136-141.
194. Lo, H.J., et al., *Nonfilamentous C. albicans mutants are avirulent.* Cell, 1997. **90**(5): p. 939-949.
195. Mersondavies, L.A. and F.C. Odds, *A morphology index for characterization of cell-shape in Candida albicans.* Journal of General Microbiology, 1989. **135**: p. 3143-3152.
196. Vylkova, S., et al., *Distinct antifungal mechanisms: beta-defensins require Candida albicans Ssa1 protein, while Trk1p mediates activity of cysteine-free cationic peptides.* Antimicrobial Agents and Chemotherapy, 2006. **50**(1): p. 324-331.
197. Liu, T.T., et al., *Genome-wide expression profiling of the response to azole, polyene, echinocandin, and pyrimidine antifungal agents in Candida albicans.* Antimicrobial Agents and Chemotherapy, 2005. **49**(6): p. 2226-2236.
198. Orth, P., et al., *Structural basis of gene regulation by the tetracycline inducible Tet repressor-operator system.* Nature Structural Biology, 2000. **7**(3): p. 215-219.
199. Saraswat, D., et al., *Signalling mucin Msb2 Regulates adaptation to thermal stress in Candida albicans.* Molecular Microbiology, 2016. **100**(3): p. 425-441.
200. Breslow, D.K., et al., *A comprehensive strategy enabling high-resolution functional analysis of the yeast genome.* Nature Methods, 2008. **5**(8): p. 711-718.

201. Andersen, K.S., et al., *Genetic Basis for Saccharomyces cerevisiae Biofilm in Liquid Medium.* G3-Genes Genomes Genetics, 2014. **4**(9): p. 1671-1680.
202. El Khoury, P., et al., *Proteomic analysis of a Candida albicans pir32 null strain reveals proteins involved in adhesion, filamentation and virulence.* Plos One, 2018. **13**(3): p. 16.
203. Li, S.X., et al., *The F1Fo-ATP Synthase beta Subunit Is Required for Candida albicans Pathogenicity Due to Its Role in Carbon Flexibility.* Frontiers in Microbiology, 2018. **9**: p. 24.
204. Luna-Tapia, A., et al., *Loss of Upc2p-Inducible ERG3 Transcription Is Sufficient To Confer Niche-Specific Azole Resistance without Compromising Candida albicans Pathogenicity.* Mbio, 2018. **9**(3): p. 17.
205. Watson, R.J., et al., *The role of iron uptake in pathogenicity and symbiosis in Photorhabdus luminescens TT01.* Bmc Microbiology, 2010. **10**: p. 12.
206. Vlisidou, I., et al., *The KdpD/KdpE two-component system of Photorhabdus asymbiotica promotes bacterial survival within M. sexta hemocytes.* Journal of Invertebrate Pathology, 2010. **105**(3): p. 352-362.
207. Castillo, J.C., S.E. Reynolds, and I. Eleftherianos, *Insect immune responses to nematode parasites.* Trends in Parasitology, 2011. **27**(12): p. 537-547.
208. Hedrick, T.L., J. Martinez-Blat, and M.J. Goodman, *Flight motor modulation with speed in the hawkmoth Manduca sexta.* Journal of Insect Physiology, 2017. **96**: p. 115-121.
209. Boman, H.G., et al., *Cell-Free Immunity in Cecropia - a Model System for Antibacterial Proteins.* European Journal of Biochemistry, 1991. **201**(1): p. 23-31.
210. Horwath, K.L. and N.E. Stamp, *Use of dietary rutin to study most initiation in Manduca sexta larvae.* Journal of Insect Physiology, 1993. **39**(11): p. 987-1000.
211. Kramer, K.J., et al., *Toxicity of purothionin and its homologs to the tobacco hornworm, Manduca sexta (L) (Lepidoptera sphingidae).* Toxicology and Applied Pharmacology, 1979. **48**(1): p. 179-183.
212. Kawahara, A.Y., et al., *Evolution of Manduca sexta hornworms and relatives: Biogeographical analysis reveals an ancestral diversification in Central America.* Molecular Phylogenetics and Evolution, 2013. **68**(3): p. 381-386.
213. Bradfield, J.Y. and G.R. Wyatt, *X-Linkage of a Vitellogenin Gene in Locusta migratoria.* Chromosoma, 1983. **88**(3): p. 190-193.

214. Sahara, K., A. Yoshido, and W. Traut, *Sex chromosome evolution in moths and butterflies.* Chromosome Research, 2012. **20**(1): p. 83-94.
215. Stillwell, R.C., A. Daws, and G. Davidowitz, *The Ontogeny of Sexual Size Dimorphism of a Moth: When Do Males and Females Grow Apart?* Plos One, 2014. **9**(9): p. 7.
216. Beetz, S., et al., *Correlation of hemocyte counts with different developmental parameters during the last larval instar of the tobacco hornworm, Manduca sexta.* Archives of Insect Biochemistry and Physiology, 2008. **67**(2): p. 63-75.
217. Summerbell, C.D., J.P. Perrett, and B.G. Gazzard, *Causes of weight-loss in human-immunodeficiency-virus infection.* International Journal of Std & Aids, 1993. **4**(4): p. 234-236.
218. Garey, K.W., et al., *Time to initiation of fluconazole therapy impacts mortality in patients with candidemia: A multi-institutional study.* Clinical Infectious Diseases, 2006. **43**(1): p. 25-31.
219. Morrell, M., V.J. Fraser, and M.H. Kollef, *Delaying the empiric treatment of Candida bloodstream infection until positive blood culture results are obtained: a potential risk factor for hospital mortality.* Antimicrobial Agents and Chemotherapy, 2005. **49**(9): p. 3640-3645.
220. Schneider, D.S. and J.S. Ayres, *Two ways to survive infection: what resistance and tolerance can teach us about treating infectious diseases.* Nature Reviews Immunology, 2008. **8**(11): p. 889-895.
221. Sandell, L.L. and V.A. Zakian, *Telomeric position effect in yeast*. 1992: Treands in Cell Biology. p. 10-14.
222. Baur, J.A., et al., *Telomere position effect in human cells.* Science, 2001. **292**(5524): p. 2075-2077.
223. Castano, I., et al., *Telomere length control and transcriptional regulation of subtelomeric adhesins in Candida glabrata.* Molecular Microbiology, 2005. **55**(4): p. 1246-1258.
224. Liu, T.Y., et al., *Riches of phenotype computationally extracted from microbial colonies.* Proceedings of the National Academy of Sciences of the United States of America, 2016. **113**(20): p. E2822-E2831.
225. Bedalov, A., et al., *NAD(+)-dependent deacetylase Hst1p controls biosynthesis and cellular NAD(+) levels in Saccharomyces cerevisiae.* Molecular and Cellular Biology, 2003. **23**(19): p. 7044-7054.
226. Revollo, J.R., A.A. Grimm, and S. Imai, *The NAD biosynthesis pathway mediated by nicotinamide phosphoribosyltransferase regulates Sir2 activity in*

mammalian cells. Journal of Biological Chemistry, 2004. **279**(49): p. 50754-50763.

227. Perrod, S., et al., *A cytosolic NAD-dependent deacetylase, Hst2p, can modulate nucleolar and telomeric silencing in yeast.* Embo Journal, 2001. **20**(1-2): p. 197-209.
228. Erdeniz, N., U.H. Mortensen, and R. Rothstein, *Cloning-free PCR-based allele replacement methods.* Genome Research, 1997. **7**(12): p. 1174-1183.
229. Krejci, L., et al., *Homologous recombination and its regulation.* Nucleic Acids Research, 2012. **40**(13): p. 5795-5818.
230. Silva-Dias, A., et al., *A novel flow cytometric protocol for assessment of yeast cell adhesion.* Cytometry Part A, 2012. **81A**(3): p. 265-270.
231. Silva-Dias, A., et al., *Adhesion, biofilm formation, cell surface hydrophobicity, and antifungal planktonic susceptibility: relationship among Candida spp.* Frontiers in Microbiology, 2015. **6**: p. 8.
232. Caplan, T., et al., *Functional Genomic Screening Reveals Core Modulators of Echinocandin Stress Responses in Candida albicans.* Cell Reports, 2018. **23**(8): p. 2292-2298.
233. Bergstrom, C.T., M. Lo, and M. Lipsitch, *Ecological theory suggests that antimicrobial cycling will not reduce antimicrobial resistance in hospitals.* Proceedings of the National Academy of Sciences of the United States of America, 2004. **101**(36): p. 13285-13290.
234. Brown, E.M. and D. Nathwani, *Antibiotic cycling or rotation: a systematic review of the evidence of efficacy.* Journal of Antimicrobial Chemotherapy, 2005. **55**(1): p. 6-9.
235. Hill, J.A., T.R. O'Meara, and L.E. Cowen, *Fitness Trade-Offs Associated with the Evolution of Resistance to Antifungal Drug Combinations.* Cell Reports, 2015. **10**(5): p. 809-819.
236. Martel, C.M., et al., *A Clinical Isolate of Candida albicans with Mutations in ERG11 (Encoding Sterol 14 alpha-Demethylase) and ERG5 (Encoding C22 Desaturase) Is Cross Resistant to Azoles and Amphotericin B.* Antimicrobial Agents and Chemotherapy, 2010. **54**(9): p. 3578-3583.
237. Morio, F., et al., *Amino acid substitutions in the Candida albicans sterol Delta(5,6)-desaturase (Erg3p) confer azole resistance: characterization of two novel mutants with impaired virulence.* Journal of Antimicrobial Chemotherapy, 2012. **67**(9): p. 2131-2138.

238. zur Wiesch, P.A., et al., *Population biological principles of drug-resistance evolution in infectious diseases.* Lancet Infectious Diseases, 2011. **11**(3): p. 236-247.
239. Perron, G.G., et al., *Fighting microbial drug resistance: a primer on the role of evolutionary biology in public health.* Evolutionary Applications, 2015. **8**(3): p. 211-222.
240. Brown, S.P., et al., *Social evolution in micro-organisms and a Trojan horse approach to medical intervention strategies.* Philosophical Transactions of the Royal Society B-Biological Sciences, 2009. **364**(1533): p. 3157-3168.
241. Ross-Gillespie, A., Z. Dumas, and R. Kummerli, *Evolutionary dynamics of interlinked public goods traits: an experimental study of siderophore production in Pseudomonas aeruginosa.* Journal of Evolutionary Biology, 2015. **28**(1): p. 29-39.
242. Diezmann, S., M.D. Leach, and L.E. Cowen, *Functional Divergence of Hsp90 Genetic Interactions in Biofilm and Planktonic Cellular States.* Plos One, 2015. **10**(9): p. 20.